Master of Science Thesis in Electrical Engineering
Department of Electrical Engineering, Linköping University, 2017

Model Based Control of Throttle, EGR and Wastegate

A System Analysis of the Gas Flows in an SI-Engine

Henrik Andersson

LINKÖPING UNIVERSITY

Master of Science Thesis in Electrical Engineering

Model Based Control of Throttle, EGR and WastegateA System Analysis of the Gas Flows in an SI-Engine

Henrik Andersson

LiTH-ISY-EX--17/5035--SE

Supervisor: **Kristoffer Ekberg**
ISY, Linköping University
Svante Löthgren
SCANIA CV AB
Erik Klingborg
SCANIA CV AB

Examiner: **Professor Lars Eriksson**
ISY, Linköping University

Division of Vehicular Systems
Department of Electrical Engineering
Linköping University
SE-581 83 Linköping, Sweden

Abstract

Due to governmental requirements on low exhaust gas emissions and the drivers request of fast response, it is important to be able to control the gas flow in a spark ignited engine accurately. The air into the cylinder is directly related to the torque generated by the engine. The technique with recirculation of exhaust gases (EGR) affect the air flow into the cylinder and increase the complexity of the control problem. In this thesis a mean value model for a spark ignited engine has been created. The basis was a diesel model from Linköping University that has been modified and parameterized with data from a test cell. The model has been used to study the gas exchange system with respect to the dynamic behaviors and nonlinearities that occur when the three actuators (throttle, wastegate and EGR-valve) are changed. Based on this analysis, some different control strategies have been developed and tested on the model. The presented results show that different control strategies give different behaviors and there is a trade-off between fast torque response and high precision for controlling the EGR-ratio. A control strategy is proposed containing two main feedback loops, prefiltering of the reference signal and a feedforward part.

Contents

Notation

Symbol	Description
A	Effective area
$(A/F)_s$	Stoichiometric air-fuel ratio
γ	Heat capacity ratio
n_e	Engine speed
n_t	Turbo speed
p	Pressure
P	Power
Π	Pressure ratio (upstream divided by downstream)
R	Gas constant
T	Temperature
u	Control signal
$\tilde{u}$	Actual actuator position
W	Mass flow
τ	Time constant
τ_d	Time delay

Index	Description
a	Air
amb	Ambient
bc	Before compressor
c	Compressor
e	Exhaust
egr	Exhaust gas recirculation
ei	Engine in
eo	Engine out
em	Exhaust manifold
f	Fuel
ic	Intercooler volume
im	Intake manifold
ref	Reference
t	Turbine
tc	Turbocharger
th	Throttle
wg	Wastegate

Abbreviation	Description
CNG	Compressed natural gas
EGR	Exhaust gas recirculation
FGT	Fixed geometry turbocharger
PID	Proportional, integral, differential (regulator)
VGT	Variable geometry turbocharger

1 Introduction

The chapter Introduction contains the background, the purpose and the goal with this thesis. There is also a short section with a motivation of the work and some limitations.

1.1 Background

In the automotive industry the emission regulations from the government constantly get stricter. The customers on the other hand require higher performance, faster response and lower fuel consumption. To achieve this the hardware and software have to be improved and new techniques have to be developed.

Most of the heavy duty vehicles today are running on diesel. A more environment friendly option is engines running on gas (called CNG-vehicles), for example biogas produced from food waste. The interest for this kind of fuel is increasing because of the possibility of renewable fuel. In most cases these engines are, compared to diesel engines, of spark ignited (SI-engines) types and follow the otto-cycle. From a control perspective there is a difference. An SI-engine is required to run at $\lambda = 1$ (if a three-way catalyst is used), compared to a diesel engine, which implies that the torque produced is directly related to the amount of air in the cylinder.

To receive good performance and low emissions with an SI-engine several techniques are used. One of them is the three-way catalyst to keep the emission low. For a catalyst to work optimally the engine needs to run at $\lambda = 1$. This means that the ratio between the air and fuel is constant and follow the stoichiometric ratio. Due to this the torque that is produced is limited to the amount of air that flow into the cylinder. The fuel is easier to control and there is no problem to inject enough fuel to combust all the oxygen.

To receive good driveability it is of interest to control and to be able to rapidly

change the amount of air into the cylinder. There is also a balance to achieve low fuel consumption. One way to do this in a heavy-duty vehicle running on gas is with a throttle and turbocharger (controlled with wastegate called fixed geometry turbo, FGT). Most of the current CNG-vehicles also have exhaust gas recirculation (EGR) which means that exhausted gas is recycled to the fresh air and back into the cylinder. The advantages of this are reduced nitrogen oxides and decreased exhaust temperature, which spare the catalyst [19].

This type of system have three actuators: throttle, wastegate and EGR-valve that controls the air and EGR-gases into the cylinder. In Wahlström [15] the problem with a diesel engine with EGR and variable geometry turbo (VGT) is described. This engines gives an advanced control problem with sign reversal and non-minimum phase behavior. If another actuator is added, in this case the throttle, the complexity will grow.

Here follows some short examples of the dilemma with controlling the air flow and EGR-ratio into the cylinder. For example, if the EGR-valve opens up, to increase the EGR-flow, the exhaust gas through the turbine is reduced and to keep the same boost from the compressor the wastegate must be closed. Or if the throttle is closed the air flow into the intake manifold is reduced and to keep the same level of EGR, the EGR-valve also needs to be closed.

To receive good performance according to driveability and low emissions modeling the air through the cylinder is of interest. One way to do this is with a mean value model and submodels, according to Andersson [1]. This makes it possible to analyze the system and evaluate different control strategies.

1.2 Motivation

The motivation to develop a mean value model of a real engine, is to be able to study the behavior of the gas flow through the cylinder. Doing measurements on real hardware is both expensive and time-consuming. The model makes it possible to analyze the system and to find non-linearities and study how fast the different actuators impact the output from the system. Analyzing the model also gives information about cross connections between the inputs and outputs of the system.

The analysis will form the basis for developing a control strategy for the three actuators. The model also gives the opportunity to test and evaluate the controllers in a simulation environment before testing on real hardware.

1.3 Purpose and goal

The purpose of this thesis is to investigate the dynamics and the cross connections between the throttle, the EGR-valve and the wastegate for a heavy-duty vehicle with an SI-engine. To be able to analyze the system a mean value model for the specific engine will be created in Matlab/Simulink. The model will be based on Wahlström and Eriksson [16] diesel model but with modifications and changes to

get the same behavior as for a 9-liter gas engine with port injection, throttle, EGR and FGT. The model will be analyzed and a controller implemented and tested.

During the modeling part, focus is on the behavior during transients and not the stationary values. What happen to the gas flows and pressures when the actuators are changed? This is relevant to be able to analyze the system and propose suitable control strategies.

Another goal with the model is that it will be built modular. This will simplify tests and updates. With submodels each part can be tested individually. It is also possible to improve the different submodels without making changes in the whole model. Wahlström and Eriksson [16] diesel model is based on both physical relations and black-box models that suit the measured data well. The objective is to use as much physical modeling as possible. This is because of the easiness to be able to adjust the model to suit different engines. For example if the volumes will be changed for the manifolds.

The overall purpose is to investigate the dynamic behaviors and propose a control strategy for the three actuators mentioned before. The system is nonlinear and therefore analyzing the system to find sign-reversal and non-minimum phase behaviors will be necessary. In the end a couple of control strategies will be developed and tested.

1.4 Problem description

As mentioned in Section 1.1, the three actuators throttle, wastegate and EGR create an advanced control problem with sign-reversals and non-minimum phase behaviors. Creating a model will simplify the analysis of the system. It will also be easier to evaluate and test different control strategies. This saves both money and time instead of doing tests on hardware. However, it is important that the model captures the dynamic right and that it is a good representation of the real engine. Otherwises the analysis will be inaccurate.

The model will be an extension of Wahlström and Eriksson [16] diesel model. To suit the SI-engine modeled in this thesis some changes will be made. The two biggest changes are:

- **Turbine:** The original model has a turbo with VGT. The engine in this thesis has a FGT turbo with a wastegate.
- **Throttle:** The original model has no throttle. A throttle model and an extra control volume between the compressor and the throttle will therefore be implemented.

Besides changing the model, the parameters in the model should be parameterized. All submodels will be validated and tested before merged together. This will give information if the submodels that are used fit the data well or if changes are needed.

From the model an analysis will be performed and a control strategy developed for the three actuators (the throttle, the wastegate and the EGR-valve). To control the engine in the entire operating area is a complex problem because

of the non-linearities described in Section 1.1. The controller will therefore be tested and evaluated in a couple of different transients and not the whole operating area for the engine.

Questions to be answered in this rapport are:

1. Which non-linearities have the system?
2. How could a controller be designed based on the system analysis?
3. Is it possible to decrease the calibration time of the engine with this controller?
4. Does the controller work even if part of the engine is changed?

1.5 Overall approach

During the thesis a model will be developed based on Wahlström and Eriksson [16] diesel model. Changes will be made to suit the 9-liters gas engine with a throttle, EGR and FGT, see Figure 1.1. The figure shows an illustration of the model with submodels modeled in this thesis. The arrows show the gas flow starting in the lower right corner. To parametrize the model measurements from a real engine will be used. The measurements are both from statics and dynamics measurement series. There is also a combination of old and new measurements performed at Scania in Södertälje. Before finishing the modeling part each submodel will be validated.

Next step in this thesis will be to analyze the system to find non-linear behaviors that affect the design of the controller. The analysis will be used to develop a control strategy for the throttle, wastegate and EGR-valve.

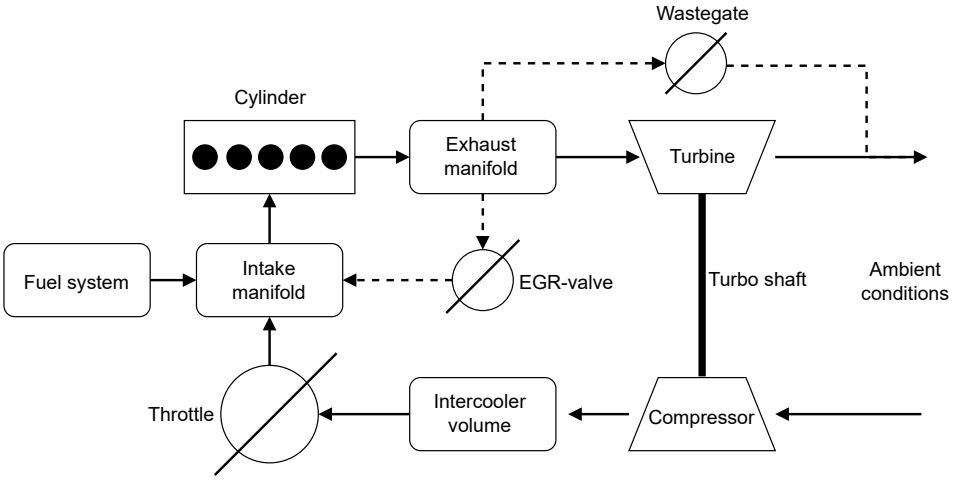

Figure 1.1: *Schematic illustration over the modeled engine. The arrows show the gas flow starting in the lower right corner.*

1.6 Limitations

Due to the complex problem and the time limits of the thesis, some limitations have been necessary. Simplifications in the model can be found in the description for each submodel, here major boundaries of the system will be presented.

- The model in this thesis contains no torque model. Instead the pressure in the intake manifold is used to get information about "available" torque. This is because the torque produced by the engine is strongly connected to the ignition angle and this is not considered in this model.
- The model supposes a perfect fuel controller, always running at $\lambda = 1$.
- The intercooler and EGR-cooler are assumed to be ideal which means they only lower the temperature to the ambient temperature and not change the pressure. Notice that the volume of the coolers give a dynamic effect of the pressure build up.
- The controllers are only parametrized for one operating point.
- The controllers are only tested on the model and not the real engine.

2

State of Art

In this chapter the theory and the State of Art of the subject are introduced. There are two main areas for the thesis, the modeling part and the controller part. Most of the theory for the modeling has been collected from research at Linköping University, and especially Eriksson and Nielsen [5]. The controller part has the root in Wahlström [15] with influence from other sources.

2.1 Modeling

Wahlström and Eriksson [17] have developed a Simulink model for a diesel engine with VGT and EGR [16] and also a control strategy. The model in Wahlströms work is based on research from Linköping University and a model library described in Eriksson [4]. In this paper the submodels and equation are presented and described. The convenience with a model library with submodels are the easiness of doing changes. Adaption to different kind of engines with other configuration are no problem. The submodels can also be more or less complex depending of the situation and the goal with the simulation.

Other sources for information to the thesis have been Heywood [12] and Eriksson and Nielsen [5]. The first one contains the basis of all kind of knowledges regarding combustion engines. The second one also discusses the ground for combustion engines but also give an introduction for different kind of models. Submodels are presented for different parts of the engine, and for a lot of them there are different kinds of complexity depending of which accuracy are sought. Models form Eriksson and Nielsen [5] except from the already existing model from Wahlström and Eriksson [16] diesel model. Modeling the throttle has also been studied in Wahlström and Eriksson [18], but the model from that work is not public and therefore not used.

The engine in this thesis is a spark ignited engine running on compressed

natural gas (CNG). There are some differences between an engine running on gasoline and CNG, which are described in Dyntar et al. [2]. For example there is no need to model wall wetting because of the fuel injected in the system is already gases.

As mentioned before it is common to use EGR to reduce the exhaust temperature, which spare the three-way catalyst, according to Fonsa et al. [7]. There are also some other benefits as decreased temperature during combustion which reduces the likelihood of knocking, [19]. The disadvantage with EGR is reduced volumetric efficiency which decrease the output of the power from the engine. In this thesis the impact of EGR is neglected during the combustion.

2.2 Controller

There is a lot of research in the area of control strategies for combustion engines. In Eriksson and Nielsen [5] a control design is proposed where a wanted pressure in the intake manifold, depending on the requested torque, is the reference signal to the controller. The controller adjust the throttle to give the right response. A boost controller is added to control the wastegate to give a specified pressure ratio over the throttle. This strategy controls the throttle and wastegate to give the requested torque but does not handle the EGR. This type of feedback loops is used in this thesis, after inspiration from Eriksson and Nielsen [5].

Most of the research for heavy duty vehicles are for diesel engines with different control strategies for controlling the gas exchanges with a turbocharger and EGR-valve. For example, Wahlström and Eriksson [17] describe a control strategy for an engine with VGT and EGR. The proposed main feedback loops are that the VGT is controlled by the requested EGR-ratio and the EGR-valve is controlled by the requested λ. The controller is also extended with a non-linear compensator to handle the non-linearities. The analysis chapter from Wahlström and Eriksson [17] is used to analyze the system. The control approach is not tested because of the differences between a SI-engine running with $\lambda = 1$ and a diesel engine that does not.

Another approach described in Friedrich et al. [8] is by using the EGR-valve and the throttle to control the EGR-ratio. The described method uses the EGR-valve as main actuator and the throttle as an auxiliary actuator. If the right EGR-ratio cannot be achieved by opening the EGR-valve the throttle closes to increase the EGR-flow. The EGR-flow depends on the pressure difference between the intake and exhaust manifold and closing the throttle will increase the difference between these. To keep the same pressure in the intake manifold the wastegate needs to be closed so the power from the turbo increases. When the wastegate closes the pressure in the exhaust manifold increases and the pressure drop over the EGR-valve increases. But this will also increases the pump work which gives a higher fuel consumption. Therefore, the throttle is used as a secondary actuator so throttling will be avoided if possible. This technique is note tested in this work but could be of interest for future work.

In Thomas and Sharma [14] one can read of the advantage with model-based

controllers. The comparison is made with look-up tables which need to be calibrated for changes in the engine. If a model based approach is used, changes in the engine can be done directly in the model. This saves a lot of time during calibration. The model-based approached is a well established technique and therefore used in this thesis.

Except from different control strategies for engines, literature about control theory have been studied. For example pole placement and stability from Glad and Ljung [10], relative gain array (RGA) from Glad and Ljung [9] and PID parametrization from Gunnarsson et al. [11]. These different techniques are used during the analysis and for developing the control strategies.

3

Engine Modeling

The modeling part of this thesis has been based on Wahlström and Eriksson [16] diesel model developed at Linköping University. That model represents an engine with VGT and EGR. Most of the submodels are based on physical relations, but to keep the model simple and the complexity low some of the models are black-box models to fit the measurements.

The submodels are mainly divided into two parts, control volumes and flow restrictions. The control volumes describe the dynamics of the engine and regulate how fast the pressure is built up. They describe the pressure in the components given the flow in and out and consist of ordinary differential equations. Examples of the control volumes are the manifolds. The flow restrictions, on the other hand, simulate pressure drop over the components. They describe the flow through the submodels given the surrounding pressures. Examples of flow restrictions are the throttle, the EGR-valve and the wastegate.

Most of the submodels from Wahlström and Eriksson [16] diesel model are used straight off. However, there have been some changes and also some new components like the throttle. An example of a changed submodel is the turbine because of the engine in this thesis has a FGT with wastegate instead of a VGT. All the models are described below, but for more information, theory and motivation the complete models can be found in Wahlström and Eriksson [17] and Eriksson and Nielsen [5].

The main purpose with the model is to capture the dynamic behaviors of the system. The right value in stationary points is less important and will not be the primary focus in this thesis. There will also be more focus of operating modes with boost pressure, which means higher pressure in the intake manifold than the ambient pressure. Using pressure in the intake manifold under ambient pressure does not require any impact of the turbocharger and the wastegate. The control strategy should include all the actuators (throttle, EGR-valve and wastegate) and

therefore operating modes where the turbocharger is needed are selected.

3.1 Method

Since most of the models already exist, the modeling part has been to adjust and parameterize. After that validation for each submodels have been performed and some models have been changed to suit the data better.

3.1.1 Parametrization

To find the parameters three different methods have been used. For linear models Matlabs least square solver has been used and for non-linear problems the function ”lsqcurvefit”. See Mathworks webpage for more details about the functions [13]. The last method was used to find delays and time constants for the dynamics in the actuators. To do this,step responses in the actuators have been analyzed by hand, and dynamic models have been adapted.

3.1.2 Measurements

Four types of measurements are used to find, adapt and validate the model. The first one is stationary measurements over the whole operating area of the engine. During the measurements, mean value measurement points are created for different engine speeds and loads. These are used to parameterize the linear and the non-linear models. These stationary measurements are from a newer engine, that is close to the one modeled in this thesis, but with one difference. The EGR-valves have different sizes and therefore an extra measurement series, over the whole operating area, has been measured for the engine with the right EGR size. This one contains fewer measurements points and not so many measured signals, compared to the measurement series on the newer engine. Due to that, this measurement series is not used to parametrize the whole model. These two stationary measurement series represents series 1 and 2 in Table 3.1.

The second type of measurements are steps in the actuators and measured positions of the valves (throttle, wastegate and EGR). These are used to be able to find the dynamic behaviors for the actuators regarding time delays and time constants. These measurements represent measurement series 3 in Table 3.1.

The third type is measurements during transients with the today’s controller for the throttle, EGR and wastegate. Different steps in the torque request are made at different engine speeds. These measurements are used for two purposes. The first one is to see how changes in the actuators effect the engine. The measured actuators position can be used to see if the model reacts in the same way as the real engine, during transients. The second purpose is to see how fast the today’s regulators work and be able to compare the control designs presented in this thesis. The transients are made for different engine speeds and different loads and represent measurement series 4 in Table 3.1.

Table 3.1: *Measurement series for parametrization and validation of the model.*

Measurement series	Type	Description
1	Stationary	Measured point over whole operating area, wrong EGR-valve.
2	Stationary	Fewer operating points than 1, right EGR-valve.
3	Dynamic	Step in the actuators position on at the time.
4	Dynamic	Short driven cycle with a couple of step response at different engine speeds.
5	Turbo map	From the manufacturer.

The last type of measurements is a turbo map from the manufacturer. This is used to find the parameters for the compressor and the turbine and represents measurement series 5 in Table 3.1.

In Table 3.2 the measured signals for measurement series 1 to 4 is presented. Measurement series 5 differ a bit from the other one and follow the standard for turbo maps.

3.1.3 Matlab solver

To evaluate and simulate the model in Simulink an ordinary differential equation (ODE) solver must be selected. Simulink has some different types with different characteristics. The one used in this thesis is ”ode23tb” which gives good performance versus simulation time. No further investigation has been made to see why, and depending on the problem and the goal with the simulation another solver maybe suits better.

3.2 Control volumes

As mentioned before the control volumes describe the dynamics of the system with ordinary differential equation.

3.2.1 Manifolds

There are two different manifolds: intake and exhaust. The pressure in these (p_{im} and p_{em}) are both described with isothermal models which means no temperature changes in the system. The equations are given by deriving the ideal gas law for the pressure and inserting the mass conversation, which gives

$$\begin{aligned} \frac{d}{dt}p_{im} &= \frac{T_{im}}{V_{im}}\left(R_a W_{th} + R_e W_{egr} + R_f W_f - R_a W_{ei}\right) \\ \frac{d}{dt}p_{em} &= \frac{R_e T_{em}}{V_{em}}\left(W_{eo} - W_t - W_{egr}\right). \end{aligned} \tag{3.1}$$

Table 3.2: *Measured signals for measurement series 1 to 4 in Table 3.1.*

Signal	Description	Measurement series
M_e	Engine torque	1,2,3,4
n_e	Engine speed	1,2,3,4
n_t	Turbo speed	1
p_{amb}	Ambient pressure	1,2,3,4
p_c	Pressure after compressor	1,2,3,4
p_{em}	Exhaust manifold pressure	1,2,3,4
p_{im}	Intake manifold pressure	1,2,3,4
T_{amb}	Ambient temperature	1,2,3,4
T_c	Temperature after compressor	1,2,3,4
T_{em}	Exhaust manifold temperature	1,2,3,4
T_{im}	Intake manifold temperature	1,2,3,4
T_t	Temperature after the turbine	1,2,3,4
u_{th}	Throttle control signal. 0 - closed, 100 - open	1,2,3,4
u_{egr}	EGR control signal. 0 - closed, 100 - open	1,2,3,4
u_{wg}	Wastegate control signal. 0 - open, 100 - closed	1,2,3,4
$\tilde{u}_{th}$	Actual throttle position. 0 - closed, 100 - open	1,2,3,4
$\tilde{u}_{egr}$	Actual EGR-valve position. 0 - closed, 100 - open	1,2,3,4
$\tilde{u}_{wg}$	Actual wastegate position. 0 - open, 100 - closed	3
W_c	Compressor mass flow	1,2,3,4
W_f	Injected fuel mass	1,2,3,4
x_{egr}	EGR fraction	1,2,3,4

The mass flow into the intake manifold comes from the throttle, W_{th}, the EGR-system, W_{egr}, and the injected fuel, W_f. The flow out from the intake manifold is the flow into the cylinder (engine), W_{ei}. For the exhaust manifold is the flow in the mass from the cylinder (engine), W_{eo}, and the flow out is the turbine flow (included the flow through the wastegate), W_t, and the EGR-flow, W_{egr}. The different gas constants for air, R_a, exhausts, R_e and fuel R_f are given. The only parameters that need to be quantified are the volumes in the intake manifold V_{im} and exhaust manifold V_{em}. Observe that no EGR-cooler is modeled and this volume is included in the intake manifold volume. Because of different types of gases in the intake manifold the gas constants are multiplied with respective gas flow.

A simplification, as mentioned before, is that the engine always runs at $\lambda = 1$. This means "perfect" combustion according to the stoichiometric ratio. In the original Wahlström and Eriksson [16] model, the model keep tracks of the fraction of oxygen in the EGR-gases to be able to know the amount of oxygen when combining fresh air with EGR. Because of the simplification, there is no need of these two states of oxygen fraction in the intake and exhaust manifold.

Another simplification is that the temperature is assumed to be constant over the whole operating region in the intake manifold, T_{im}. This assumption requires an ideal intercooler and that the impact of the temperature from the EGR is negligible (the reinstated EGR is much warmer than the fresh air because the EGR-cooler is cooled with engine water). Studying the measurements shows that the temperature only differs around 7 degrees for the different operating modes. Because of this, the impact of different intake manifold temperature has been neglected.

3.2.2 Intercooler volume

The intercooler volume is added because of the new throttle model. The throttle is a restriction like the compressor, therefore a control volume is needed between these two. The intercooler is assumed to be ideal which means that the temperature is constant and the same in the whole volume. For this model the temperature in the intercooler volume is assumed to be the same as the intake manifold ($T_{ic} = T_{im}$). The pressure in the intercooler volume is modeled in the same way as the manifolds, where W_c is the flow from the compressor

$$\frac{d}{dt}p_{ic} = \frac{R_a T_{ic}}{V_{ic}}\left(W_c - W_{th}\right) \tag{3.2}$$

and the only unknown parameter is the volume of the intercooler, V_{ic}.

3.2.3 Fuel system

As mentioned before this paper does not consider any fuel controller and the engine is assumed to run at $\lambda = 1$. The fuel still takes space in the intake manifold and affect the pressure. To consider this a simple model, calculating the amount of fuel according to the amount of air flowing through the throttle, has been

created. The ratio between the fuel and the air should follow the stoichiometric ratio $(A/F)_s$ and the model is

$$W_f = \frac{W_{th}}{(A/F)_s}. \tag{3.3}$$

No unknown parameters are needed to be found. The reason to use the flow through the throttle, W_{th}, instead of the flow into the cylinder, W_{ei}, is that the amount of fuel should only correspond to the amount of fresh air into the cylinder. For example if the EGR-flow is increased the fuel should not be increased to keep the same air-fuel ratio.

3.3 Throttle

The throttle consists of two parts, part one describes the flow through the throttle and part two expresses the dynamics of the actuator. The control signal to the throttle goes from 0 % (closed) to 100 % (open).

3.3.1 Throttle flow

The flow through the throttle is modeled with a throttle model

$$W_{th} = \frac{p_{ic}}{\sqrt{R_a T_{ic}}} A_{th}(\tilde{u}_{th}) \Psi(\Pi_{th}) \tag{3.4}$$

where

$$\Pi_{th} = \frac{p_{im}}{p_{ic}}. \tag{3.5}$$

The effective area as a function of the actual throttle position, $\tilde{u}_{th}$, is modeled with a third-order polynomial.

$$A_{th}(\tilde{u}_{th}) = a_0 + a_1 \tilde{u}_{th} + a_2 \tilde{u}_{th}^2 + a_3 \tilde{u}_{th}^3 \tag{3.6}$$

In Eriksson and Nielsen [5] the Ψ-function is modeled as

$$\Psi(\Pi_{th}) = \sqrt{\frac{2\gamma_a}{\gamma_a - 1} \left(\Pi_{th,lim}^{2/\gamma_a} - \Pi_{th,lim}^{1+1/\gamma_a} \right)} \tag{3.7}$$

where γ_a is the heat capacity ratio for air and

$$\Pi_{th,lim} = \max \left(\Pi_{th}, \left(\frac{2}{\gamma_a + 1} \right)^{\frac{\gamma_a}{\gamma_a - 1}} \right). \tag{3.8}$$

The unknown parameters are the coefficients for the effective area (a_0, a_1, a_2 and a_3). These are quantified by calculating the A_{th} from stationary measurements (measurement series 1 in Table 3.1) with (3.4). After that the calculated A_{th} is used with (3.6) and minimized with the least square method. Figure 3.1 shows the validation of the throttle. In the upper plot the effective area is given as a function of the throttle position. The blue line is the model and the red line

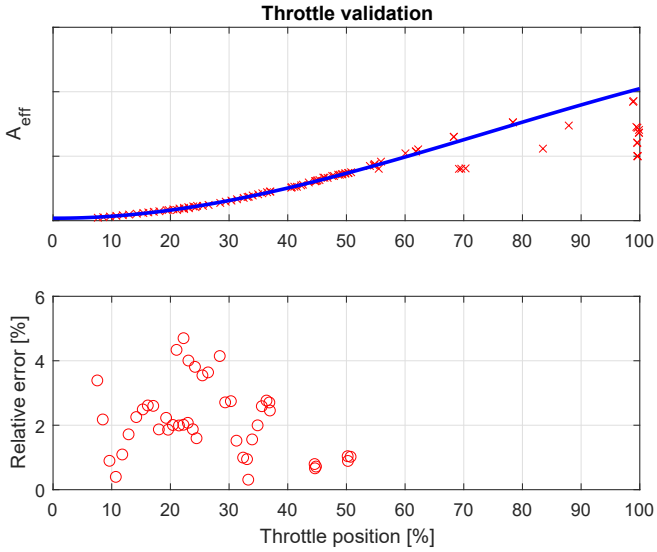

Figure 3.1: *The upper plot shows the model (blue line) of the effective area as a function of the throttle angle and the red marks are the measurements. The lower plot shows the relative error for the measurements. The relative errors are only showed for the points used during the calibration.*

is the measurements. The lower plot shows the relative errors for the measurements that were used.

Only measurements with $\Pi_{th} < 0.9$ were used when quantifying the parameters. This is because of the uncertainty of the measurement. If the difference between p_{im} and p_{ic} is big the impact of errors in measurements is small. If the pressure before and after the throttle on the other hand is close to each other an error in the measurements will affect the pressure ratio a lot. Therefore, only lower pressure ratios are used during parameterization. This can also be seen in Figure 3.1 where the relative errors only are showed for the measurements that are used. For higher throttle positions the effective area differ a lot which is the reason of not using these measurements. Instead the effective area at 100% is compared with the physical area, to give a reasonable value.

3.3.2 Actuator

The actual throttle position, $\tilde{u}_{th}$, is modeled as a function of the control signal to the throttle, u_{th}, with a first order system according to

$$\frac{d}{dt}\tilde{u}_{th} = \frac{1}{\tau_{th}}\left((u_{th} - \tau_{dth}) - \tilde{u}_{th}\right) \tag{3.9}$$

with the unknown parameters: the time constant τ_{th} and the time delay τ_{dth}. To find the parameters, steps in the actuators have been analyzed (measurement

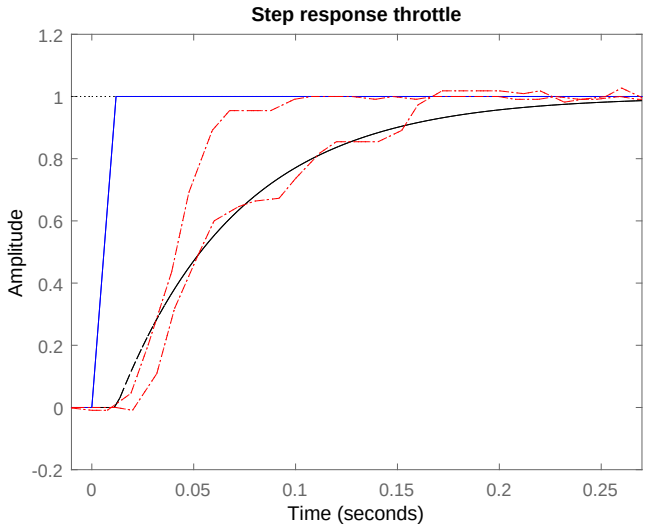

Figure 3.2: *Validation of throttle actuator where the blue line shows the step in the control signal, the red lines shows the measured positions and the black line the shows the adapted system. The steps are normalized.*

series 3 in Table 3.1) by hand and the result is presented in Figure 3.2. The blue line shows the step in the control signal, the red lines shows the measured positions and the black line shows the adapted system. Two different steps have been performed and they are both normalized and start at $t = 0$.

3.4 EGR

The EGR-system is modeled as a throttle and the EGR-cooler is assumed to be ideal and is neglected. An ideal EGR-cooler means that the mass flow from the EGR is cooled to a constant temperature and that the temperature in the whole EGR-cooler is the same. In this case also assumed to be the same as for the intake manifold, T_{im}. The volume of the EGR-cooler is added to the intake manifold volume to receive the right dynamic behaviors.

Like the throttle the EGR-valve is described with two parts, one for the flow and one for the dynamics of the actuator. The model assumes that the pressure in the exhaust manifold is higher than the pressure in the intake manifold ($p_{em} > p_{im}$). If $p_{em} < p_{im}$ the ratio between these is saturated and set to 1, see (3.13).

3.4.1 EGR flow

The EGR flow over the EGR-valve is modeled with a throttle model according to

$$W_{egr} = \frac{A_{egr} p_{em} \Psi_{egr}(\Pi_{egr})}{\sqrt{T_{em} R_e}}. \tag{3.10}$$

where

$$\Pi_{egr} = \frac{p_{em}}{p_{im}}. \tag{3.11}$$

Measurements show that the Ψ_{egr}-function can be calculated as a parabolic function of the pressure ratio over the EGR-valve (see the end of the section for further discussion).

$$\Psi_{egr} = 1 - \left(\frac{1 - \Pi_{eqr}}{1 - \Pi_{eqropt}} - 1 \right)^2 \tag{3.12}$$

with the restrictions

$$\Pi_{egr} = \begin{cases} \Pi_{egropt} & \text{if } \frac{p_{im}}{p_{em}} < \Pi_{egropt} \\ \frac{p_{im}}{p_{em}} & \text{if } \Pi_{egropt} \leq \frac{p_{im}}{p_{em}} \leq 1 \\ 1 & \text{if } 1 < \frac{p_{im}}{p_{em}} \end{cases} \tag{3.13}$$

The effective area, A_{egr}, as a function of the actual EGR-valve position, $\tilde{u}_{egr}$ is

$$A_{egr} = A_{egrmax} f_{egr}(\tilde{u}_{egr}) \tag{3.14}$$

described with a second degree polynomial

$$f_{egr}(\tilde{u}_{egr}) = \begin{cases} c_{egr1} \tilde{u}_{egr}^2 + c_{egr2} \tilde{u}_{egr} + c_{egr3} & \text{if } \tilde{u}_{egr} \leq -\frac{c_{egr2}}{2c_{egr1}} \\ c_{egr3} - \frac{c_{egr2}^2}{4c_{egr1}} & \text{if } \tilde{u}_{egr} > -\frac{c_{egr2}}{2c_{egr1}} \end{cases} \tag{3.15}$$

The unknown parameters are the coefficients in the effective area in (3.15) (c_{egr1}, c_{egr2} and c_{egr3}) and the parameter Π_{egropt} in (3.12). The problem is nonlinear and solved with stationary measurements (measurement series 2 in Table 3.1).

As mentioned above the Ψ_{egr} is modeled as a parabolic function. In the upper plot in Figure 3.3 is the blue line the model and the red marks the measurements for the Ψ_{egr} as a function of Π_{egr}. The measurements suit the data well for higher pressure ratio. But the measurement series contains few measurements which gives big uncertainty, and therefore the parabolic model proposed in Wahlström [15] is tried out even if the model does not suit well in the whole region.

The f_{egr}-function is displayed in the lower plot in Figure 3.3. The blue line in the plot is the model and the red marks the measurements. The function is a second degree polynomial with a maximum value around 16 %. This means that opening up the EGR-valve any more than 16 % would decrease the effective area. In (3.15) is a saturation used (second line in the equation) to keep the same

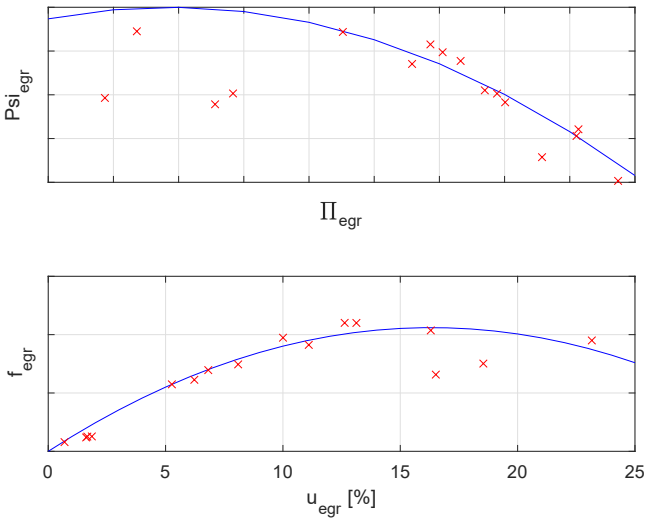

Figure 3.3: *The upper plot shows the Ψ_{egr} as a function of Π_{egr}, the blue line is the model and the red marks the measurements. The lower plot shows the f_{egr} as a function of the EGR-valve position.*

effective area for all the EGR-positions over the value that gives the maximum value.

The parametrization gives strange results. If there is a pressure drop over the EGR-valve and the actuator is open from 16 % to 20 % nothing will happen. Therefore, the parameterization from the origin Wahlström and Eriksson [16] diesel model has been tested. The result can be found in Figure 3.4, along with the results from the parametrization made in this thesis. In the upper plot are the red marks the validation for the parameterization in this thesis and the black marks when using the parametrization from Wahlström. They should both follow the blue line which correspond to that the model and the measurements give the same results. The lower plot shows the relative errors for both the parametrizations.

The parametrization from Wahlström and Eriksson [16] model seems to suit the data well except for four outliers. Even if these give a higher mean error the parametrization from Wahlström and Eriksson [16] is used in the model because the number of available measurements for quantify the parameters for the EGR have been few. The parameterization from Wahlström and Eriksson [16] also gives a saturation around 85 % instead of 16 % for f_{egr} which means that a bigger operating area of the EGR-valve affects the result.

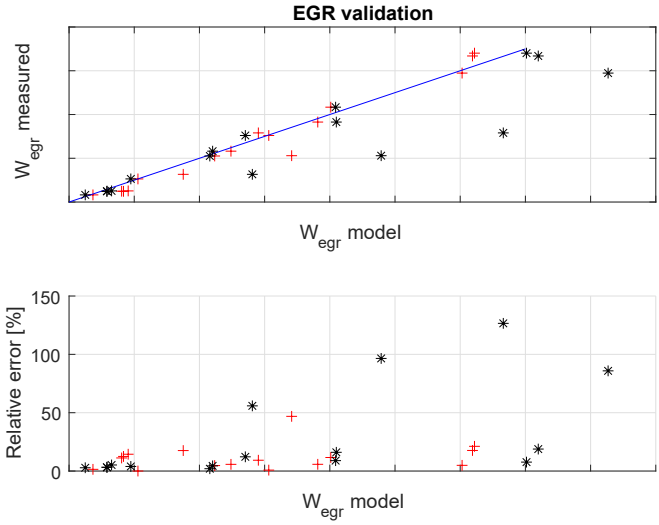

Figure 3.4: *Validation of the EGR-valve. The upper plot shows the model vs. measurement and the result should follow the blue line (model and measurements give the same value then). The parametrization performed in this thesis are the red marks and the parametrization from the Wahlström and Eriksson [16] the black marks. The lower plot show the relative errors.*

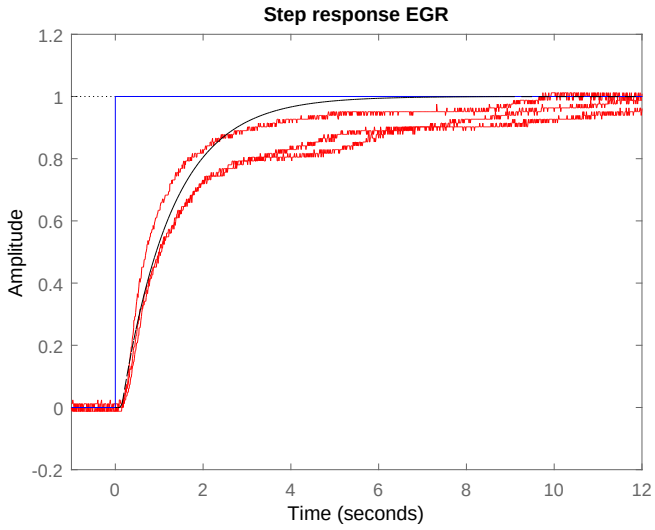

Figure 3.5: *Validation of EGR actuator where the blue line shows the step in the control signal, the red line shows the measured position and the black line the shows the adapted system for three different steps. The steps are normalized.*

3.4.2 Actuator

The dynamic behavior for the EGR actuator has been decided in the same way as for the throttle actuator. Steps in the control signal, u_{egr}, both up and down, have been analyzed by hand and the dynamic behavior is described with a first order system

$$\frac{d}{dt}\tilde{u}_{egr} = \frac{1}{\tau_{egr}}\left(\left(u_{egr} - \tau_{degr}\right) - \tilde{u}_{egr}\right) \tag{3.16}$$

with the unknown parameters: the time constant, τ_{egr}, and the time delay, τ_{degr}. The validation can be found in Figure 3.5 where the blue line shows the step in the control signal, the red lines the measured positions and the black line the adapted system. The measurements are from measurement series 3 in Table 3.1. If one analyzes the result more carefully one can see that the steps at first reach around 90 % of the final value. And after eight seconds the actuator increases to the final value. A more advanced model suits the dynamics better and may increase the accuracy of the model result. This is not investigated in this thesis, due to time limitations. More measurements, for different steps in the control signal, are needed to improve the model.

3.5 Cylinder

The model in this master thesis contains no torque model. Instead the pressure in the intake manifold is used as a performance variable. The motivation of this can be found in Section 1.6. The cylinder model contains a model of the flow through the cylinder and a temperature model for the exhaust gases.

3.5.1 Flow through cylinder

The flow into the cylinder, W_{ei}, is described by

$$W_{ei} = \frac{\eta_{vol} p_{im} n_e V_d}{120 R_a T_{im}} \tag{3.17}$$

which, except the intake manifold pressure, p_{im}, and the engine speed, n_e, depends of the volumetric efficiency η_{vol}. The rest of the terms are constant in the model: the displacement volume for the engine, V_d and the gas constant for air, R_a. The number 120 comes from that n_e is in RPM (divide by 60 to get SI-units), and the engine is a four-stroke-engine (only receives air every other revolution, divide by two). The volumetric efficiency can be described as a function of p_{im} and n_e.

$$\eta_{vol} = c_{vol1}\sqrt{p_{im}} + c_{vol2}\sqrt{n_e} + c_{vol3} \tag{3.18}$$

The three unknown parameters c_{vol1}, c_{vol2} and c_{vol3} can be found with stationary measurements (measurement series 1 in Table 3.1 are used). For stationary points are $W_{ei} = W_{th} + W_{egr} + W_f$ and $W_{th} + W_{egr} = W_c/(1 - x_{egr})$, which are measured along with W_f. The η_{vol} can be calculated from the measurements with (3.17) and the parameters can be quantified with the least square method.

The validation of the volumetric efficiency is presented in Figure3.6. The upper plot shows the modeled values on the x-axis and the measured values on the y-axis. The red marks are the measured points and should follow the blue line. The lower plot shows the relative errors for the measurements. For higher efficiency the measurements seem to suit well, but for lower efficiency the model constantly gives to high values. For better results the physical process has to been analyzed and the impact of the residual gases. For more information see for example Eriksson and Nielsen [5]. For this purpose the results are good enough, since the most interesting points are with boost pressure which result in high p_{im} and therefore higher η_{vol} according to (3.18).

3.5.2 Temperature model

The temperature model describes the temperature of the exhaust gases out from the cylinder, which for this model is the same as the temperature in the exhaust manifold. From the stationary measurements two sensor positions have been available, one next to the exhaust valve and one before the turbine. The one used in this thesis is the position closest to the turbine. The temperature affects the energy in the gases and there is of interest to has as correct knowledge about the energy in the exhaust gas as possible. This will has impact of the power produced

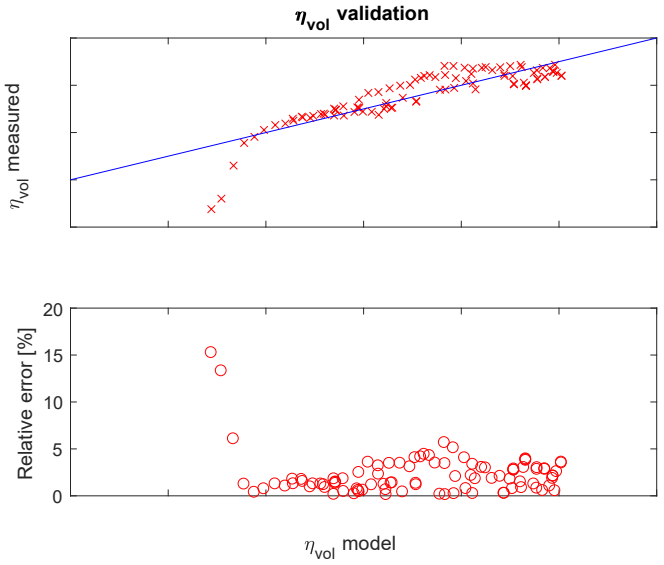

Figure 3.6: *Validation of the volumetric efficiency, in the upper plot are the red marks the measurements and the blue line the model. The lower plot shows the relative errors.*

by the turbine and therefore is the position closest to the turbine selected. In Eriksson [3] is the exhaust temperature, T_{em}, investigated as a function of the mass flow out from the cylinder, W_{eo}. The article presented good results for an SI-enginge that run at maximum break torque (MBT) with $\lambda = 1$.

$$T_{em} = T_{vec1} + T_{vec2}\sqrt{W_{eo}} \tag{3.19}$$

The two unknown parameters T_{vec1} and T_{vec2} can be found with stationary measurements (measurement series 1 in Table 3.1). In the stationary case $W_{eo} = W_{ei} = W_{th} + W_{egr} + W_f$ and the flow can be calculated from the measurements in the same way as in Section 3.5.1. From measured T_{em} and calculated W_{eo} the coefficients can be quantified with the least-square method and (3.19). The validation of the model can be found in Figure 3.7 where the upper plot shows the measurements as red marks and the model as a blue line and the lower plot shows the relative errors. The model suits well for higher mass flows, but for lower mass flows there are some more dependencies, probably of the engine speed. These are not investigated in this theses and the model is considered to be good enough.

A more advanced model could be preferred to capture the impact of lower exhaust temperature if EGR is used. As mentioned in Section 1.1 EGR is used to lower the temperature out of the cylinder and therefore a model taking into account the EGR-ratio would be interest to to be able predict the temperature in the exhaust manifold better. One reason to improve the model is to capture the dynamic behavior of the temperature during transients. This is of interest because

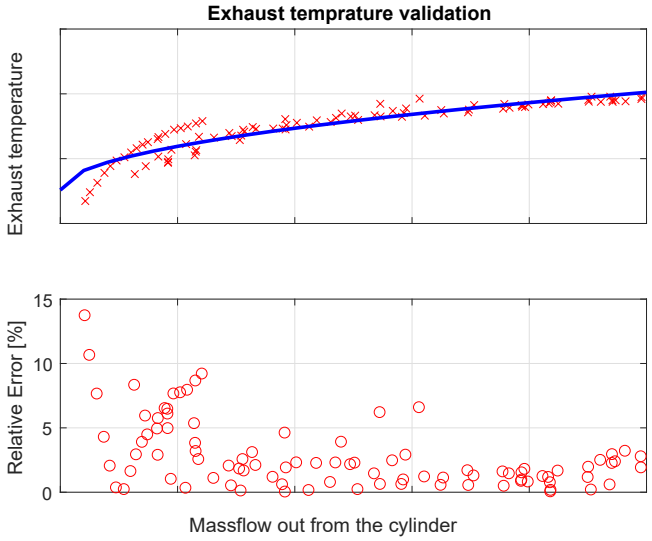

Figure 3.7: *Validation of the exhaust temperature, in the upper plot the red marks are the measurements and the blue line the model. The lower plot shows the relative errors.*

the turbine is highly dependent on the energy from the gases which is affected by the temperature. The temperature is also affected of the ignition timing, [5], and an extension of the model as a function of that could be of interest.

3.6 Turbocharger

The model for the turbocharger is divided into six parts: the turbo shaft, the compressor efficiency, the compressor mass flow, the turbine efficiency, the turbine mass flow and the wastegate. Most of these models are not physical but suit the data well. The parametrization is made with data from a turbo map (measurement series 5 in Table 3.1). The original Wahlström and Eriksson [16] diesel model contains a VGT instead of a FGT with wastegate. Therefore, the turbine massflow model is changed and a wastegate model is added. The other submodels are described in Wahlström [15].

3.6.1 Turbo shaft

The turbo shaft describes the dynamic for the turbo as a function of changes in turbo speeds, ω_t. It is a first order system with the power consumed by the compressor, P_c, and the power delivered by the turbine, P_t. There is also some

energy losses in the shaft, η_m. The model is

$$\frac{d}{dt}\omega_t = \frac{P_t\eta_m - P_c}{J_{tc}\omega_t} \tag{3.20}$$

where the only unknown parameter is the inertia for the turbo charger, J_{tc}. The parameter is estimated with dynamic measurements to get the right behavior during transients (measurement series 3 in Table 3.1). The initial inertia was first given from Scania and after that tuned to suit the measurements well.

One way to extend the model is to add a friction term. In Eriksson and Nielsen [5] one can read that this is especially good for lower turbo speeds. This is not tested in this thesis due to time limits.

3.6.2 Compressor efficiency

The compressor contains flow friction losses (see [5] for more information) and due to that all the energy that is delivered from the shaft is not used to force the air into the intercooler volume. The power consumed by the compressor can be described as

$$P_c = \frac{P_{c,s}}{\eta_c} = \frac{W_c c_{pa} T_{amb}}{\eta_c}\left(\Pi_c^{1-1/\gamma_a} - 1\right) \tag{3.21}$$

where $P_{c,s}$ is the power from the isentropic process. To calculate the consumed power the efficiency, η_c, has to be modeled. To do this the efficiency is studied as a function of the mass flow through the compressor, W_c and the pressure ratio, $\Pi_c = p_{ic}/p_{amb}$. Figure 3.8 shows that the efficiency can be described as ellipses with non-linear transformations on the axis for the pressure ratio.

$$\eta_c = \eta_{c,max} - X^T Q_c X \tag{3.22}$$

where X is a vector which contains the inputs

$$X = \begin{bmatrix} W_c - W_{c,opt} \\ \pi_c - \pi_{c,opt} \end{bmatrix} \tag{3.23}$$

and π_c is a non-linear transformation of Π_c according to

$$\pi_c = (\Pi_c - 1)^{c_\pi}. \tag{3.24}$$

Q_c is a symmetric positive definite matrix with three parameters

$$Q_c = \begin{bmatrix} Q_{11} & Q_{12} \\ Q_{12} & Q_{22} \end{bmatrix} \tag{3.25}$$

The unknown parameters in the model are $\eta_{c,max}$ in (3.22), $W_{c,opt}$ and $\pi_{c,opt}$ in (3.23), c_π in (3.24), and Q_{11}, Q_{12} and Q_{22} in (3.25). The problem is non-linear and the parameters are optimized with ”lsqcurvefit”. The validation is presented in Figure 3.8 with compressor mass flow on the x-axis and the pressure ratio on the y-axis. The values of the efficiency are presented with different types of marks. In the contour plot the measured data is the red marks and the calculated limits the lines. The plotted lines are the lower limits for the respective region.

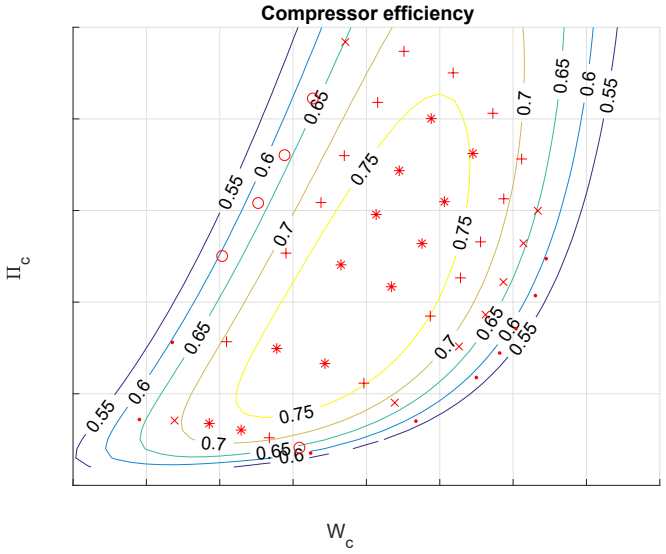

Figure 3.8: *Validation of the compressor efficiency, the red marks are the measured points from the turbo map and the lines represent the model. The marks for the measurements represent . = 0.55-0.60, o = 0.60-0.65, x = 0.65-0.70, + = 0.70-0.75 and * > 0.75.*

3.6.3 Compressor mass flow

To model the compressor mass flow two dimensionless variables are used. The first one is the energy transfer coefficient:

$$\Psi_c = \frac{2c_{pa}T_{amb}\left(\Pi_c^{1-1/\gamma_a} - 1\right)}{R_c^2\omega_t^2} \tag{3.26}$$

with the compressor radius, R_c, and the other one is the volumetric flow coefficient

$$\Phi_c = \sqrt{\max\left(0, \frac{1 - c_{\Psi 1}(\Psi_c - c_{\Psi 2})^2}{c_{\Phi 1}}\right)} + c_{\Phi 2}. \tag{3.27}$$

The relation between these two variables can be described by a part of ellipse according to

$$c_{\Psi 1}(\omega_t)\left(\Psi_c - c_{\Psi 2}\right)^2 + c_{\Phi 1}(\omega_t)\left(\Phi_c - c_{\Phi 2}\right)^2 = 1 \tag{3.28}$$

where the two variables $c_{\Psi 1}$ and $c_{\Phi 1}$ are modeled as polynomial functions of the turbo speed, ω_t.

$$c_{\Psi 1}(\omega_t) = c_{\omega\Psi 1}\omega_t^2 + c_{\omega\Psi 2}\omega_t + c_{\omega\Psi 3} \tag{3.29}$$

$$c_{\Phi 1}(\omega_t) = c_{\omega\Phi 1}\omega_t^2 + c_{\omega\Phi 2}\omega_t + c_{\omega\Phi 3} \tag{3.30}$$

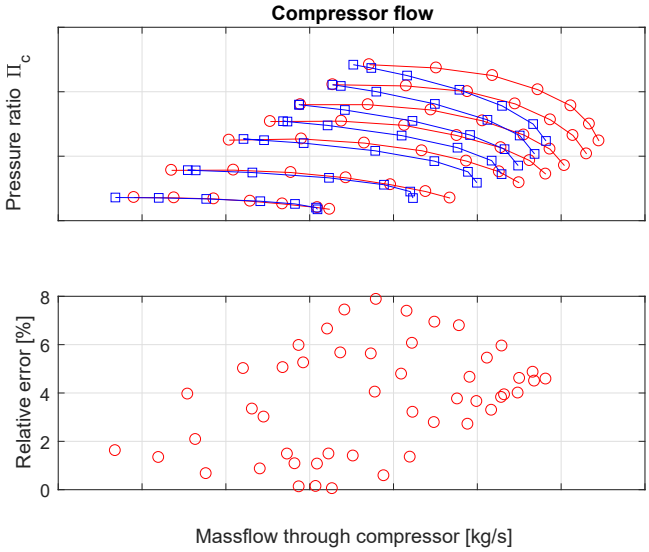

Figure 3.9: *Validation of the compressor flow, in the upper plot the blue lines are the measured data from the turbo map and the red lines are the model. The different lines represent different turbo speeds. The lower plot shows the relative errors for respective measurement.*

The compressor mass flow is then

$$W_c = \frac{p_{amb}\pi R_c^3 \omega_t}{R_a T_{amb}} \Phi_c. \tag{3.31}$$

The unknown parameters for the compressor efficiency are $c_{\Psi 2}$ and $c_{\Phi 2}$ in (3.27), $c_{\omega\Psi 1}$, $c_{\omega\Psi 2}$ and $c_{\omega\Psi 3}$ in (3.29) and $c_{\omega\Phi 1}$, $c_{\omega\Phi 2}$ and $c_{\omega\Phi 3}$ in (3.30). This problem is non-linear and the parameters can be optimized with ”lsqcurevfit”. The validation of the model can be found in Figure 3.9, where the measured data from the turbo map are the blue lines and the calculated data are the red ones. The plot shows the pressure ratio as a function of the mass flow for different turbo speeds. The lower plot shows the relative errors for the measurements.

3.6.4 Turbine efficiency

The turbine efficiency can be described as the ratio between the power delivered to the shaft and the power from the isentropic process. There is also some losses in the shaft from the turbine to the compressor. If one includes these losses, the efficiency from the turbine to the compressor is called η_{tm}. This efficiency is the ratio between the power from the isentropic process in the turbine, $P_{t,s}$, and the

power consumed by the compressor, P_c.

$$\eta_{tm} = \frac{P_c}{P_{t,s}} = \frac{W_c c_{pa}(T_c - T_{amb})}{W_t c_{pe} T_{em}\left(1 - \Pi_t^{1-1/\gamma_e}\right)} \tag{3.32}$$

From (3.20) one can see that $P_t \eta_{tm} = P_c$ at steady state. This together with (3.32) gives

$$P_t \eta_m = \eta_{tm} P_{t,s} = \eta_{tm} W_t c_{pe} T_{em}\left(1 - \Pi_t^{1-1/\gamma_e}\right). \tag{3.33}$$

The ratio between the speed of the blades edge and the speed of the air is called the blade speed ratio (BSR) and is given by:

$$\text{BSR} = \frac{R_t \omega_t}{\sqrt{2 c_{pe} T_{em}\left(1 - \Pi_t^{1-1/\gamma_e}\right)}} \tag{3.34}$$

A common choice is to use a quadratic function for the efficiency in BSR [5]

$$\eta_{tm} = \eta_{tm,max}\left(1 - \frac{\text{BSR} - \text{BSR}_{opt}}{BSR_{opt}}\right)^2 \tag{3.35}$$

where measurements show that both $\eta_{tm,max}$ and BSR_{opt} depends on the turbo speed ω_t.

$$\eta_{tm,max} = \eta_{tm,vec1} + \eta_{tm,vec2} \cdot \omega_t \tag{3.36}$$

$$\text{BSR}_{opt} = BSR_{vec1} + BSR_{vec2} \cdot \omega_t \tag{3.37}$$

The unknown parameters are the two coefficients that describe the BSR_{opt} in (3.37) and the two coefficients in (3.36) that describe $\eta_{tm,max}$. The problem is nonlinear and solved with ”lscurevfit” and measurements from measurement series 5 in Table 3.1.

3.6.5 Turbine mass flow

The mass flow through the turbine, W_t, has been changed from the Wahlström and Eriksson [16] model. This is because the original model simulates a VGT and the engine in this thesis has a FGT. The model can be found in Eriksson and Nielsen [5] and is a simple function of the pressure ratio over the turbine, $\Pi_t = p_{amb}/p_{em}$, corrected with the temperature and pressure in the exhaust manifold.

$$W_{t,co} = k_0 \sqrt{1 - \Pi_t^{-k_1}} \tag{3.38}$$

where

$$W_t = \frac{p_{em}}{\sqrt{T_{em}}} W_{t,co} \tag{3.39}$$

The unknown parameters to be quantified are k_0 and k_1 in (3.38). The problem is linear and solved with the least square method and measurements from measurement series 5 in Table 3.1. The result can be found in Figure 3.11 where the

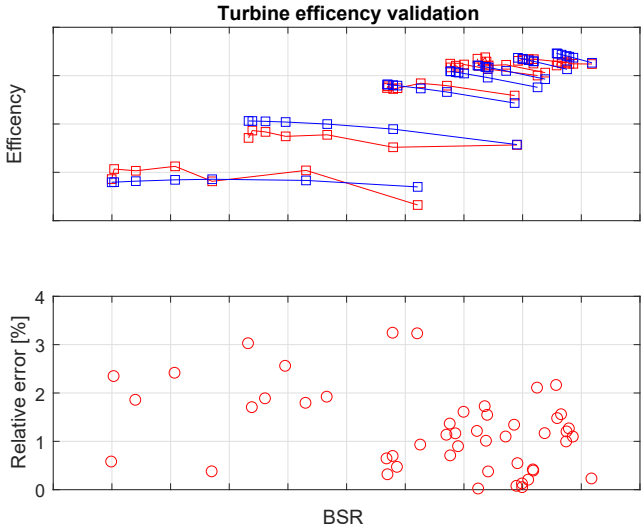

Figure 3.10: *Validation of the turbine efficiency for the measured points in the turbo map. In the upper plot the red lines represent the measurements and the blue lines the model. The different lines represent different turbo speeds. The lower plot shows the relative error.*

corrected turbine flow is plotted as a function of the pressure ratio for the given data from the turbo map. The blues line are the measurements and the red lines are the modeled values. The different lines represent different turbo speeds.

3.6.6 Wastegate

Like the throttle and EGR-valve, the wastegate has one model for the flow and one for the dynamics of the actuator. Notice that opposed to the EGR and throttle, 0 % is fully open and 100 % is closed.

Wastegate flow

The flow through the wastegate, W_{wg}, is modeled with a throttle equation according to

$$W_{wg} = \frac{p_{em}}{\sqrt{R_e T_{em}}} A_{wg}(\tilde{u}_{wg}) \Psi(\Pi_{wg}) \tag{3.40}$$

where

$$\Pi_{wg} = \frac{p_{amb}}{p_{em}}. \tag{3.41}$$

The upper plot in Figure 3.12 shows that from the measurements (red marks) a linear model is a good approximation of the effective area as a function of the

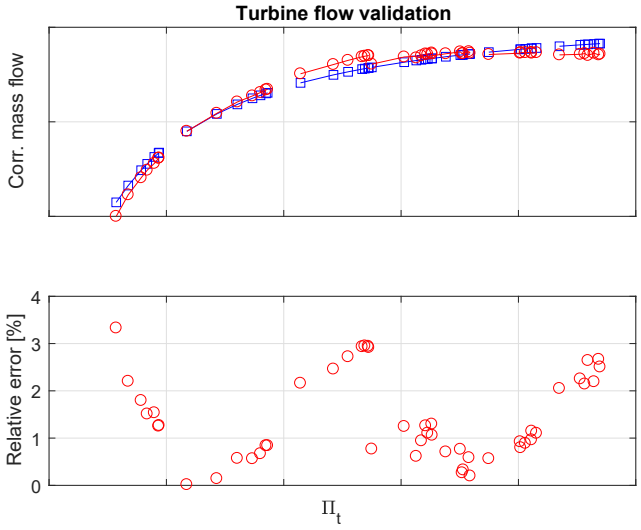

Figure 3.11: *Validation of the turbine flow, in the upper plot the red lines are the measurements and the blue line represent the model. The y-label shows the corrected mass flow, see (3.39). The lower plot shows the relative errors.*

actual wastegate position, $\tilde{u}_{wg}$.

$$A_{wg}(\tilde{u}_{wg}) = a_0 + a_1 \tilde{u}_{wg} \tag{3.42}$$

In the end the Ψ-function is modeled in the same way as for the throttle

$$\Psi(\Pi_{wg}) = \sqrt{\frac{2\gamma_e}{\gamma_e - 1}\left(\Pi_{wg,lim}^{2/\gamma_e} - \Pi_{wg,lim}^{1+1/\gamma_e}\right)} \tag{3.43}$$

where

$$\Pi_{wg,lim} = \max\left(\Pi_{wg}, \left(\frac{2}{\gamma_e + 1}\right)^{\frac{\gamma_e}{\gamma_e - 1}}\right). \tag{3.44}$$

The unknown parameters are a_0 and a_1 in the effective area (3.42). To be able to optimize these parameters the flow through the wastegate must be calculated from the measurements. For stationary measurements (measurement series 1 in Table 3.1) the flow through the wastegate is calculated as $W_{wg} = W_c + W_f - W_t$ and the flow through the turbine is estimated with the turbine flow in Section 3.6.5. The other signals are measured. The problem becomes linear and the optimization is solved with the least square method.

The validation of the model is presented in Figure 3.12. The plot shows that for around 50 % closed wastegate the effective area is zero and there is no flow through the wastegate. This is not correct due to the physical component. However, the uncertainty of the calculated W_{wg} and the actual wastegate position,

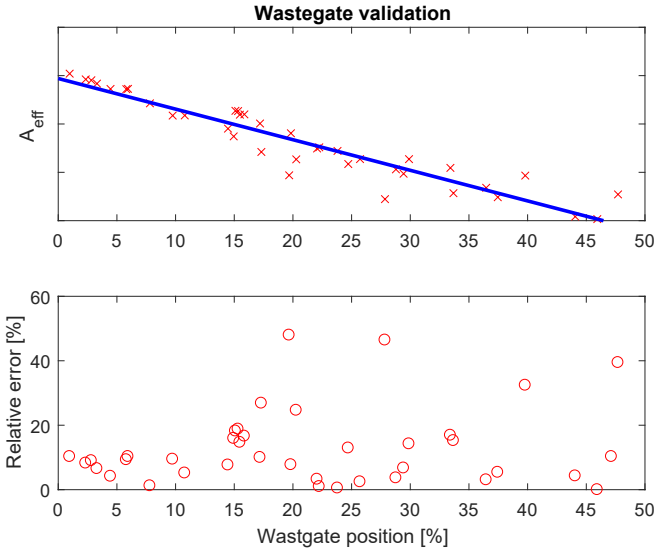

Figure 3.12: *Validation of the wastegate. The upper plot shows the effective area as a function of the wastegate position. The red marks are the measurements and the blue line the model. The lower plot shows the relative errors.*

$\tilde{u}_{wg}$, makes it hard to do a better model. The model will therefore only react on control signals from 0 % to 50 %. The high uncertainty in $\tilde{u}_{wg}$ depends on that there is no feedback for the wastegate position.

Wastegate actuator

The wastegate actuator is modeled as a first order system

$$\frac{d}{dt}\tilde{u}_{wg} = \frac{1}{\tau_{wg}}\left(u_{wg} - \tilde{u}_{wg}\right) \tag{3.45}$$

with the unknown time constant τ_{wg}. The step response in the control signal u_{wg} is analyzed (measurement series 3 in Table 3.1) and the normalized results are plotted in Figure 3.13. The red lines are the measurements, the blue line the step in the control signal and the black line the adapted model. The plot shows five different steps both up and down from different positions.

It is hard to see where the control signal change, and therefore it is not possible to be able to add a time delay to the model. The time constant τ_{wg} is on the other hand so big that a short delay would not affect the result substantially.

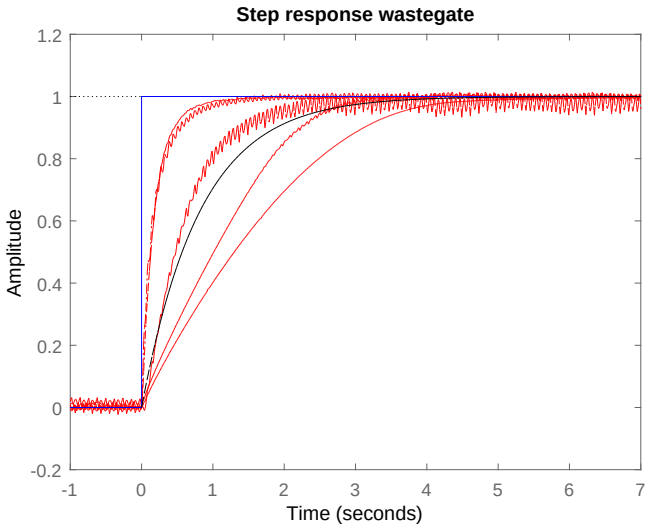

Figure 3.13: *Validation of wastegate actuator where the blue line shows the step in the control signal, the red lines the measured positions and the black line the adapted system, for five different steps. The steps are normalized.*

3.7 Result

In Table 3.3 one can find the mean and maximum relative errors of each submodel. The relative errors are calculated as

$$\text{relative error}(i) = \frac{|y_{meas,stat}(i) - y_{mod,stat}(i)|}{\frac{1}{N}\Sigma_{i=1}^{N} y_{meas,stat}(i)}. \tag{3.46}$$

Only the measurements used for the parameterization are included in the table. For example has the throttle only measurements with a pressure ratio below 0.9. See each submodel for information which measurements that are used.

Table 3.3: *The mean and maximum relative errors of the submodels are presented in the table.*

Model	Mean relative error	Maximum relative error
Throttle flow	2.11 %	4.68 %
EGR own parameters	11.94 %	45.77 %
EGR [16] parameters	23.832 %	79.69 %
Volumetric efficiency	2.21 %	15.24 %
Exhaust temperature	2.18 %	10.92 %
Compressor flow	3.71 %	7.87 %
Compressor efficiency	1.29 %	7.59 %
Turbine flow	1.42 %	3.33 %
Turbine efficiency	1.22 %	3.24 %
Wastegate flow	12.84 %	47.95 %

4

System Analysis

This chapter contains an analysis of the system. The first section shows a validation of the model compared to measured data from the real engine. The second section contains different types of analysis over the whole operating area for the engine.

4.1 Model validation

From measurement series number 4 in Table 3.1 a couple of steps in torque request are made at different engine speeds. The actual positions for the three actuators (u_{th}, u_{wg} and u_{egr}) were measured and set as input to the model to see how well the model follow the real engine. The result for one step is presented in Figure 4.1. The two left plots show the measured (red line) and the modeled (blue line) values for the intake manifold pressure and EGR-ratio. The right plot shows the measured signals for the engine speed and the torque to give information which operating point the engine worked within.

The intake manifold pressure rise above for the model and gets higher than the measured values. When studying the signals in the model, there seem to be some problem with the turbo model. The turbo spins fast and reach a high turbo speed. No measurements with turbo speeds during transients are available and therefore it is hard to know if the behavior of the turbo is right.

If one neglect the stationary errors the dynamic behaviors is similar which is the priority in this thesis. The rise time is the same and they capture the same dynamics. For the EGR-ratio is the stationary values more close and the dynamic behaviors are similar. The reason why the EGR-ratio gives reasonable value while the pressure in the intake manifold is to high is because the other pressure and flow in the engine also is much higher than the measured once.

The validation has been performed in more operating modes for other torque

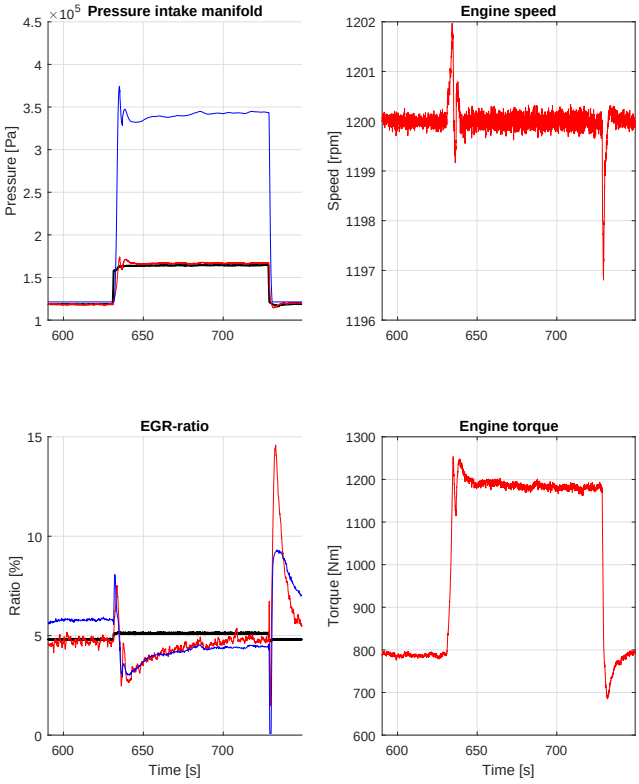

Figure 4.1: *Validation of the model. The blue lines show the modeled values, the red lines the measured once and the black lines the reference values. The left plots are for validation and the right plots to show the operating area of the engine.*

requests and engine speeds. The behavior is similar in these points, with to high pressures but with the right dynamic behaviors. And therefore the model will be useful for this thesis and is assumed to be good enough for the task.

4.2 Mapping of the system properties

Mapping of the system properties show how the characteristics change for the different operating modes of the engine. To do the mapping the system has been linearized at steady state for the whole operating area. The linearized models have been tested with step response and the relative gain array (RGA) has been calculated for $\omega = 0$, which means stationary. The choice of $\omega = 0$ is to see the

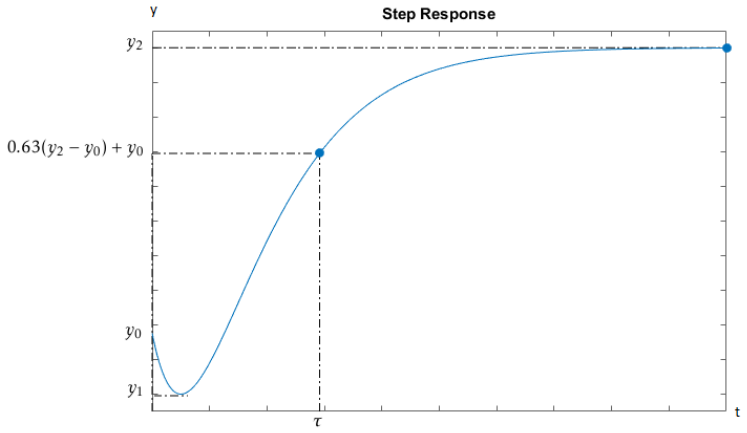

Figure 4.2: *A step response with an initial value y_0, final value y_2, a non-minimum phase behavior with an undershoot y_1 and a response time τ*

Table 4.1: *Actuator positions used to linearize the model for n_e = 1000, 1500 and 2000 rpm.*

Actuator	Position [%]
u_{th}	0, 10, 20, 30, 40, 50, 60, 70, 80, 90, 100
u_{egr}	0, 3, 6, 9, 12, 15, 18, 21, 24, 27, 30
u_{wg}	0, 10, 20, 30, 40, 50

effect of the cross connections at stationary conditions and possible instability, see [9] for more information.

The notation "channel" used in this section means the result for a specific actuator (input of the system) to a specific performance variable (output of the system). The inputs analyzed in this section are the control signals to the three actuators (u_{th}, u_{wg} and u_{egr}) and the outputs are the pressure in the intake manifold (p_{im}) and the EGR-ratio in the intake manifold (x_{egr}).

Figure 4.2 shows a typical step response for a linearized model with an initial value y_0, final value y_2, a non-minimum phase behavior with an undershoot y_1 and a response time τ. Step responses have been made for the linearized models in the whole operating area. The linearization has been made by setting the actuators to a constant value and let the system reach steady state and for this point linearize the system. This has been done for the actuator positions in table 4.1 and n_e = 1000, 1500 and 2000 rpm.

The actual values in the contour plots in Section 4.2.1 to 4.2.3 are of minor interest because they show the response for a unit step in the respective actuator position. This would correlate from fully closed to fully open for an actuator since the range of the actuators is 0 to 1 (or 0 % to 100 %). However, the value

can be of interest relative each other because they show how big impact each channel have for different operating modes.

Section 4.2.1 to 4.2.4 describe the DC-gain, non-minimum phase behaviors, response time and RGA for each actuator (u_{th}, u_{egr} and u_{wg}) to the two performance variables p_{im} and x_{egr}. In this section only one plot for each subsection is presented to show the principle. The plots for the whole operating area can be found in Appendix A. Notice that the plots cover the whole operating area and have combinations of actuator positions that are not possible operating modes for the real engine.

4.2.1 DC-gain

The DC-gain shows the static gain at the linearized point for a unit step in the actuator position. From Figure 4.2 the contour plots for the DC-gain show $(y_2 - y_0)$/step size, which is the gain for a step in the actuator. In Figure 4.3 one of the contour plots is presented for $n_e = 1000$, $u_{wg} = 40\%$ for a step in the wastegate actuator and how it affects the EGR-ratio. The values are not as important as the sign. For example if the engine run with $u_{th} = 50\%$ and $u_{egr} = 15\%$ and the given engine speed and wastegate position, a positive step with the wastegate actuator would give lower EGR-ratio (stationary). This is due to the negative values in the middle of the plot. If the step instead is performed with $u_{th} = 20\%$ the EGR-ratio would increase. This gives a sign reversal where the same step in the wastegate position could either increase or decrease the EGR-ratio.

From a control perspective this is important to consider when designing a feedback loop. The contour plots A.1 to A.5 show that the throttle and the wastegate have positive gain for the entire operating area to the output p_{im}. Opening the throttle will never decrease the pressure in the intake manifold because there is always a pressure drop over the throttle. The model has a saturation that always give $p_{im} < p_{ic}$. If the wastegate is closed the p_{im} will also always increase. Closing the wastegate will increases the power from the turbo which increases the boost pressure and also the pressure in the intake manifold.

For x_{egr} Figure A.5 shows positive gain from u_{egr} in the whole operating area. The throttle has negative DC-gain to the EGR-ratio according to Figure A.4 which could be of interest if the EGR-valve could not deliver enough EGR because of the low pressure drop between the intake and exhaust manifold. The reason is if the throttle opens up the flow of fresh air increases. The ratio between the EGR-flow and the fresh air decreases which means that the EGR-ratio decreases. One way to increases the EGR is therefore to close the throttle.

Another way is to close the wastegate. Due to Figure A.6 closing the wastegate increases the EGR-ratio in almost the whole operating area. The reason is that the pressure in the exhaust manifold increase which increases the pressure drop over the EGR-valve. A higher pressure drop give a higher flow according to (3.10). But closing the wastegate will also increases the boost pressure and therefore the fresh air into the intake manifold. The plot still shows that for almost the whole operating area the ratio between increasing EGR-flow and increased flow of fresh air, the EGR-flow is bigger.

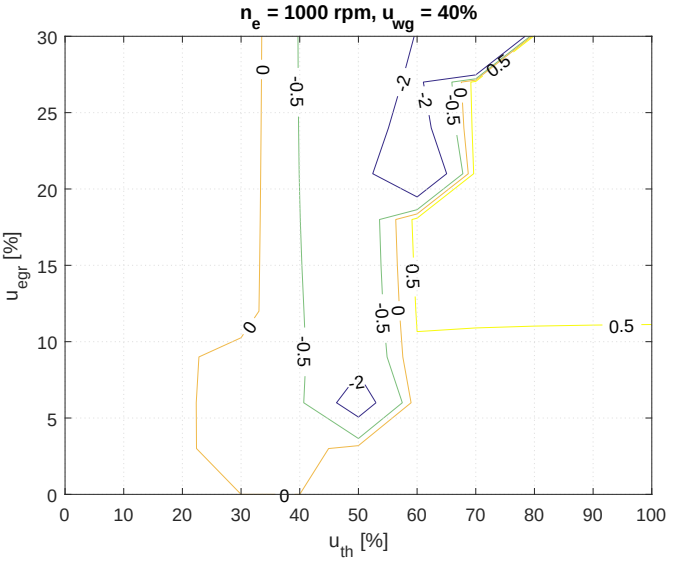

Figure 4.3: *Contour plot of the DC-gain for the channel u_{wg} to x_{egr} for $n_e = 1000$ and $u_{wg} = 40\%$. The values are the gain for a unit step.*

If the throttle or the wastegate is used to control the EGR-ratio both of them need to be included. Otherwise the pressure in the intake manifold will be changed. Opening the throttle will require to opening the wastegate to keep the same p_{im} level. Closing the wastegate will require closing the throttle as well, for same p_{im}.

4.2.2 Non-minimum phase behaviors

Non-minimum phase behaviors are also of interest from a controller design point of view. Especially when there is non-minimum phase behavior in some operating area and not in other. From Figure 4.2 the contour plots in this section show $y_0 - y_1$ for a unit step for the actuators. This correlates to the undershoot of the system and shows the non-minimum phase behaviors. Figure 4.4 shows a similar plot as for the DC-gain section. The figure shows steps from wastegate to EGR-ratio at the operating point $n_e = 1500$ and $u_{wg} = 30\%$. There is a region with undershoots which means that from wastegate to EGR-ratio non-minimum phase behaviors exist. This is because when the wastegate closes the EGR-ratio increases initial because of higher exhaust manifold pressure. The pressure drop over the EGR-valve increases which increases the EGR-flow. But after stabilization the turbo speed increases and deliver more boost. The intake manifold pressure also increases and decreases the EGR-ratio. In the region with no undershoots, a step in the wastegate increases the EGR-ratio stationary according to the corresponding DC-plot, Figure A.6.

Figure A.7 and A.9 show the channels from throttle and wastegate (u_{th} and

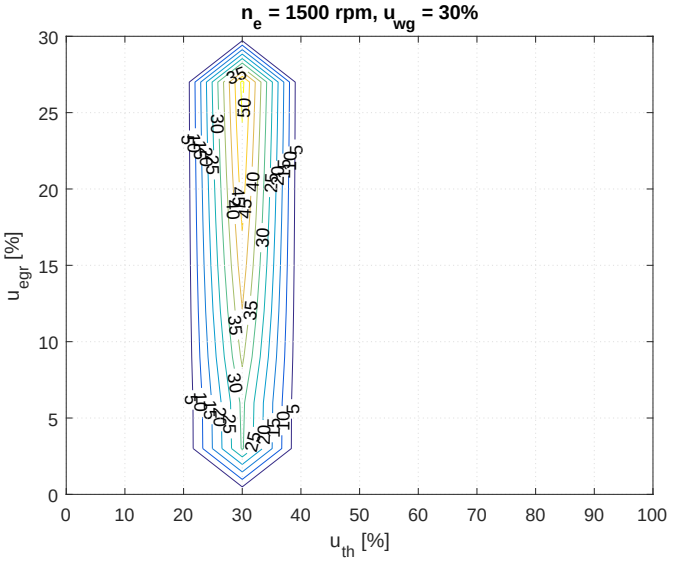

Figure 4.4: *Contour plot of the non-minimum phase behavior for the channel u_{wg} to x_{egr} for $n_e = 1500$ and $u_{wg} = 30\%$. The seen values are the percentage undershoots relative the final value.*

u_{egr}) to the pressure in the intake manifold (p_{im}). Both have a small operating area for high engine speeds where some non-minimum phase behaviors occur. This may needs to be considered if these channels are used in feedback loops. But the region are small and engine speeds around 2000 rpm are high and not normally the operating modes.

For the channel EGR-valve to EGR-ratio Figure A.11 shows that there is no non-minimum phase behaviors.

4.2.3 Response time

The response time gives information about how fast different actuators effect the different outputs of the system. In the contour plots in Appendix A.3 τ from Figure 4.2 are presented. There the step has reached 63 % of the final value.

For the channels u_{th} and u_{wg} to p_{im} the behaviors are the similar for the operating area. The throttle effects generally the intake manifold pressure faster than the wastegate, see Figure 4.5, where the response from u_{th} is presented to the left and u_{wg} to the right. The throttle is closer to the intake manifold so changes there should be seen faster in p_{im}. However when opening up the throttle the mass flow through the cylinder increases and so the turbine power. This increases the boost from the turbo and also the intake manifold pressure. Therefore, the dynamics of the whole engine will be included even if only the throttle is open up.

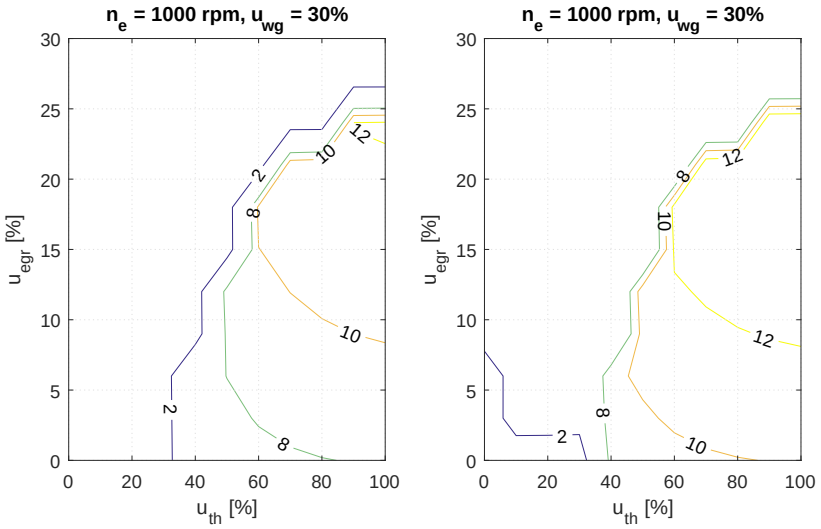

Figure 4.5: *Contour plot of the τ for the channel u_{th} to p_{im} to the left and for u_{wg} to p_{im} to the right. In both cases are $n_e = 1000$ and $u_{wg} = 30\%$. The showed values are the time for a step to reach 63 % of the final value.*

4.2.4 Relative gain array

The final analysis for the operating region is the relative gain array (RGA). This is used to see cross connections between inputs and outputs of the system. The analysis gives information which input that correlates the most with which output. An RGA-value close to one means that the channel is good choice for a feedback loop according to Glad and Ljung [9]. The more the RGA-value differs from one the impacts of the other control signals will increase.

See for example Figure 4.6. The EGR-actuator has an RGA value close to one in almost the whole operating area for $n_e = 1500$ and $u_{wg} = 20\%$. Studying Figure A.23 shows that this also is true for almost the whole operating area of the engine. However, there are two operating modes where the other actuators have a bigger impact. The first one is for small throttle angles and high EGR-valve angles (the upper left corner in the plot). For this region has the throttle the most impacts of the EGR-ratio. The reason is that the pressure drop over the throttle is high which means that changes in the throttle position affects the content in the intake manifold a lot. And the pressure drop over the EGR-valve is small which makes the impact of the EGR-valve small.

The other area is for high EGR-flow and low engine speeds. Here the wastegate has the most impact, for the same reason. The pressure drop over the EGR-valve is small but if the wastegate closes a little the pressure in the exhaust manifold increases which will increase the EGR-flow due too the higher pressure drops over the EGR-valve. Closing the wastegate will of course also increases the intake manifold pressure because of higher turbo boost. But according to this analysis

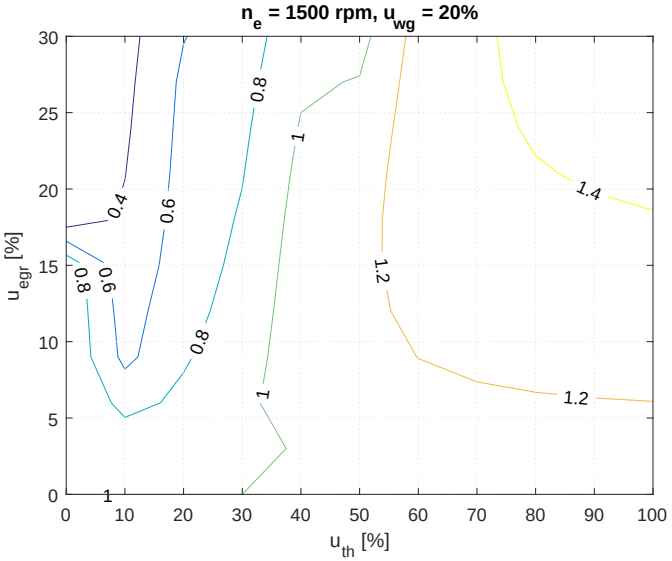

Figure 4.6: *Contour plot of the RGA-value for the channel u_{egr} to x_{egr} for $n_e = 1500$ and $u_{wg} = 20\%$.*

the impact of the increased pressure in the exhaust manifold is bigger. The reason for this effect has not been investigated but can maybe be explained by different efficiency for the turbine and the compressor depending on the operating area for the turbo.

Which channels that affect the pressure in the intake manifold the most are not clear. The throttle has an RGA-value close to one when the throttle is in a region around 30 % open according to Figure A.19. For higher throttle angles the pressure drop over the throttle decreases which gives the result that the impact of the throttle decreases.

For operating area with more open throttle (> 50 %) one can see in Figure A.21 that the wastegate has a RGA-value around one and could be a good choice in a control loop. The pressure drop over the throttle is low and the impact of the throttle as well. Therefore, the impact of the wastegate is bigger in these areas.

The EGR-valve also affect the p_{im} but has negative RGA-value for some operating modes, which makes it more difficult to use in a feedback-loop.

4.3 Conclusion

From the analysis in Chapter 4 one simple approach is to use the throttle and the wastegate to control the intake manifold pressure and the EGR-valve to control the EGR-ratio. The first two actuators could be in series where the throttle gives the faster response due to the response time analysis. For good control performance, the throttle should be in a position to be able to both increase and

decrease the pressure. The wastegate should regulate to adjust the throttle to this operating area for example with a pressure ratio over the throttle. There are no non-minimum phase behaviors in this loop except for some small regions. In this thesis will these be neglected.

Using the EGR-valve to control the pressure would work fine for some operating modes but due to the change from positive to negative RGA this will require selectors and a more advanced control strategies. Therefore, the EGR-valve will not be used in a feedback loop with p_{im}. One way to extend the control design is to see u_{egr} as a disturbance at p_{im} and feedforward the change from the EGR-valve.

For the EGR-ratio a control loop with the EGR-valve is a good alternative. The RGA analysis shows that RGA is one for a large area for this channel. There is no sign-reversals and no non-minimum phase behaviors. As mentioned in Section 4.2.4 there are two operating modes where the other actuators affect the EGR-ratio more. One way to solve this is to include these in the EGR-ratio controller for example with selectors or requiring a certain pressure ratio over the EGR-valve with the throttle or wastegate. To improve the performance, there is a possibility to see the throttle and the wastegate as a disturbance at the EGR-controller.

5

Controller

This chapter will present the different control strategies that are used and investigated in this thesis. The results can be found in Chapter 6 and the analysis of the results in Chapter 7. There have been two types of approaches to find the control structures. The first one is through system analysis. What is a good choice for a basic controller? The second one is to add some different techniques to se how the controller could be improved, more of this further on.

The system has three control signals, u_{th}, u_{egr} and u_{wg}, and two performance variables, p_{im} and x_{egr} that should follow the reference signals $p_{im,ref}$ and $x_{egr,ref}$. Except from these p_{ic} will be used as an output in the feedback system. The performance variable, p_{im}, is selected because it gives a perception of the generated torque. This together with the EGR-ratio, x_{egr}, are of interest to be able to control with the three actuators.

5.1 Proposed control strategy from system analysis

In Chapter 4 the system is linearized and analyzed for the whole operating region of the engine. The analysis shows the DC-gain, time response, non-minimum phase behaviors and RGA for the three control signals u_{th}, u_{egr} and u_{wg} to the two performance variables p_{im} and x_{egr}.

As mentioned in Section 4.3 one simple approach is to use the throttle and the wastegate to control the pressure in the intake manifold, and the EGR-valve to control the EGR-ratio. These two controllers will work as feedback loops with PID-controllers, see Figure 5.1. The control loop for the intake manifold contains two actuators but only one performance variable. One way to use them is to select the throttle to regulate directly on the measured p_{im} signal. This choice is due to the faster response from u_{th} to p_{im} in relation to u_{wg} to p_{im}. The wastegate, on the other hand, is selected to be used in a feedback loop to control the

pressure ratio over the throttle. This will give the opportunity to change the requested pressure ratio over the throttle, Π_{th}, depending on if response time or fuel economy are most important [5]. A higher pressure drop over the throttle means faster response and higher fuel consumption. In this case, the wastegate will be more closed which will increases the exhaust manifold pressure. The pump works for the engine increases which gives higher fuel consumption. The response time gets faster because the power from the turbo increases which result in higher boost pressure. That, in turn, increases the p_{im} faster when opening up the throttle. The opposite is true for low pressure drops over the throttle. For all the feedback loops are PID-controllers used which are designed according to Section 5.5.

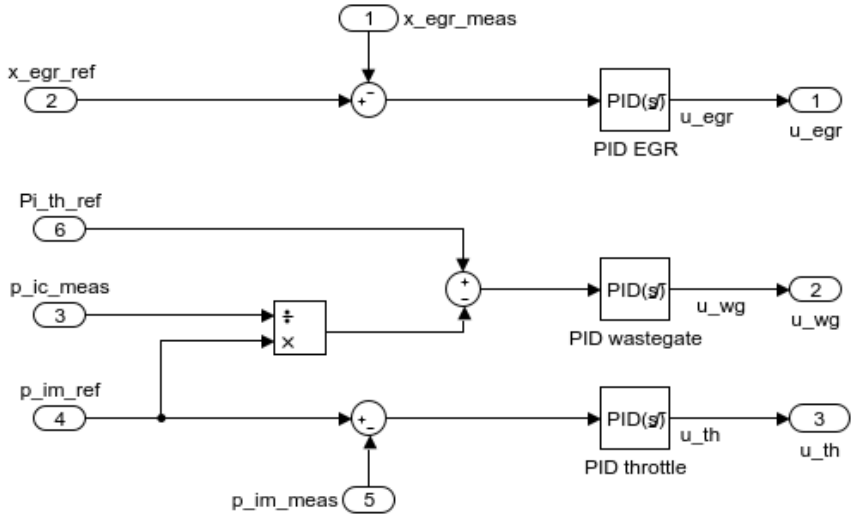

Figure 5.1: *Control structure of a controller with only feedback loops.*

5.2 Feedforward with models

Feedforward information to a given control signal gives faster response time. The knowledge about how something will affect a performance variable makes it possible to set the control signal to the right value directly. The concept is easier to illustrate with a concrete example and in this thesis two feedforward controllers are tested, both are showed in Figure 5.2. These are selected to increase the reference tracking for the EGR-ratio.

1. Feedforward from $x_{egr,ref}$ to u_{egr}. This require a model from u_{egr} to x_{egr}.
2. Feedforward from $p_{im,ref}$ to u_{egr}. This require a model from $p_{im,ref}$ to u_{egr} and from u_{egr} to x_{egr}.

The first feedforward controller reacts on the reference signal for the EGR-ratio, x_{egr}, and changes the control signal to the EGR-valve, u_{egr}. This requires a model for how the system reacts for changes from u_{egr} to x_{egr}. Physically this is given from the throttle model that is used in the submodel for the EGR-flow. The approach here is instead to use the linearized model developed in Chapter 4. An operating mode is selected and the given linearization is used to find out how x_{egr} reacts on changes in u_{egr}. In the feedforward controller the inversed model is used to give information about how the EGR-valve should reacts depending on a given EGR-ratio. As mentioned before, this model is developed for one operating mode.

The second feedforward controller works in the same way but needs two type of models. First a model for how the p_{im} affect the x_{egr} (called H). And a second model, that is the same as in the first feedforward controller, that describes the behavior from u_{egr} to x_{egr} (called G). Combine these according to

$$\text{Feedforward } p_{im} \text{ to } u_{egr} = -HG^{-1}$$

and add that to the control signal for the EGR-actuator will reduce the impact of changes in $p_{im,ref}$ at x_{egr}. The changes in the intake manifold pressure are seen as a disturbance of the EGR-ratio, see [11] for more theory. The model from p_{im} to x_{egr} can not be found in the linearization in Chapter 4. Therefore a new linearization has been made with the Matlabs toolbox "Control Design". As input the p_{im} signal is selected and as output the x_{egr}. The physically model for that is harder to find and therefore the linearization model is a good choice. The model from u_{egr} to x_{egr} was found in the same way as for feedforward controller number one.

The inverted model of u_{egr} to x_{egr} is used in both the controllers. It is important that the used system is stable and proper [11]. A stable system means that all poles are in the left side of the s-plane. A proper function has at least as many poles as zeros. Therefore a pole has been added with the same placement as the pole closest to origo. The placement of the pole will impact the behavior of the feedforward part. This could thus be changed and different placements could be tested. The choice in this thesis is to give the modified inversed model as close behavior as possible to the real inversed model [9].

5.3 Prefiltered reference

To receive better performance due to under- and overshoots, one way is prefiltering the reference signals. The system can be made slower and has a reference signal it is more likely to follow. For example, the EGR-ratio which is affected from all the actuators but only controlled with the u_{egr}. The response from the EGR-actuator is slower than the throttle-actuator which means that fast changes in the throttle will affect the EGR-ratio before the EGR-valve is able to compensate. Therefore, prefiltering the $p_{im,ref}$ is a suggested control strategy, which slows down the fast changes in the throttle. The prefiltering selected in this the-

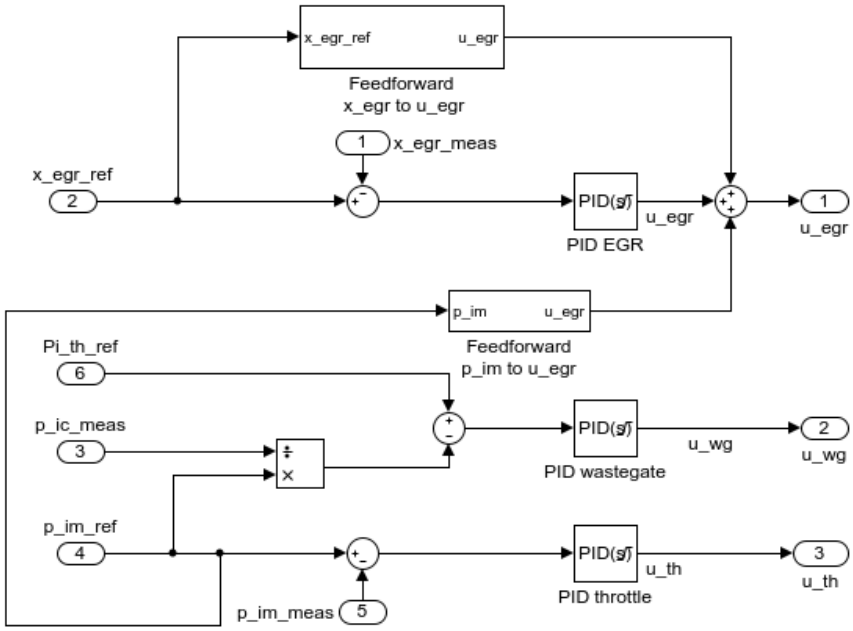

Figure 5.2: *Control structure of a controller with feedback loops and feed-forward parts from $x_{egr,ref}$ to u_{egr} and $p_{im,ef}$ to u_{egr}.*

sis is a first order system according to

$$F_f = \frac{1}{1 + sT} \tag{5.1}$$

where T is the preferred time constant for the system and has been selected through testing. A higher time constant (slower system) will improve the EGR-ratio tracking on one hand but slows down the pressure built up in the intake manifold on the other. A lower time constant will do the opposite. See Figure 5.3 for a control structure with the proposed prefiltering part.

5.4 Min-max selector

The last control approach tested in this thesis is with min-max-selectors. This can be used in many different ways, for example, to keep restrictions or reach certain limits. The approach here is with a max-selector and a controller from the EGR-ratio error to the control signal of the wastegate, see Figure 5.3. The "PID EGR to wastegate" controller will increase u_{wg} if the EGR-ratio is lower than the reference signal. If the error is big enough, this will override the Π_{th} controller and close the wastegate. Observe that this controller is connected to a max-selector which means that it will only be ”activated” if the EGR-ratio is to low. There will be no impact of this during decreased EGR-steps. To keep the controller simple but still reach the stationary level a PI-controller is used.

There are two reasons to use the wastegate to improve the EGR-tracking. The first one is that the system analysis shows that the DC-gain is positive for almost the entire operating area. If u_{wg} is increased the x_{egr} will also be increased. The second reason why using the wastegate instead of the throttle is to keep the design that gives a fast p_{im} response. The throttle is the fastest actuator, and therefore it will only be used for the p_{im} controller.

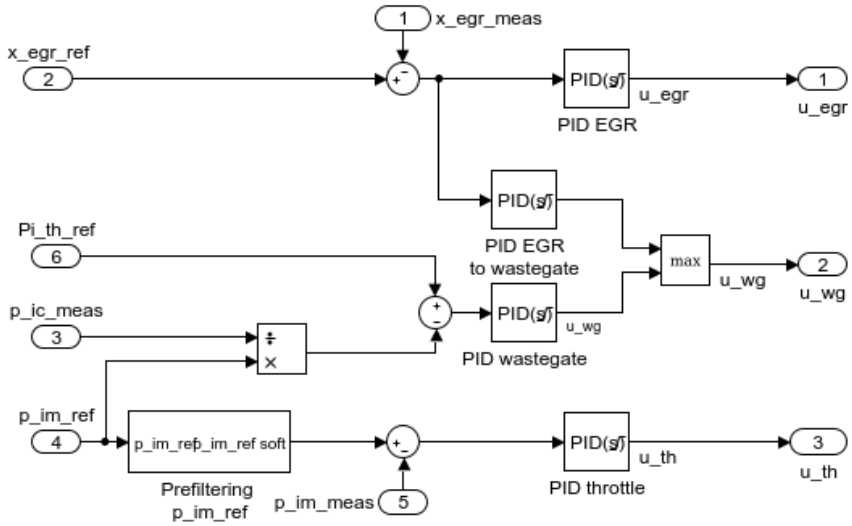

Figure 5.3: *Control structure of a controller with prefiltering of $p_{im,ref}$ and min-max-selector. The wastegate is controlled to either keep the $\Pi_{th,ref}$ or if the EGR-ratio is to low, closes the wastegate, to increases the EGR-flow.*

5.5 Controller parameterization

In the previous sections there are a couple of different control strategies proposed, but these still includes PID-controllers. There are a lot of different methods to adjust these. The method used here is called IMC-tuning and use a three parameters model of the controlled system to find the parameters for the controller. More information can be found in [11].

The used form of the PID-controller is the parallel form

$$\text{PID} = K\left(1 + \frac{1}{T_i s} + \frac{T_d s}{T_d s + 1}\right). \tag{5.2}$$

where the parameters to quantify are K, T_i and T_d. To find the parameters the model has been linearized around a stationary point and the input and output have been selected according to where the controller should operate. For example should the "PID-throttle" controls u_{egr} and reacts on p_{im}. The model

to be controlled has therefore u_{egr} as input and p_{im} as output. The linearization is preformed with the linearization tool in Matlabs toolbox "Control design", in the same way as for the system analysis. A three parameters model is adapted according to

$$G(s) = \frac{K_p}{1 + sT} e^{-sL} \tag{5.3}$$

where K_p is the gain, T the time constant and L the time delay. The three parameters for the PID controllers are then

$$K = \frac{L}{K_p(T_c + L)} \left(\frac{1}{\tau} - \frac{1}{2} \right) \qquad T_i = L \left(\frac{1}{\tau} - \frac{1}{2} \right) \qquad T_d = L \frac{1 - \tau}{2 - \tau} \tag{5.4}$$

where

$$\tau = \frac{L}{L + T}. \tag{5.5}$$

T_c on the other hand is a design parameter

$$\lambda = \frac{T_c}{T} \tag{5.6}$$

where λ is optimized to give the desired response. A $\lambda < 1$ will give a faster feedback system and $\lambda > 1$ a slower one, than the open system.

5.6 Fuel economy versus fast response

Fuel economy and fast response time are two important factors for an engine. During this thesis the focus has not been to optimize according to the fuel consumption. A parameter that still reflect the fuel consumption is the pressure drop over throttle, see Section 5.1 for more information. A more closed throttle and wastegate will generally give higher fuel consumption according to Eriksson et al. [6]. Therefore, the Π_{th} signal is plotted in the result for all tests. If the controllers have different Π_{th} before a transient the condition to give good performance are unequal.

5.7 Controller summary

As described in this chapter five different controllers are developed. These are presented in Table 5.1 with a short description. In chapter Result and Analysis (Chapter 6 and 7) these controllers will be referred to with the number in the Table 5.1.

5.8 Sensitivity analysis

A simple sensitivity analysis has been performed on one of the controllers. The controller that has been tested is a combination of controller number 1, 2 and 4

Table 5.1: *The table presents the five different controllers that have been developed and tested in this thesis.*

Controller	Description
1	Only feedback loops, see Figure 5.1
2	Feedforward from $x_{egr,ref}$ to u_{egr}, see Figure 5.2
3	Feedforward from $p_{im,ref}$ to u_{egr}, see Figure 5.2
4	Prefiltering the reference signal $p_{im,ref}$, see Figure 5.3
5	Max-selector for WG between Π_{th} and EGR error, see Figure 5.3

in Table 5.1. This contain a feedforward part and a prefiltering part together with the ordinary feedback loops. The analysis has been made in three steps:

1. Disturbances have been added to the measured x_{egr}. The disturbances contain both white noise and a static offset. The purpose is to see how the EGR-loop is affected. The measured EGR-ratio is disturbed because this one is included in the feedback loop.

2. Disturbances have been added to the measured p_{im} and p_{ic}. The disturbances contain both white noise and a static offset. The purpose is to see how the intake manifold pressure loop is affected. This two signals are chosen because these are used in the feedback loop to control the intake manifold pressure.

3. The effective area of the wastegate is multiplied with a gain. This is to see how model error impacts the result. The wastegate is selected because of the high uncertainty in this model due to Table 3.3.

The white noise is generated with a Simulink block and fitted to look like real measurements noises. The offset is a constant added to the signal with a reasonable value to give an impact of the output. All the result can be found in Chapter 6 where a transient with a step in the $p_{im,ref}$ and $x_{egr,ref}$ is performed. The output in the plot will show the ”real” value of the measured signal before the disturbances are added.

6 Results

Chapter number 6 contains the results of the controllers described in Chapter 5. Two kinds of results will be analyzed. The first part contains some steps in $p_{im,ref}$ and $x_{egr,reg}$, where the initial conditions for all the controllers are the same and the reaction during the transients will be studied. The second part is to compare one controller with the response from real measurements. In that section the result will be presented along with the measured signals together with a comparison between the controllers developed in this thesis and the controllers used today.

6.1 Transients

The results during six different transients, for the five controllers described in Chapter 5, will be presented in this section. The transients either have a step in the reference signal to the intake manifold pressure, $p_{im,ref}$, or in the reference signal to the EGR-ratio, $x_{egr,ref}$, or both. The transients are presented in Table 6.1, and they will also be presented in the beginning of each "Transient"-section. For all the results the control signals to the three actuators are showed along with p_{im}, x_{egr} and Π_{th}. The transients have reasonable values for an engine to work within, and have been selected to illustrate the difference between the different controllers. All the steps are performed at time = 100 s, which allows the system to find stationary points before the steps are made. In the plots the lines are only labeled with a number which corresponds to the controller in Table 5.1.

In Appendix B tables with rise times and overshoots for p_{im} and x_{egr} for the different transients can be found.

Table 6.1: *The table presents six different transients where the controllers developed in Chapter 5 are tested. The transients contain different steps for $p_{im,ref}$ and $x_{egr,ref}$, but all with same engine speed and requested pressure ratio over the throttle.*

Number	$p_{im,ref}$		$x_{egr,ref}$		n_e	$\Pi_{th,ref}$
A	1.2 bar	1.7 bar	5 %	5 %	1500 rpm	0.88
B	1.7 bar	1.2 bar	5 %	5 %	1500 rpm	0.88
C	1.2 bar	2.3 bar	0 %	0 %	1500 rpm	0.88
D	1.7 bar	1.7 bar	5 %	15 %	1500 rpm	0.88
E	1.7 bar	1.7 bar	15 %	5 %	1500 rpm	0.88
F	1.7 bar	2.3 bar	5 %	15 %	1500 rpm	0.88

6.1.1 Transient A

Number	$p_{im,ref}$		$x_{egr,ref}$		n_e	$\Pi_{th,ref}$
A	1.2 bar	1.7 bar	5 %	5 %	1500 rpm	0.88

Transient A contains a step in the $p_{im,ref}$ which exemplifies a step around intermediate load. Figure 6.1 shows the result. Studying the p_{im}-signal it is shown that controller number 4 is the slowest one. This is because the reference signal to the p_{im} is prefiltered with a first order system. The PID, controlling the throttle will therefore reacts slower and the total response gets slower. But notice that the overshoot for the p_{im} is smaller in this case. The rest of the controllers have the same response for p_{im}.

Looking at x_{egr} there are four different behaviors. Number 1 and 2 react in the same way. The only difference between these are the feedforward from $x_{egr,ref}$ to u_{egr} for controller number 2. In this transient is the reference for the EGR-ratio constant which gives no influence on controller number 2. The EGR-ratio drops rapidly when the p_{im} suddenly increases for these controllers.

Controller number 5 reacts in the same way. The impact of EGR-ratio error to wastegate is therefore low. The wastegate is already closed down, so the impact of closing the wastegate to increase the EGR will not be seen. During the slow down of p_{im} (around T = 102 s) the wastegate never opens up fully but the impact of this does not change the result. Remember that 0 % wastegate means fully open and 50 % fully closed.

Controller number 3 has a feedforward part from the $p_{im,ref}$. The impact can be seen when the EGR-valve opens up. The response is faster than the other and also opens up the EGR-valve more. The EGR-ratio gets an overshoot and oscillates around the reference value before stabilizing to the stationary point. The initial drop is still there.

The last controller, number 4, does not give the initial drop. This is because of the slower response in p_{im}. Moreover, during the transient the EGR-controller cannot compensate to keep the EGR-ratio, before p_{im} has been stabilized.

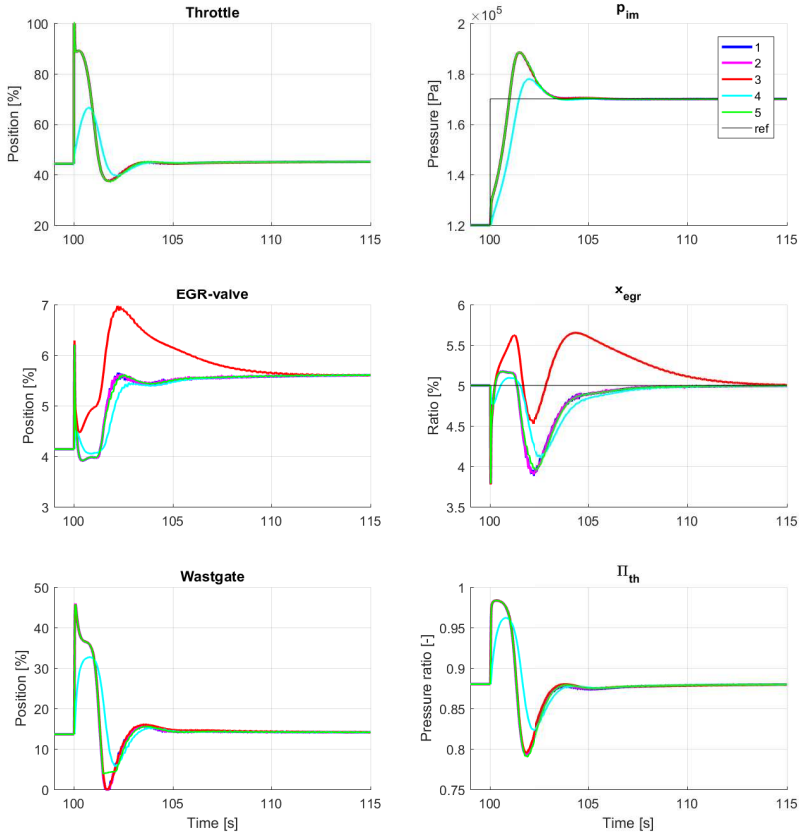

Figure 6.1: *The result of the 5 controllers from Table 5.1 with a step in $p_{im,ref}$ according to transient A in Table 6.1. The different colored lines represent the different controllers and the black line the reference signal.*

6.1.2 Transient B

Number	$p_{im,ref}$		$x_{egr,ref}$		n_e	$\Pi_{th,ref}$
B	1.7 bar	1.2 bar	5 %	5 %	1500 rpm	0.88

Transient B (see Figure 6.2) contains a decreasing step in $p_{im,ref}$ instead of a rising one as in transient A. Except from this all the data are the same. Studying the p_{im}-signal it is shown that controller number 4 reacts much slower corresponding to the other. It is easier to decrease the pressure than build it up, which results in a bigger difference between controller number 4 and the other during this transient. This can be seen in the throttle signal which does not close completely. The other controllers react in the same way for the p_{im}-signal.

The x_{egr}-signal shows that the fast pressure drop gives a peak in the EGR-ratio. But controller number 4 only rise around 20 % compare to the other who rises nearly 120 %. The slower response in the p_{im}-controller helps the EGR-controller to keep the right EGR-ratio.

Controller number 3 closes the EGR-valve more than the other but the delay in the EGR-valve still gives the initially peak. After the peak, there is an undershoot and the controller takes longer time to stabilize. The rest of the controllers react in the same way for the x_{egr}-signal.

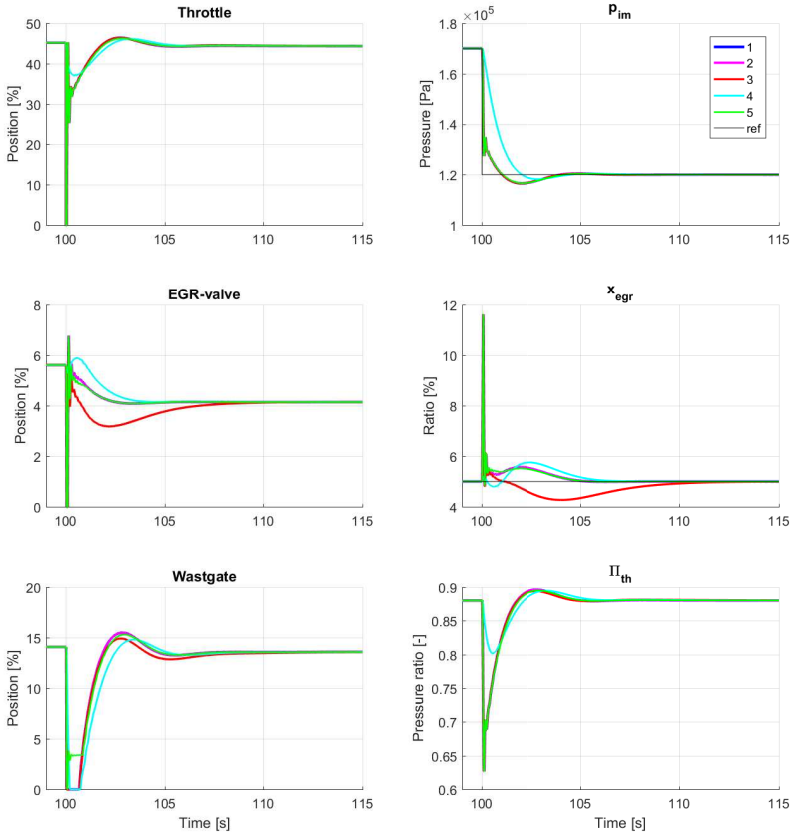

Figure 6.2: *The result of the 5 controllers from Table 5.1 with a step in $p_{im,ref}$ according to transient B in Table 6.1. The different colored lines represent the different controllers and the black line the reference signal.*

6.1.3 Transient C

Number	$p_{im,ref}$		$x_{egr,ref}$		n_e	$\Pi_{th,ref}$
C	1.2 bar	2.3 bar	0 %	0 %	1500 rpm	0.88

Transient C contains a step from intermediate to high load and is presented in Figure 6.3. The EGR-ratio reference is kept to zero during the whole transient. The p_{im} response is same for all the controllers except number 4 and the reason is the same as for transient A (see Section 6.1.1).

For the x_{egr}-signal the controller number 3 opens up and gives an EGR-flow into the intake manifold. The controller is linearized around a point where higher p_{im} needs more open EGR-valve for same EGR-ratio. This is not the case for zero EGR-ratio and needs to be considered if a feedforward part from the $p_{im,ref}$ to the EGR-loop is implemented.

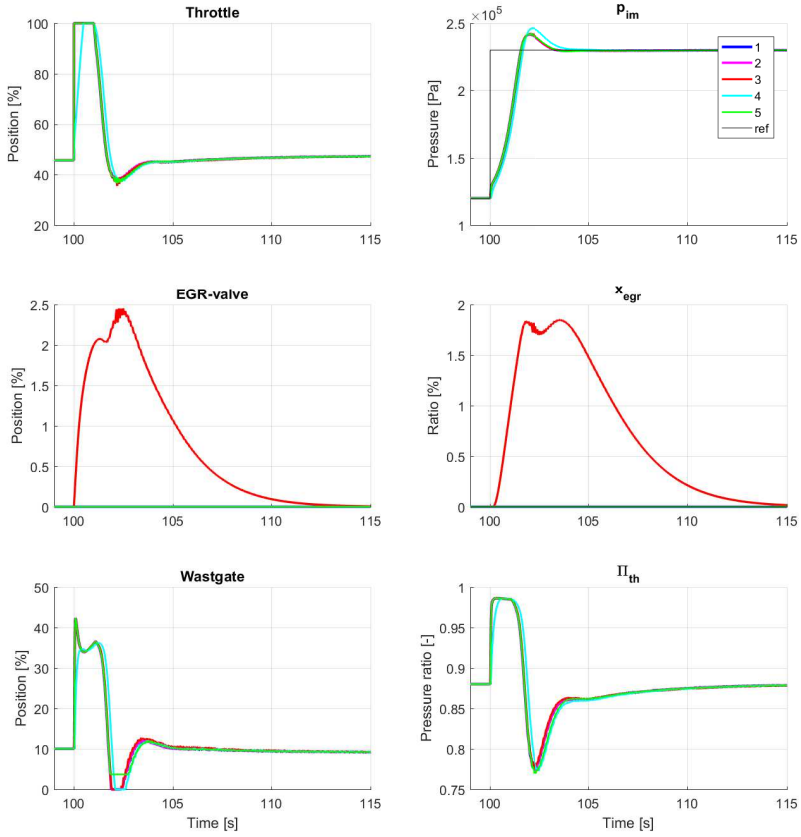

Figure 6.3: *The result of the 5 controllers from Table 5.1 with a step in $p_{im,ref}$ according to transient C in Table 6.1. The different colored lines represent the different controllers and the black line the reference signal.*

6.1.4 Transient D

Number	$p_{im,ref}$		$x_{egr,ref}$		n_e	$\Pi_{th,ref}$
D	1.7 bar	1.7 bar	5 %	15 %	1500 rpm	0.88

The first three transients have contained steps in the reference signal to the intake manifold pressure and constant EGR-ratio. Transient D on the other hand has a step in $x_{egr,ref}$ while keeping the $p_{im,ref}$ constant, see Figure 6.4. The step is from 5 % to 15 % EGR-ratio while driving with intermediate load (1.7 bar in the intake manifold).

Controller number 1, 3 and 4 have similar behavior, the difference between these depends only on $p_{im,ref}$, and because there is no change in this signal the transient behavior is the same. The response in the EGR-ratio is slowest for these three compared to the other two, but there is also less oscillations in p_{im}.

Controller number 2 reacts by opening up the EGR-valve more than the other. This is because of the feedforward part from the $x_{egr,ref}$. The rise time is improved for the EGR-ratio but also gives an overshoot, and the oscillations in p_{im} are bigger.

The last controller, controller number 5, closes the wastegate faster than the others. The control strategy, controls the wastegate depending of the error in the EGR-ratio, which increases fast. The pressure in the intake manifold, p_{im}, first gets an overshoot and then an undershoot because of this. The EGR-response is the same as for the response with just feedback loops.

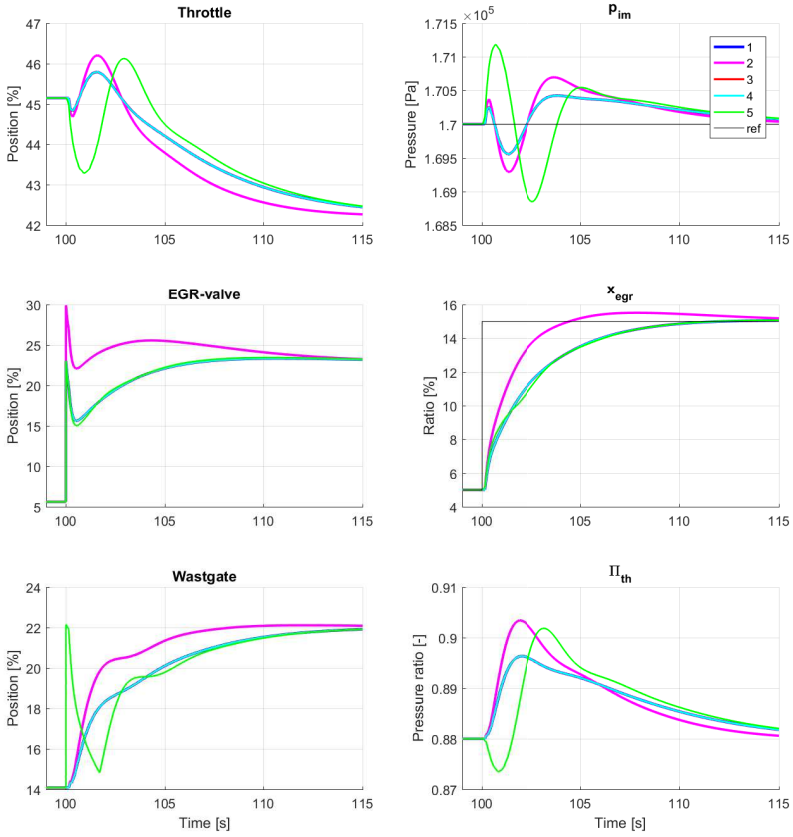

Figure 6.4: *The result of the 5 controllers from Table 5.1 with a step in* $x_{egr,ref}$ *according to transient D in Table 6.1. The different colored lines represent the different controllers and the black line the reference signal.*

6.1.5 Transient E

Number	$p_{im,ref}$		$x_{egr,ref}$		n_e	$\Pi_{th,ref}$
E	1.7 bar	1.7 bar	15 %	5 %	1500 rpm	0.88

Transient E is the same as transient D but instead of a rising step in EGR-ratio there is falling step from 15 % to 5%. The behavior is the same, see Figure 6.5. Controller number 2 reacts faster and close the EGR-valve more than the other according to the feedforward part. Controller number 1,3 and 4 react in the same way, slower EGR-ratio tracking but less oscillations than controller number 2.

One can also notice that controller number 5 reacts in the same way as the other. This is because the controller that affect the wastegate depending on the EGR-ratio error is selected with a max-selector. That means it will only gives impact when the EGR-ratio is to low, compared to the reference signal.

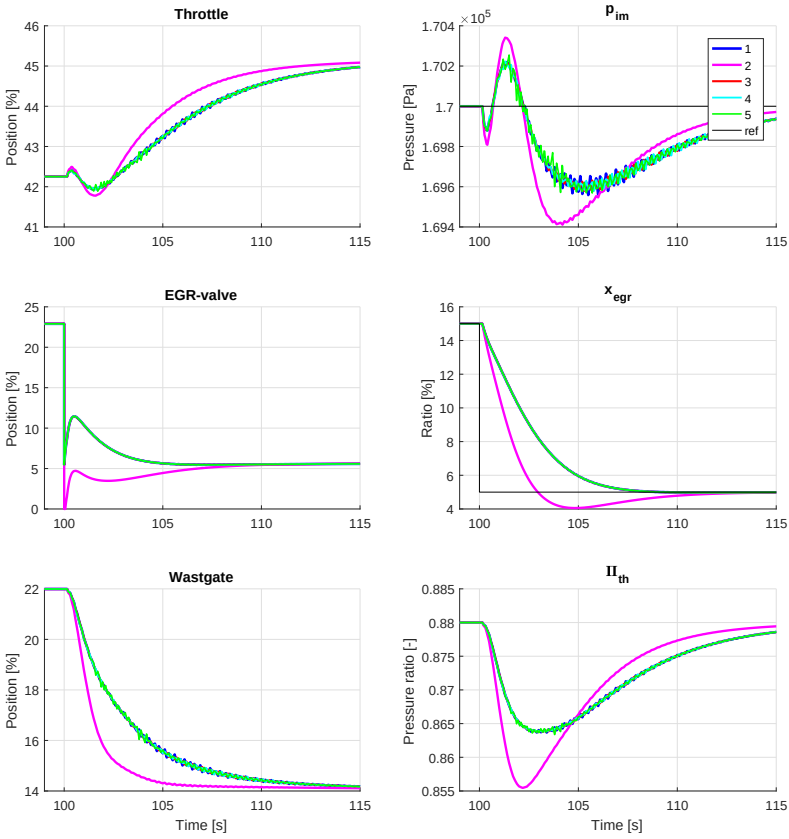

Figure 6.5: *The result of the 5 controllers from Table 5.1 with a step in $x_{egr,ref}$ according to transient E in Table 6.1. The different colored lines represent the different controllers and the black line the reference signal.*

6.1.6 Transient F

Number	$p_{im,ref}$		$x_{egr,ref}$		n_e	$\Pi_{th,ref}$
F	1.7 bar	2.3 bar	5 %	15 %	1500 rpm	0.88

The last transient, F, contains steps in both $p_{im,ref}$ and $x_{egr,ref}$. The step in the intake manifold pressure is from intermediate to high load and the EGR-ratio step is from 5 % to 10 %. The response in p_{im} is the same for all the controllers except number 4 which is slower according to the prefiltering that makes the reference signal softer.

For the EGR-ratio the difference is bigger. At first there is an undershoot except for controller number 4. The undershoot depends on the faster response in the throttle actuator and the shorter time delay for the throttle compared to the EGR-actuator. When the reference for the EGR-ratio changes the feedforward from $x_{egr,ref}$ open up the EGR-valve most. This gives faster EGR response for controller number 2. Also controller number 3 reacts faster due to the feedforward part from $p_{im,ref}$.

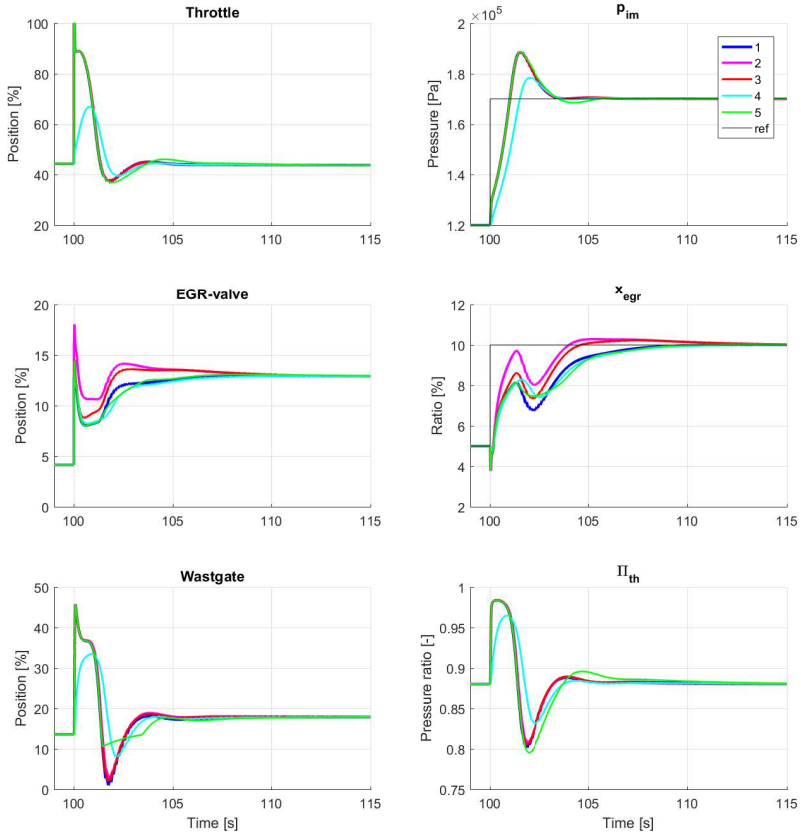

Figure 6.6: *The result of the 5 controllers from Table 5.1 with a step in $p_{im,ref}$ and $x_{ref,ref}$ according to transient F in Table 6.1. The different colored lines represent the different controllers and the black line the reference signal.*

6.2 Sensitivity analysis

A sensitive analysis is performed to see the impact of disturbances in the measured signals and model errors. The result is presented in Figure 6.7, where the blue lines are the controller with no disturbance and the purple lines with noise and off-set on the measured x_{egr}-signal. The red lines are disturbance (noise and off-set) on the measured p_{ic} and p_{im} signals and the cyan lines are a simulation with an offset of the wastegates effective area. The black lines are the reference signals. The sensitive analysis is performed with a combination of controller number 1, 2 and 4 in Table 5.1. The controller has two main feedback loops, prefiltering on the reference signal to p_{im} and a feedforward part from $x_{egr,ref}$ to u_{egr}.

In the plot the "real" values are presented. This means that the noise is added after measurements before going back to the feedback loops.

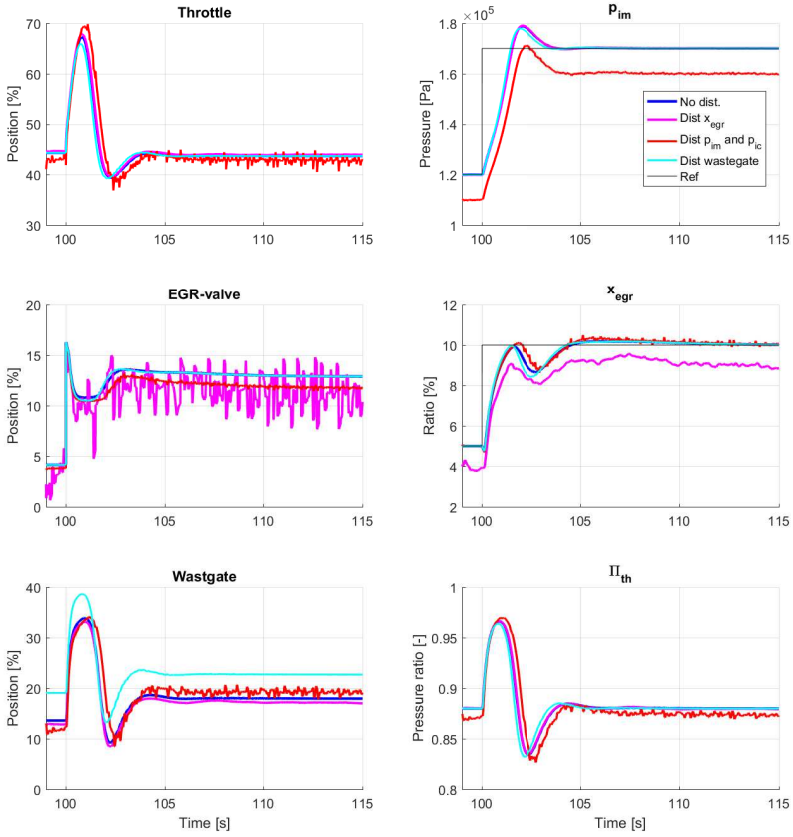

Figure 6.7: *Different kind of disturbances of measured signals and changed parameters for wastegate effective area. The disturbances are described in Section 5.8.*

6.3 Comparison with existing controller

To see the performance of the controller developed in this thesis a comparison with measurements, from a real engine, has been done. The results are presented in Figure 6.8 and 6.9, where the red lines are the measured values and the blue lines the modeled. The black lines are the reference signals. Notice that for Π_{th} the black line is only the reference signal for the real engine. The controller for the model controls to $\Pi_{th} = 0.94$ during the whole transient.

The controller that is used for the model is the same as described in the previous section (Section 6.2), a combination between controller number 1, 2 and 4 in Table 5.1.

The first transient is performed with $n_e = 1500$ rpm, from low to intermediate load. The plot, Figure 6.8, shows that p_{im} increases faster for the model but with a bigger overshoot. The EGR-regulation seems also to be better where the big peak initially is avoided. Instead the EGR-ratio decreases while the p_{im} increases.

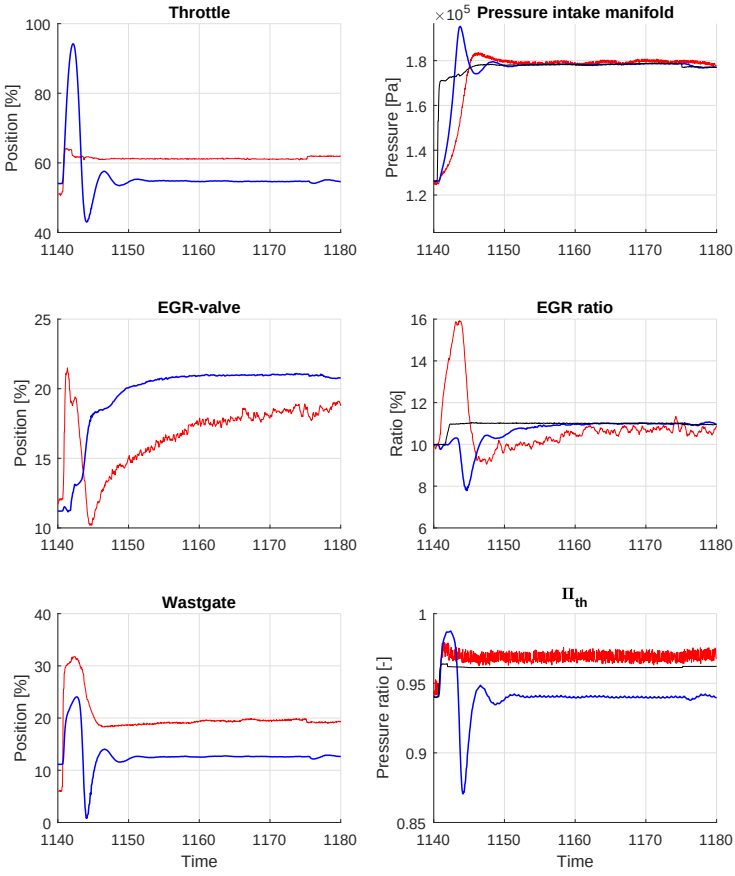

Figure 6.8: *The figure shows the real engine (red lines), the model (blue lines) and the reference signals for p_{im} and x_{egr} (black lines). Observe that for Π_{th} the model follows 0.94 meanwhile the real engine follow the black line. The transients is performed with $n_e = 1500$ rpm.*

The second transient is performed with $n_e = 1500$ rpm, from low to high load. The plot, Figure 6.9, shows that the p_{im} signals is close to each other but also here with a bigger overshoot for the model compared to the real engine. The way to reaches the set value differs a lot. The model opens up the throttle while the real engine close the wastegate to receive the same result. This may affects the EGR-ratio which increases when the step for $p_{im,ref}$ is performed for the real engine. The model on the other hand has problem to reach the right EGR-ratio and saturates around 14 % for the given operating mode.

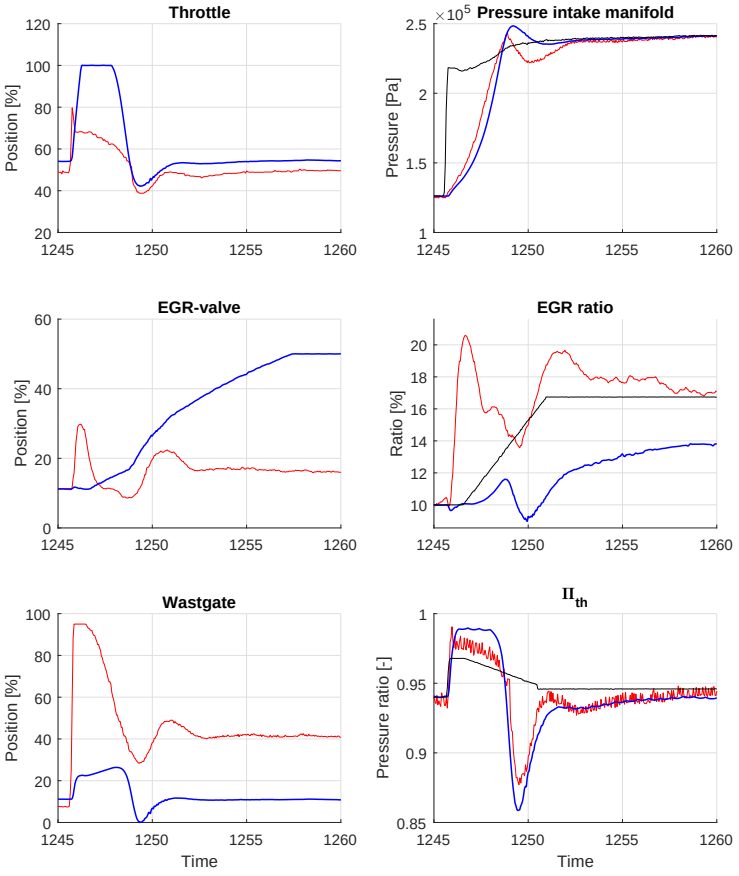

Figure 6.9: *The figure shows real engine (red lines), the model (blue lines) and the reference signal for p_{im} and x_{egr} (black lines). Observe that for Π_{th} the model follows 0.94 meanwhile the real engine follows the black line. The transient is performed with $n_e = 1500$ rpm.*

7

Analysis

The Analysis chapter contains an analysis of the result and a proposed control strategy. The first section analyzes the five different controllers described in Chapter 5 and evaluated in Chapter 6. The following parts go through the sensitivity analysis of the controllers and the comparison with the existing controller that is used today. After that will a control strategy based on the results in this thesis be presented.

7.1 Analysis of the result

This section goes through the five controllers in Table 5.1 which are evaluated in six different transients described in Table 6.1.

7.1.1 Controller 1 - Feedback loops

The first controller is the most basic one with three feedback loops to control the intake manifold pressure and the EGR-ratio. The wastegate is controlled based on the pressure ratio over the throttle, and in this thesis that reference has been kept constant. It is possible to have another degree of freedom by setting different pressure quotients for different operating modes. The controller is in most cases the slowest but has less under- and overshoots compared to the controller with feedforward techniques. The following controllers are compared against this one to see changes between the different techniques.

7.1.2 Controller 2 - Feedforward from $x_{egr,ref}$

The controller with a feedforward part from $x_{egr,ref}$ to u_{egr} gives faster EGR-response when the EGR-ratio is changed. For transients D to F studying the EGR-

valve shows that the EGR-valve is opened/closed more during these steps. The faster response, on the other hand, gives a bigger overshoot than just using feedback loops. The fast response in the EGR-valve also affects the p_{im} controller and give bigger oscillations in the intake manifold. This can also be seen for the throttle and wastegate positions which are varying faster. However, the oscillation in the p_{im} signal is still small.

7.1.3 Controller 3 - Feedforward from $p_{im,ref}$

The second tested feedforward controller is from $p_{im,ref}$ to u_{egr}. This one is tested to improve the EGR-controller during transients in $p_{im,ref}$, where quick changes in the p_{im} gives big peaks/drops in the EGR-ratio. The transients where the controller should give different results, from using feedback loops, are A, B, C and F. For the first transient where the p_{im} increases the EGR-valve opens up more to compensate. The longer time delay for the EGR-actuator compared to the throttle still gives the initial peaks. Moreover, after the peak the controller instead overcompensate and tracking the EGR-ratio seems to be no better than for using just feedback loops. For transient B the behavior is the same.

Transient C is interesting because the feedforward part opens up the EGR-valve during the transient for the p_{im}. However for no EGR-flow the EGR-valve should always be closed. If a feedforward part like this is selected this must be considered and some selector must be used.

For transient F the EGR-tracking is improved. There is still a drop before the EGR-ratio starts to increase but the rise time is faster than for just feedback loops. The controller seems to improve the result when both references are changed. The overcompensation effect that could be seen in transient A and B improves the result here. In transient A and B should the EGR-ratio be kept constant but in number 3 the EGR-ratio should increases which improve the result.

There is also a problem with the longer time delay for the EGR-valve compared to the throttle. Even if the reference signal from the p_{im} is feedforward, the EGR-valve has no chance to change before the p_{im} has changed. Therefore, this controller gives an initial peak/drop during steps in $p_{im,ref}$.

7.1.4 Controller 4 - Prefiltered reference signal

The prefiltered $p_{im,ref}$ have particularly one advantage and one disadvantage compared to the controller without any filter. The disadvantage occurs when $p_{im,ref}$ is changed which gives slower response for p_{im}. See for example transient A and B. Especially during pressure drops the controller is slower compared to the other. The advantage with the controller is that there is no peak initially in x_{egr} when the $p_{im,ref}$ is changed. These two characteristics are connected and changing one of them will affect the other.

It would be of interest to verify the peak occurred when p_{im} changes fast. For example in transient B (Figure 6.2) where the EGR-ratio rises 120 % before drop down and all this under one second. Such fast changes seems unlikely for the EGR-ratio and are perhaps a model issue. The reason is that the EGR-ratio is cal-

culated with the mass flow and not the actual mass. If the mass flow changes fast the modeled EGR-ratio will change fast but the real EGR-ratio is slower because it take a while to change the mass in a volume.

7.1.5 Controller 5 - Max-selector for the wastegate

The last controller that was tested used a max-selector to control the wastegate. If the EGR-ratio is too low the wastegate closes to increase the pressure over the EGR-valve, which increases the EGR-flow. The biggest impact can been seen for transient D where a step in the EGR-ratio is performed. The controller closes the wastegate which should increase the EGR-ratio, and a careful look shows that the EGR-response is faster at the beginning. After the initial peak the wastegate starts to open up because of the error in the EGR-ratio decreases. At the same time the pressure ratio over the throttle has decreased which implicates that the other PID, that controls the wastegate, will take longer time before it reacts. This makes the wastegate open more than for the feedback controller and the increasing EGR-ratio slows down and gets the same response time as for the feedback loops.

The initial behavior of the controller is right but the parametrization must be better. This type of controller can also be used if the reference to the pressure ratio over the throttle is set to a higher value. In that case, the EGR-valve may has problem to achieve the right EGR-ratio and this controller will close the wastegate so the wanted EGR-ratio can be reached. Higher pressure ratio implies lower fuel consumption. Therefore, it could be of interest to has as high pressure ratio over the throttle as possible and only decreases Π_{th} when the right EGR-ratio cannot be reached.

7.2 Controller parametrization

During this work only one operating mode has been selected and used to parameterize the PID-controllers. To improve the performance over the whole operating region dependent PID-variables could be one useful technique. The dependency could be the engine operating mode, for example the engine speed and the pressure in the intake manifold. There could also be a dependency from the EGR-ratio. This can easily be done from the model where different operating modes can give different PID-parameters. In the parameterization method used in this thesis, there is an optimization variable λ. The λ-parameter changes the speed of the controller and because of the non-linearities in the system, as different response time, this should be adjusted for each operating mode to optimize the controller. This is not investigated and perhaps could the parameter be the same for the whole operating region and still reach good results.

Implementing the controller in the real engine would probably require calibration of the PID-controllers. If the model represents the engine well the parameters might be used, but would probably not give the ”optimal” results.

7.3 Sensitivity analysis

The sensitivity analysis performed in this thesis is simple and just give a hint how the controllers would react on errors in the measurements and the model. The disturbance of the measured x_{egr} gives oscillation for the EGR-valve. The controller still has the same behavior. The stationary error comes from the offset that is added to the measured signal.

Disturbances in p_{im} and p_{ic} react in a similar way as for the disturbances in x_{egr}. The throttle and wastegate oscillate but the behavior is still the same. The gain added to the wastegate displace the effective area and the wastegate must close more to achieve the same result. Except for this, the dynamic behaviors during the transient the same as for the controller with the original effective area.

The analysis shows that the controller still works despite the disturbance. The actuator will start to oscillate which is not preferred. One way to solve this is to low-pass filter, before feedback, the measured signal. Offset errors are more difficult to solve and need different kind of adaptations to get rid of.

7.4 Comparison with existing controller

Two transients are presented in Section 6.3. Doing a fair comparison is difficult due to the difference between the model and the real engine. In the real engine there are also a lot of phenomenon that does not occur in the model. For example is there no disturbance on the measured signals in the model.

The first transient, presented in Figure 6.8, shows that the p_{im}-controller for the model is faster than the real engine. Also notice that the overshoot is bigger for the model. For the EGR-ratio the model follows the reference value better, even if the EGR-controller cannot compensate for the increased p_{im}. The real engine opens up the EGR-valve a lot already when the $p_{im,ref}$ change. There seems to be some kind of feedforward part to control this. The EGR-ratio peaks before the p_{im} has been stabilized. The total control strategy also work in different way. The model opens up the throttle and does not use the wastegate so much. The real engine do the opposite and keep the throttle more closed. One interesting thing is the Π_{th}. Initially both have the same value but during the transient the model increases more, this should be the case because the throttle is more open in the model which increases the pressure ratio. The controller in the engine ends up in a different value. The reference for the engine goes to a higher value than before the transient. This gives another degree of freedom and more options for the controller, which has not been tested in this thesis.

The second transient, presented in Figure 6.9, shows that the p_{im}-controller for the model and the engine is close to each other. The response time is almost the same, a little bit faster for the real engine. The model has en overshoot but the real engine on the other hand drop a little before its reach the final value. The throttle seems to close down (t = 1249 s) and therefore drops the pressure in the intake manifold.

The EGR-ratio on the other hand is similar to the first transient. For the engine

peaks the EGR-ratio the $p_{im,ref}$ is changed and the EGR-valve open up. For the model, the EGR-tracking drops in the middle of rising part (around t = 1249 s). This is because the p_{im} slows down and the wastegate will open up to keep the same pressure ratio over the throttle. The pressure in the exhaust manifold will decrease which decreases the pressure drop over the EGR-valve and also the EGR-flow. This effect could be avoided with the max-selector presented in controller number 5. The EGR-ratio for the model never reaches the final value, there is some errors in the model that make the pressure ratio over the EGR-valve too low and the EGR-flow cannot increase. This gives an indication that the model and the real engine differ.

To summaries the performance the controllers differ a lot. The p_{im} controller are closest to each other and which one is best depends of the operating mode. For the controller in the model the parameters in the PID-controllers are quantified for only one operating mode, and depending parameters would maybe increase the performance. Measuring the EGR-ratio in the engine is difficult and during transients the measurements can give strange values. Therefor, it is hard to say which controller gives the best performance. One thing is that the strategy differ according how to reach the right reference signals.

7.5 Proposed control strategy

The proposed control strategy to achieve good controller performance is to use a combination of controller number 1,2 and 4 in Table 5.1. The controller will contain feedback loops with prefiltered $p_{im,ref}$ and a feedforward part from $x_{egr,ref}$. The prefiltered part will reduce the peaks for x_{egr} during p_{im} transients. Notice that the rise time will also be decreased for p_{im}. The feedforward part will improve the EGR-following during EGR-transients and give faster EGR-response. The disadvantage with this is the increased overshoot for the EGR-ratio. Overall the controller will give faster response for the EGR-loop with fewer peaks. But the cost is slower response for the p_{im} tracking. The result of this controller can be found in Figure 7.2 for transient F in Table 6.1. The red line is the proposed controller while the blue lines show the controller number 1-5 in Table 5.1 and the black lines the reference signals. The peak in x_{egr} is reduced and it also reaches the set-value faster. The p_{im} controller, on the other hand, is slower.

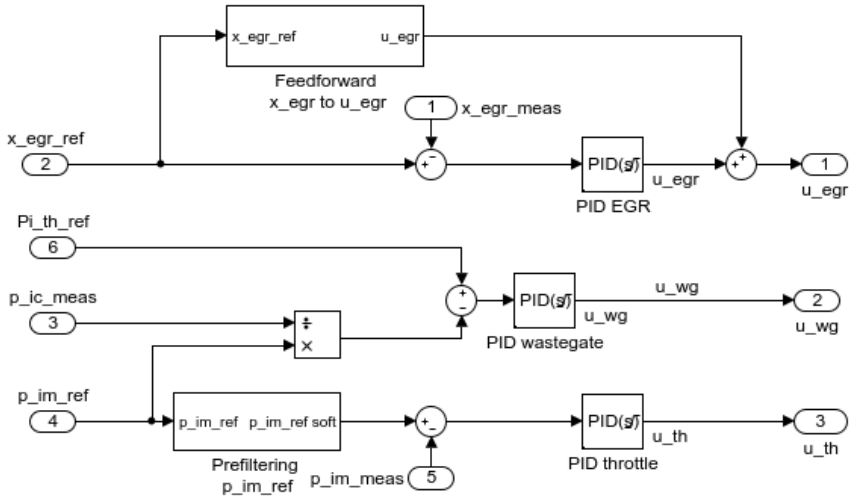

Figure 7.1: *Control structure of the proposed controller with feedback loops, feedforward part from $x_{egr,ref}$ to u_{egr} and prefiltering the $p_{im,ref}$.*

This control strategy is based on a balance between performance in the p_{im} and x_{egr} response from a controller perspective. The strategy should maybe be different depending on the controller's goal. The driver would, for example, has fast response for the p_{im}, that means faster torque response. If the engine could handle a more diverse EGR-ratio this could be preferred. If the engine is sensitive to the right EGR-ratio the control loop for the p_{im} must be slow downed so the EGR-controller could follow the EGR-reference. As for all controller problems there are always a balance between different performance variables, when there is cross connection between control signals. This together with the different dynamics in the actuators and all the non-linearities make it a difficult control problem.

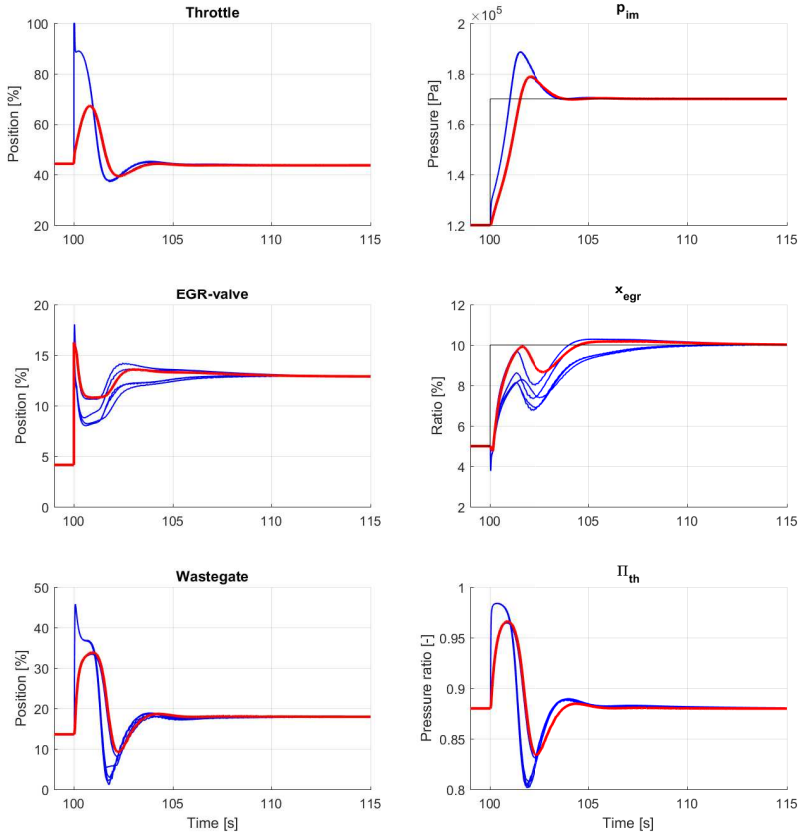

Figure 7.2: *The red lines show the result of the proposed controller and the blue lines controller number 1 to 5 from Table 5.1 for transient F in Table 6.1. The black lines are the reference signals.*

8

Conclusion and Future Work

The last chapter answers the questions asked in Chapter 1 and contains the conclusions of the thesis. There is also a section with thoughts abouts future work regarding the results from the thesis.

8.1 Conclusion

The questions investigated in this thesis are listed and answered below.

1. **Which non-linearities have the system?**
   Three types of non-linearities have been studied in this thesis. These are presented in Chapter 4 and are different non-minimum phase behaviors, different rise time and different DC-gain which also result in sign reversals in some operating modes.

2. **How could a controller be designed based on the system analysis?**
   A control strategy with feedback loops has been designed from the system analysis and is described in Chapter 5. The idea is that the EGR-valve controls the EGR-ratio, the throttle controls the intake manifold pressure and the wastegate the pressure ratio over the throttle. Further, some additional control strategies have been developed and tested where the conclusion was to add a feedforward part from the $x_{egr,ref}$ to u_{egr} and a prefilter part for $p_{im,ref}$. Both these options improved the EGR-regulation but slowed down the p_{im}-control.

3. **Is it possible to decrease the calibration time of the engine with this controller?**
   The proposed control strategy have a couple of PID-controllers and a model for how the EGR-valve affects the EGR-ratio. If the model developed in this

thesis is close to the real engine, the parameters could be found with the model and the method described in Chapter 5. Moreover, the difference between the model and the real engine will not make the controller "optimal" and therefore will calibration be needed before implementation in the real engine. The calibration time will not be decreased.

4. **Does the controller work even if part of the engine is changed?**
   This has been tested by changing the parameters in the wastegate model. The controller still works in the same way and the controllers are adapted. Robustness against disturbances have also been tested and the controller works but the actuators oscillate which is not preferred.

Besides the answered questions some more conclusions have been drawn. These are listed below.

- To achieve a good EGR-control the pressure in the intake manifold cannot change too fast. The EGR-valve is too slow and will not compensate for sudden changes in p_{im}. One way to compensate for this is to prefilter the $p_{im,ref}$ which increases the performance of the EGR-controller.
- To receive good results with feedforward, models of the behaviors are needed which differ a lot depending of the engines operating mode. If they are correct they improve the result, but on the other hand, can an incorrect model decrease the performance.

8.2 Future work

A short collection of notes of possible improvements and add-ons are listed below. These are suggestions on future works.

- **Improve the model**
  During modeling the model can always be improved and changed to better suit the real engine. The model provided in this thesis especially has two area of improvements. The first one is the temperature model for the exhaust gases. A temperature model that take into account the EGR-ratio and ignition timing would be of interest. Because this is affect the temperature leaving the cylinder. EGR is also used specific to lower the exhaust temperature and therefore it is of interest to has a temperature model depending of the EGR-ratio. The second submodel is the turbocharger with the wastegate that today has a very big uncertainty.

- **Test the parametrization on a real engine**
  The next step of developing a new controller, based on the model in this thesis, is to try it on a real engine. Would the parametrization work and will the control structure react in the same way for the model as for the real engine? This also gives an indication which part in the model that should be updated to simulate the real engine.

- **Parameterize with the system analysis**
  An interesting investigation would be to study if the system analysis could be used to quantify the parameters for the controllers. The analysis gives information about rise time and DC-gain which can be used to adapt a three parameter model. From this the parameters for the PID-controllers could be found. The analysis gives information for the whole operating area and dependent parameters could be taken from this. If the parameters found with this technique could be implemented in the real engine a lot of calibration time would be saved.

- **Control the EGR-ratio given the exhaust temperature**
  As mentioned in Chapter 1, one of the main focus of using EGR is to decrease the exhaust temperature. Today fixed values of EGR-ratio are used for different operating modes. An interesting technique would be to control the amount of EGR as a function of the exhaust temperature.

- **Extend the control structure**
  The controller can always be extended with new features and techniques. One thing that has not been investigated during this thesis is the set point of the pressure ratio over the throttle. Could this be changed and still get the same or better performance. This kind of analysis is preferred to do with an analysis of the fuel consumption. If the fuel consumptions is not considered it is easy to improve the controller by closing the wastegate and increase the pressure drop over the throttle.

Appendix

A

System analysis plot

A.1 DC-gain

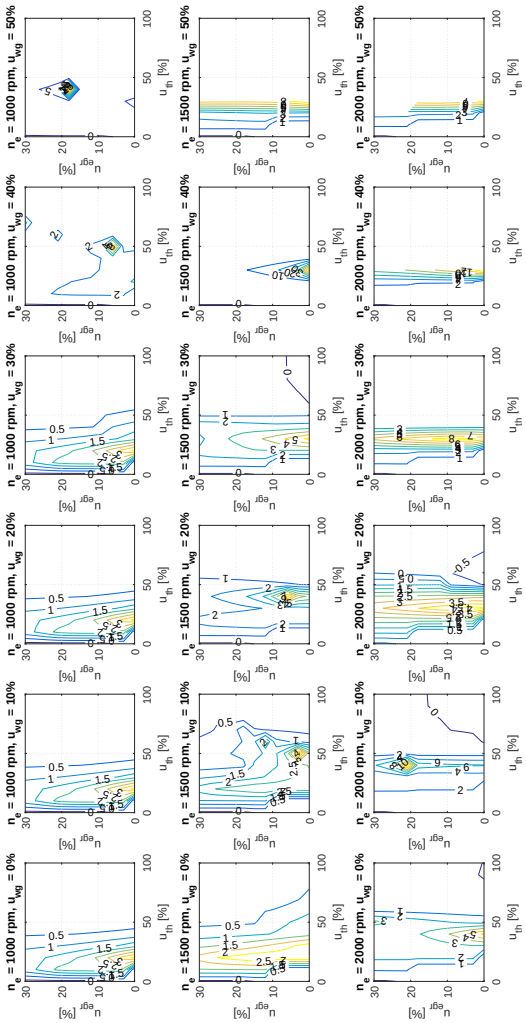

Figure A.1: *Contour plot of the DC-gain for the channel u_{th} to p_{im} at 6 different wastegate positions and 3 different engine speeds.*

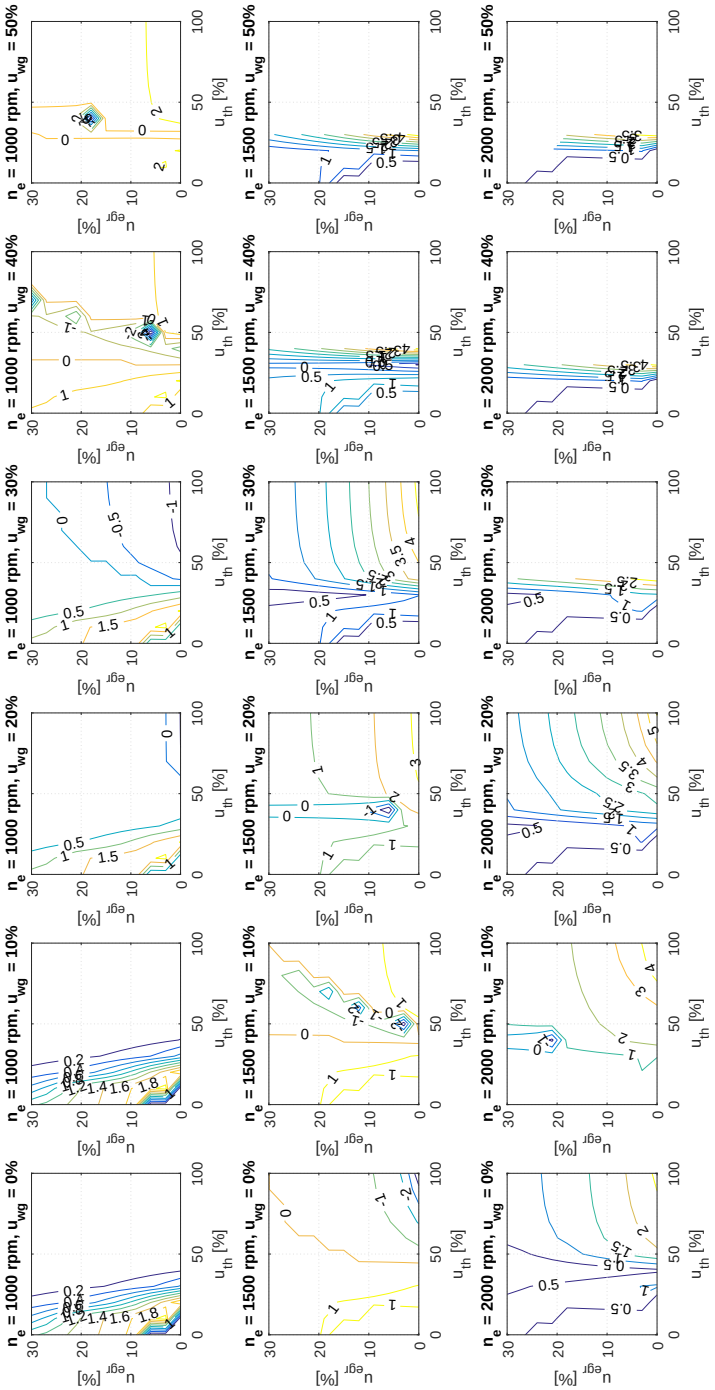

Figure A.2: *Contour plot of the DC-gain for the channel u_{egr} to p_{im} at 6 different wastegate positions and 3 different engine speeds.*

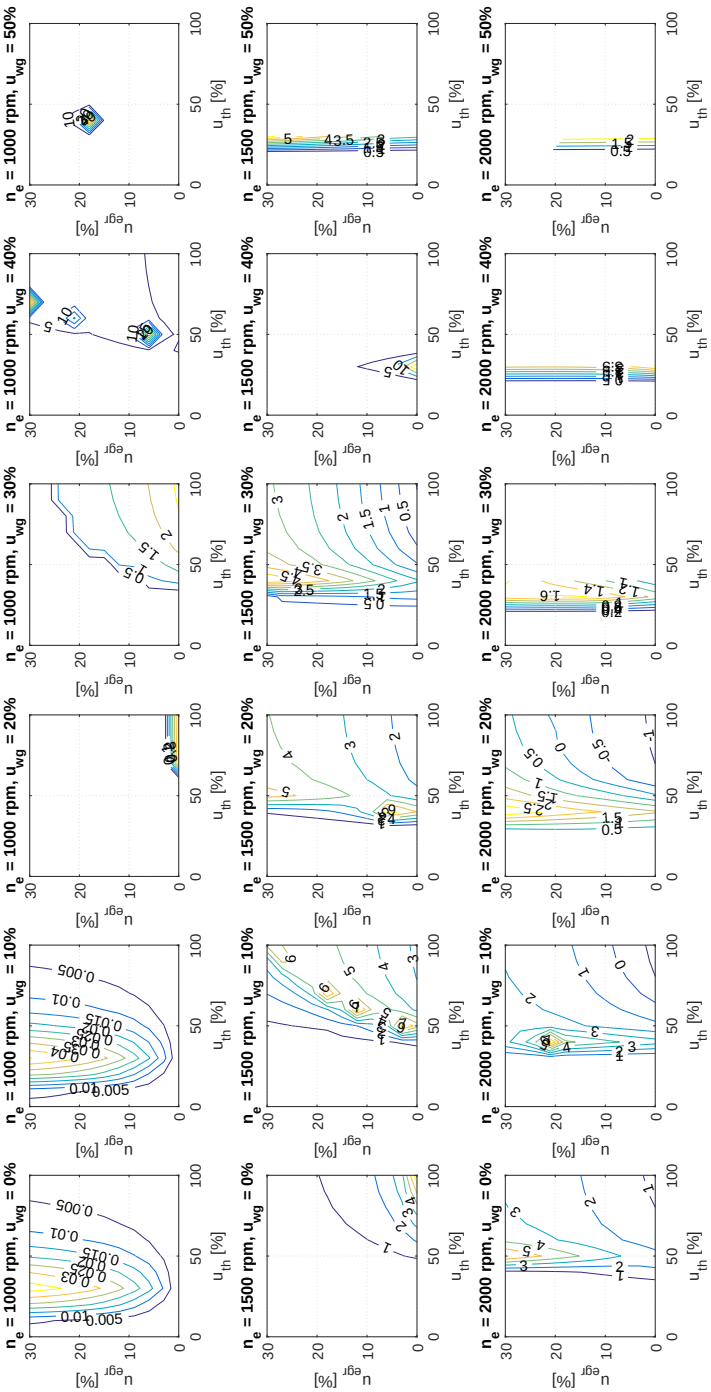

Figure A.3: *Contour plot of the DC-gain for the channel u_{wg} to p_{im} at 6 different wastegate positions and 3 different engine speeds.*

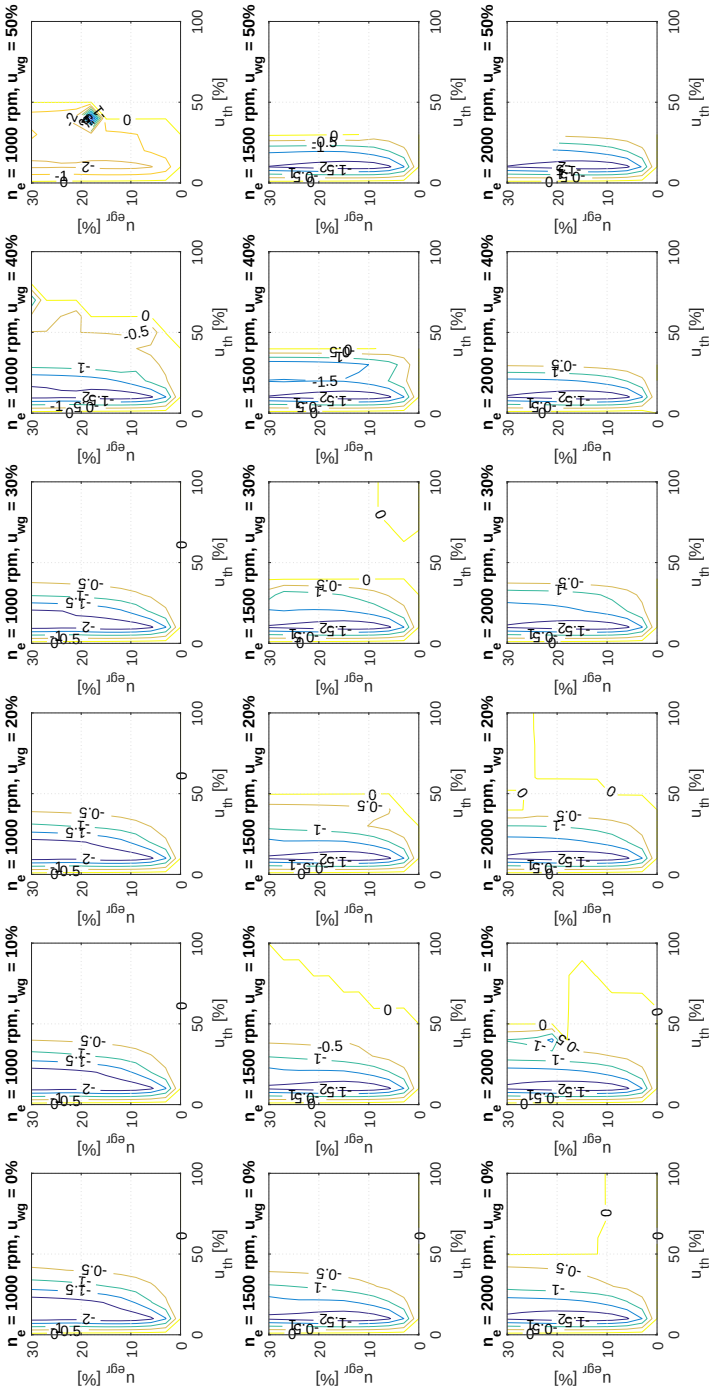

Figure A.4: *Contour plot of the DC-gain for the channel u_{th} to x_{egr} at 6 different wastegate positions and 3 different engine speeds.*

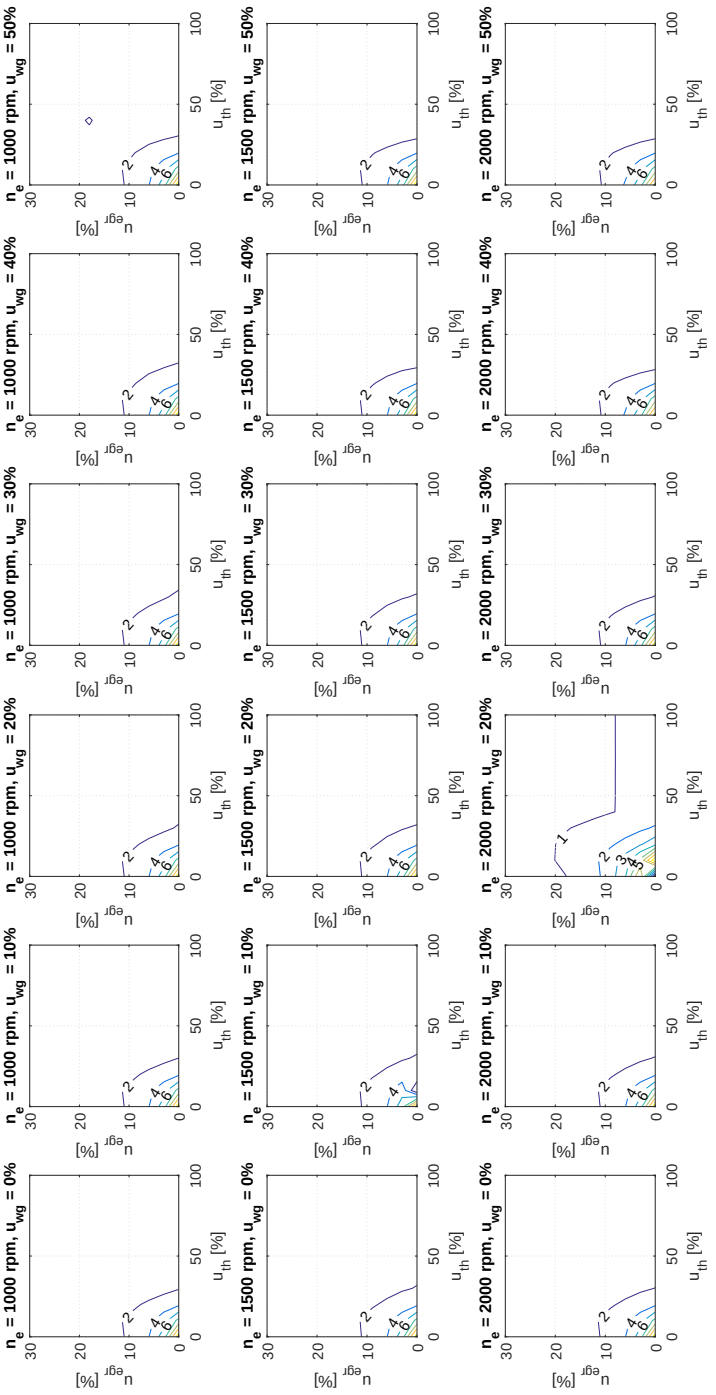

Figure A.5: *Contour plot of the DC-gain for the channel u_{egr} to x_{egr} at 6 different wastegate positions and 3 different engine speeds.*

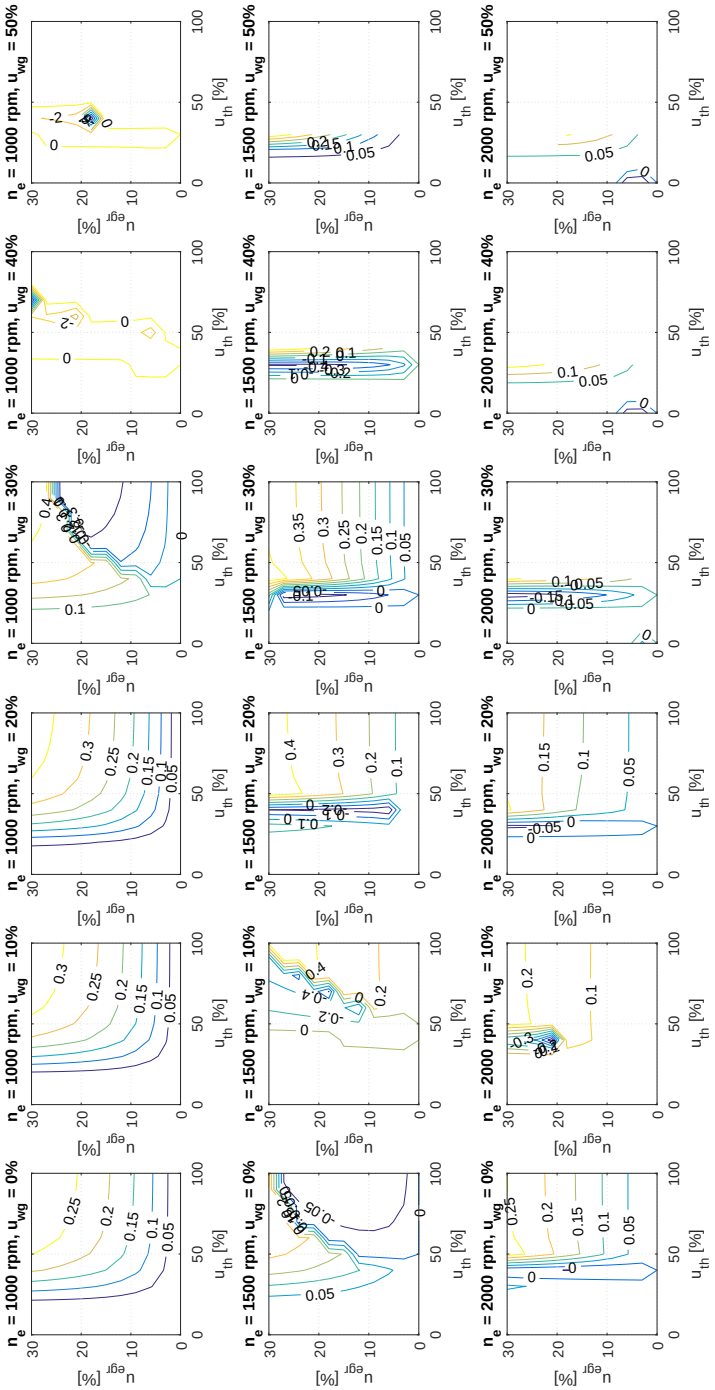

Figure A.6: *Contour plot of the DC-gain for the channel u_{wg} to x_{egr} at 6 different wastegate positions and 3 different engine speeds.*

A.2 Non-minimum phase behaviors

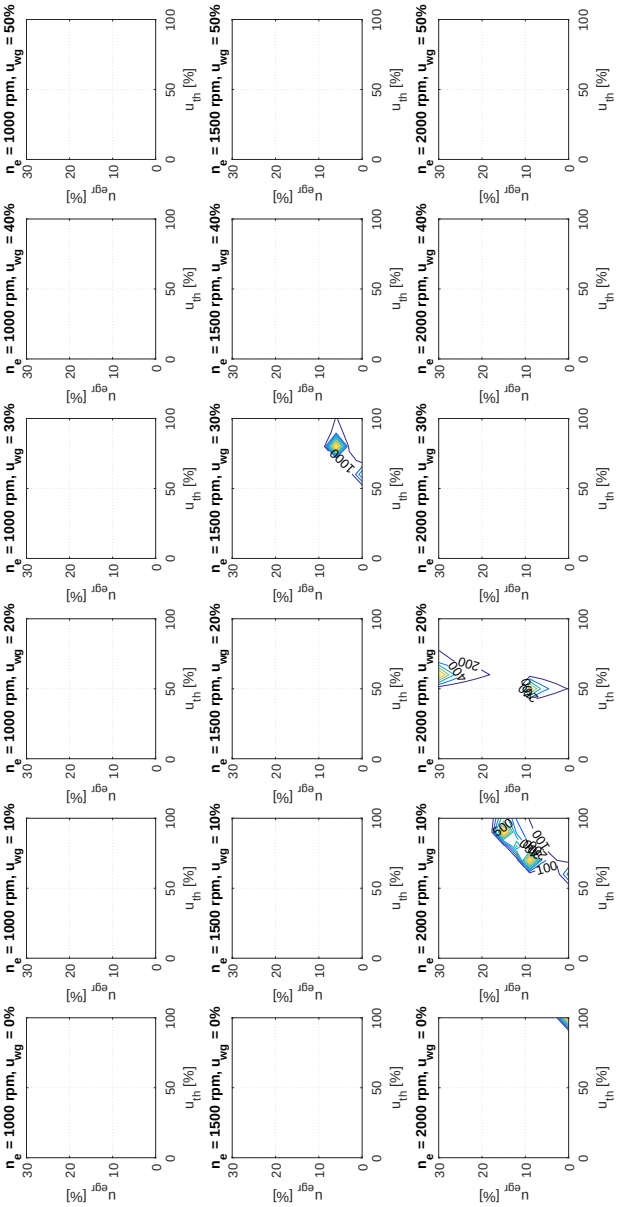

Figure A.7: *Contour plot of the undershoot for u_{th} to p_{im} for a unit step at 6 different wastegate positions and 3 different engine speeds.*

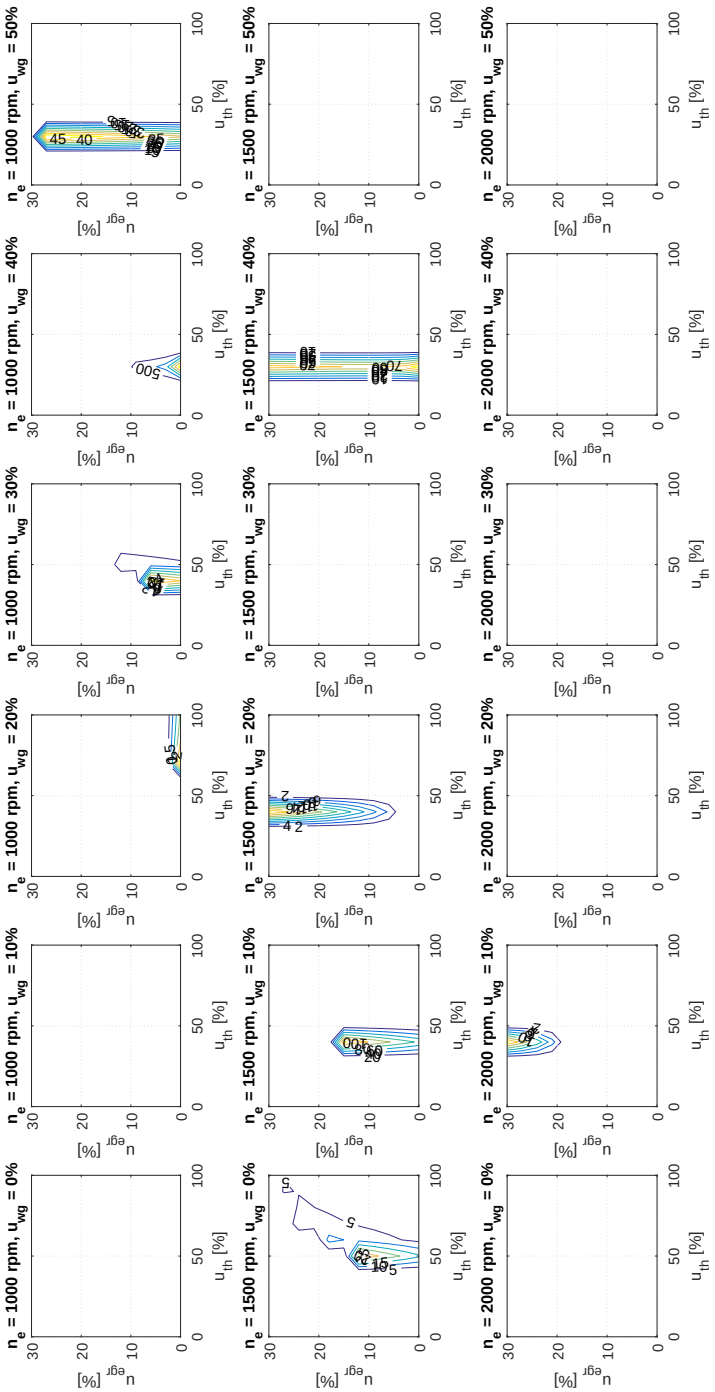

Figure A.8: *Contour plot of the undershoot for u_{egr} to p_{im} for a unit step at 6 different wastegate positions and 3 different engine speeds.*

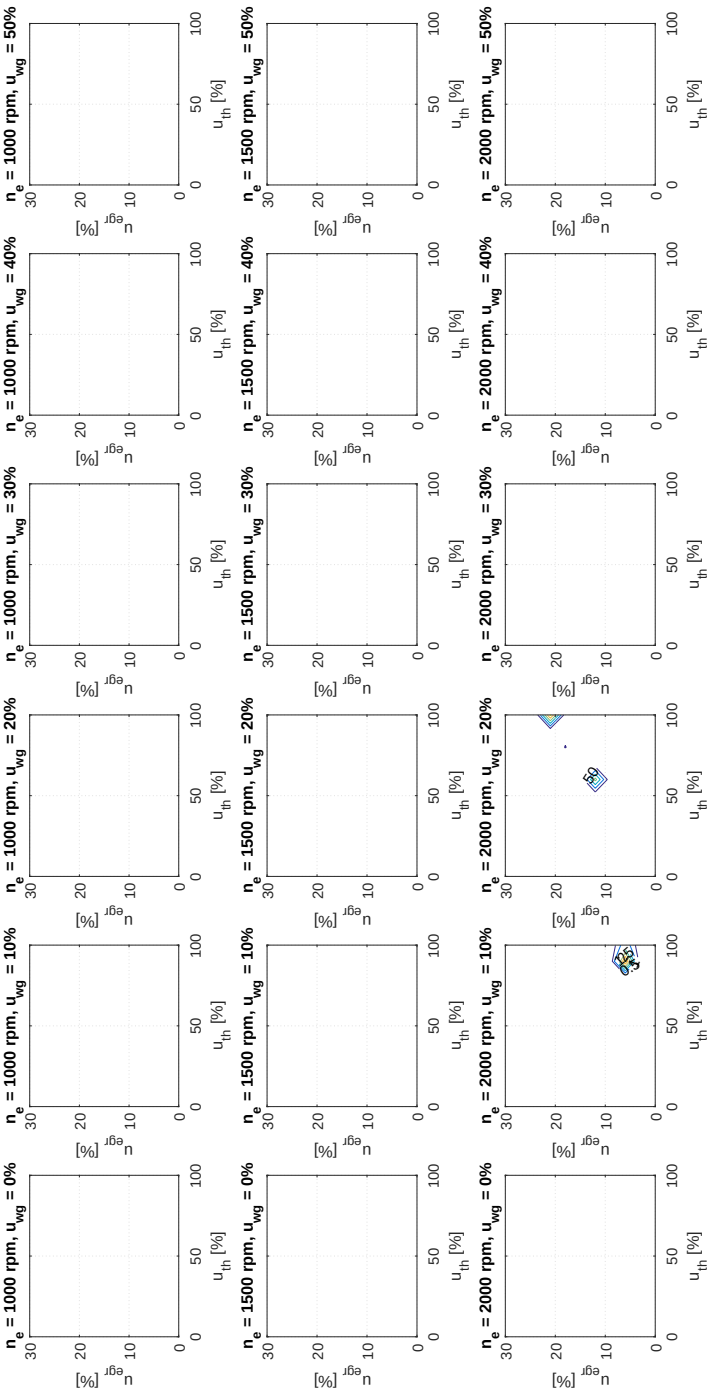

Figure A.9: *Contour plot of the undershoot for u_{wg} to p_{im} for a unit step at 6 different wastegate positions and 3 different engine speeds.*

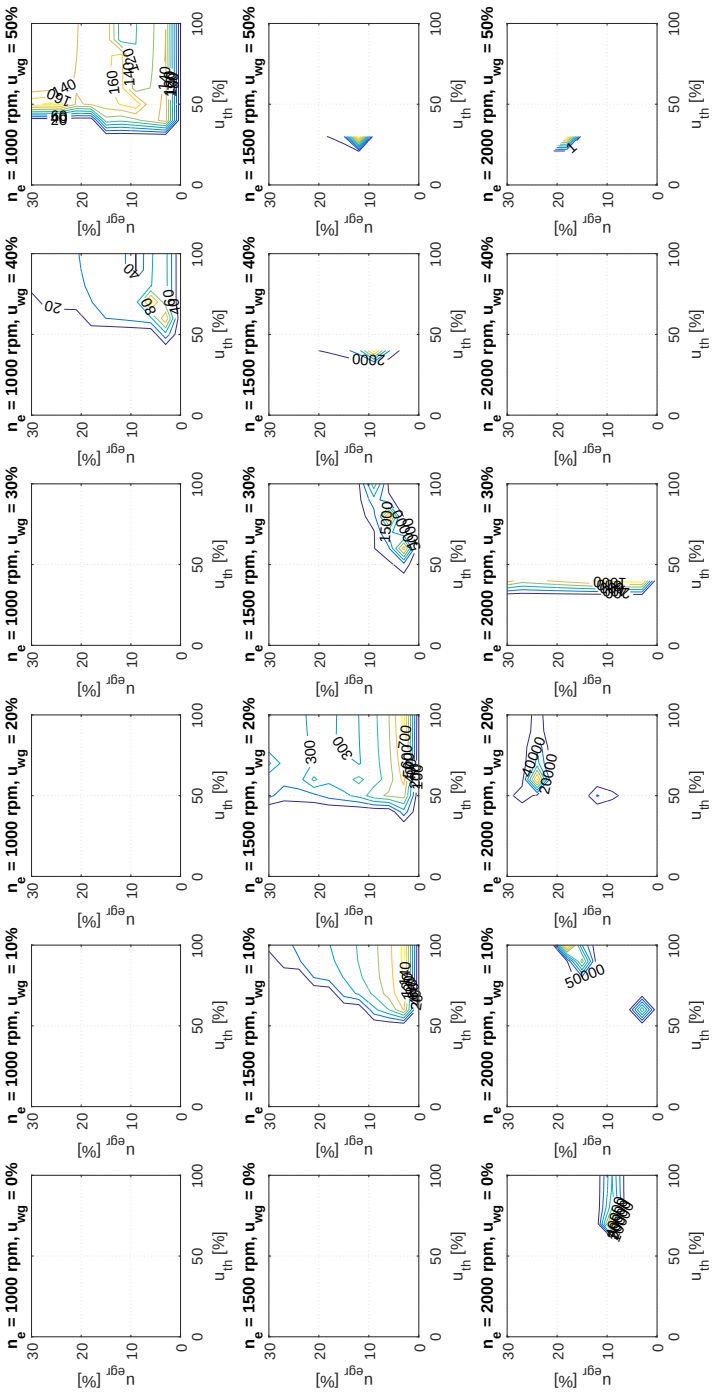

Figure A.10: *Contour plot of the undershoot for u_{th} to x_{egr} for a unit step at 6 different wastegate positions and 3 different engine speeds.*

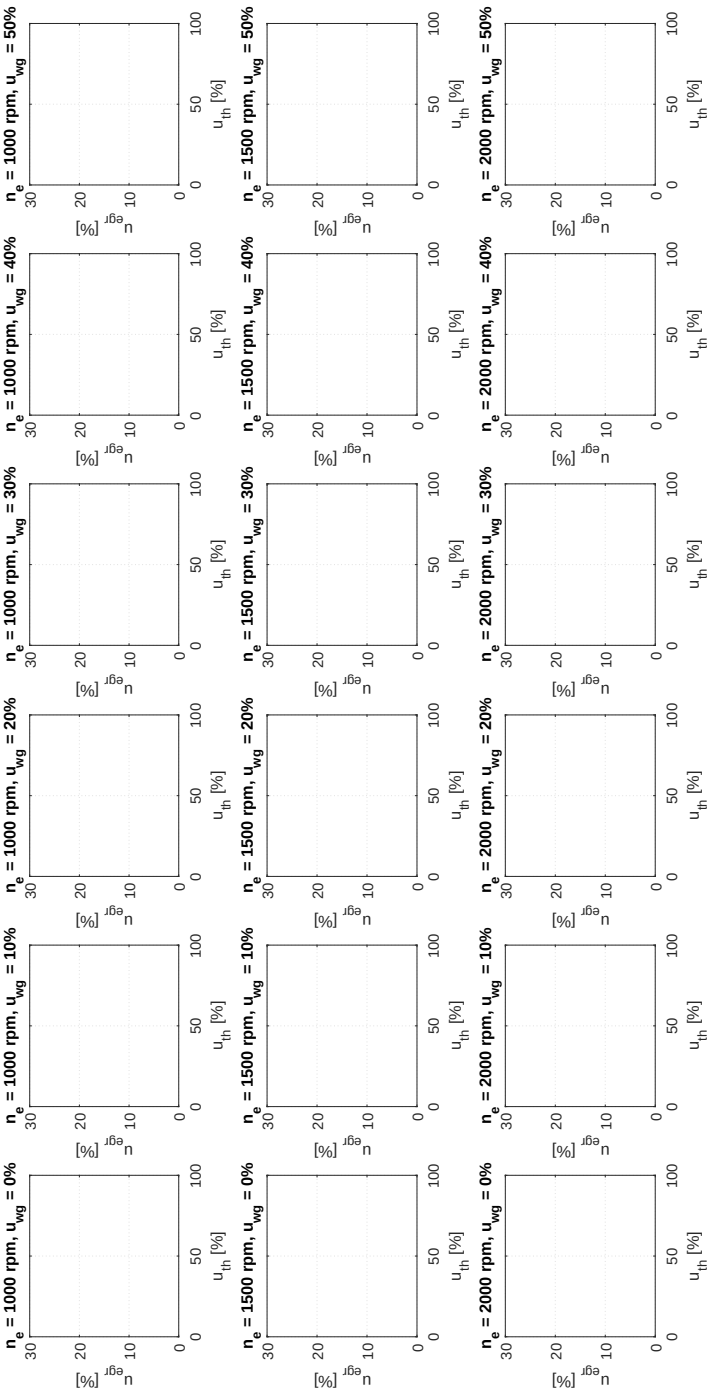

Figure A.11: *Contour plot of the undershoot for u_{egr} to x_{egr} for a unit step at 6 different wastegate positions and 3 different engine speeds.*

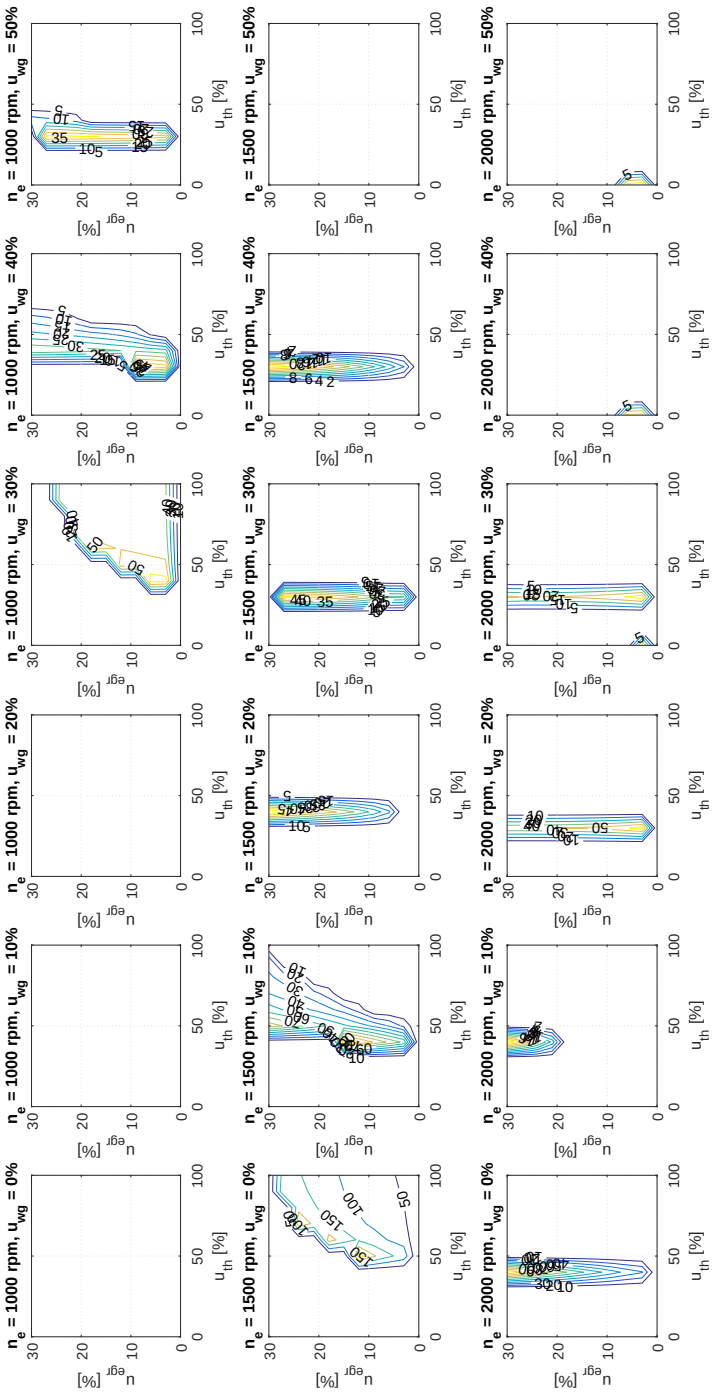

Figure A.12: *Contour plot of the undershoot for u_{wg} to x_{egr} for a unit step at 6 different wastegate positions and 3 different engine speeds.*

A.3 Response time

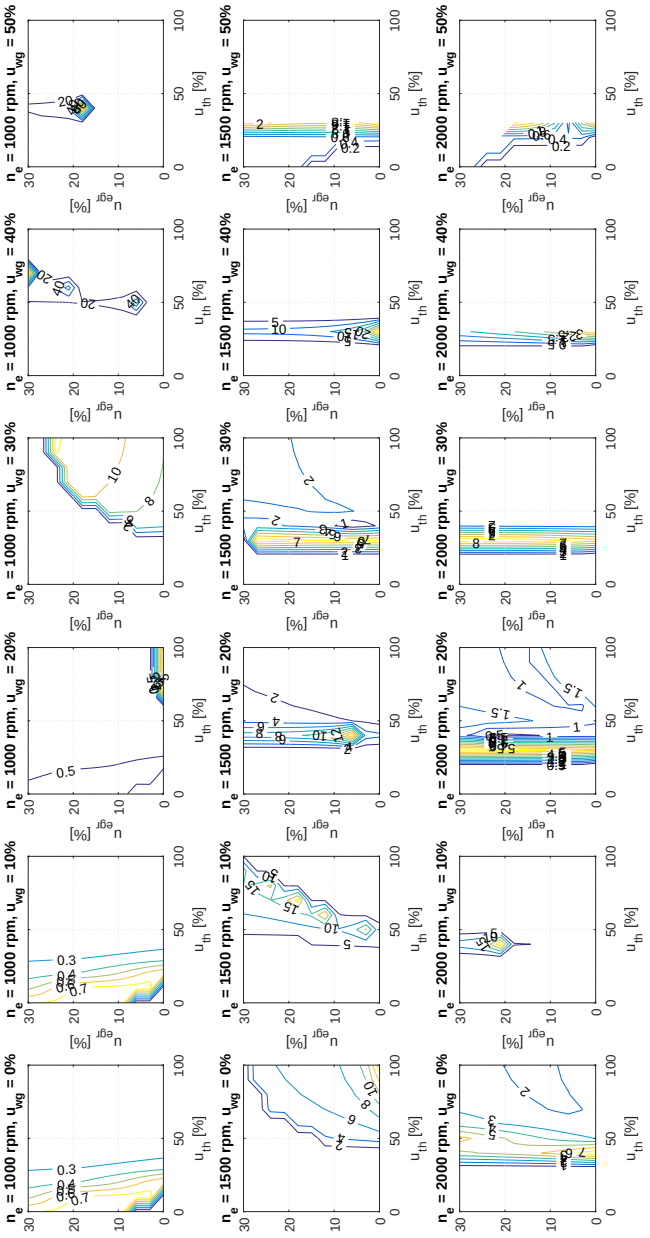

Figure A.13: *Contour plot of the time constant for u_{th} to p_{im} of a unit step at 6 different wastegate positions and 3 different speeds.*

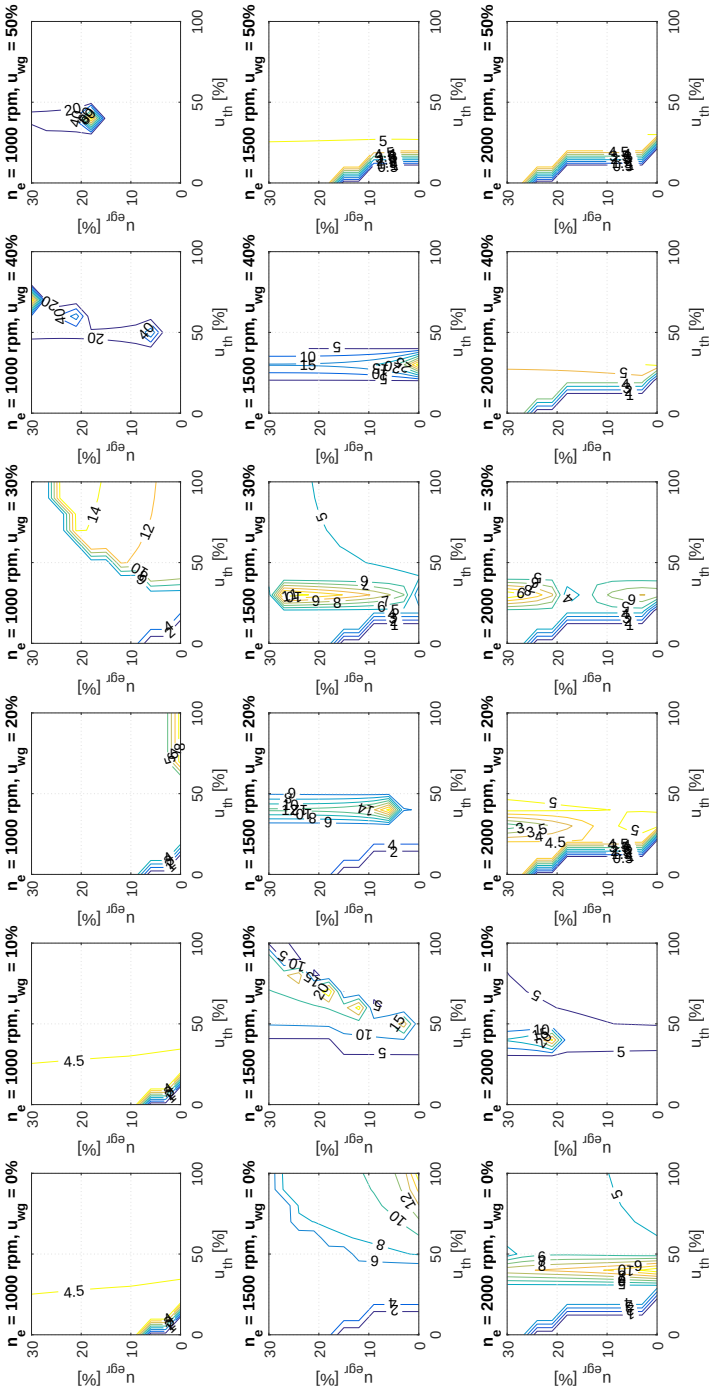

Figure A.14: *Contour plot of the time constant for u_{egr} to p_{im} of a unit step at 6 different wastegate positions and 3 different speeds.*

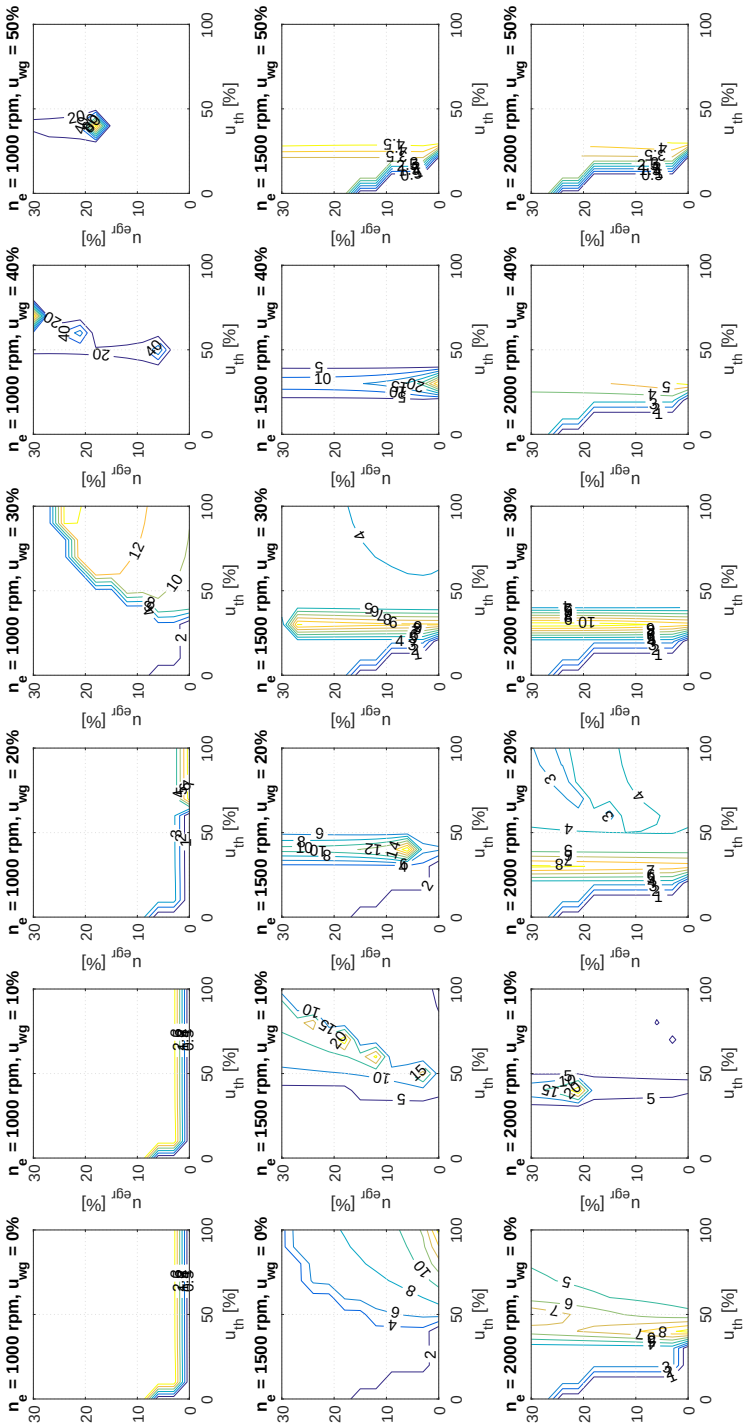

Figure A.15: *Contour plot of the time constant for u_{wg} to p_{im} of a unit step at 6 different wastegate positions and 3 different speeds.*

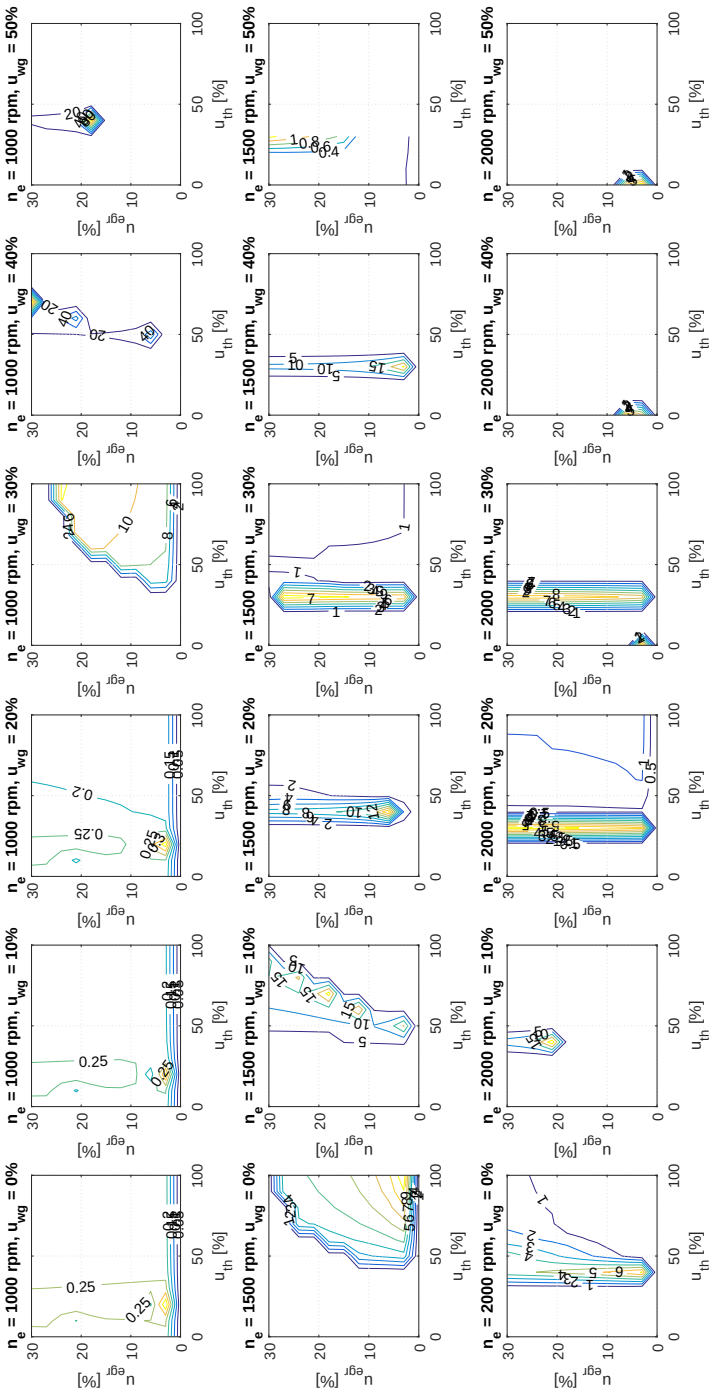

Figure A.16: *Contour plot of the time constant for u_{th} to x_{egr} of a unit step at 6 different wastegate positions and 3 different speeds.*

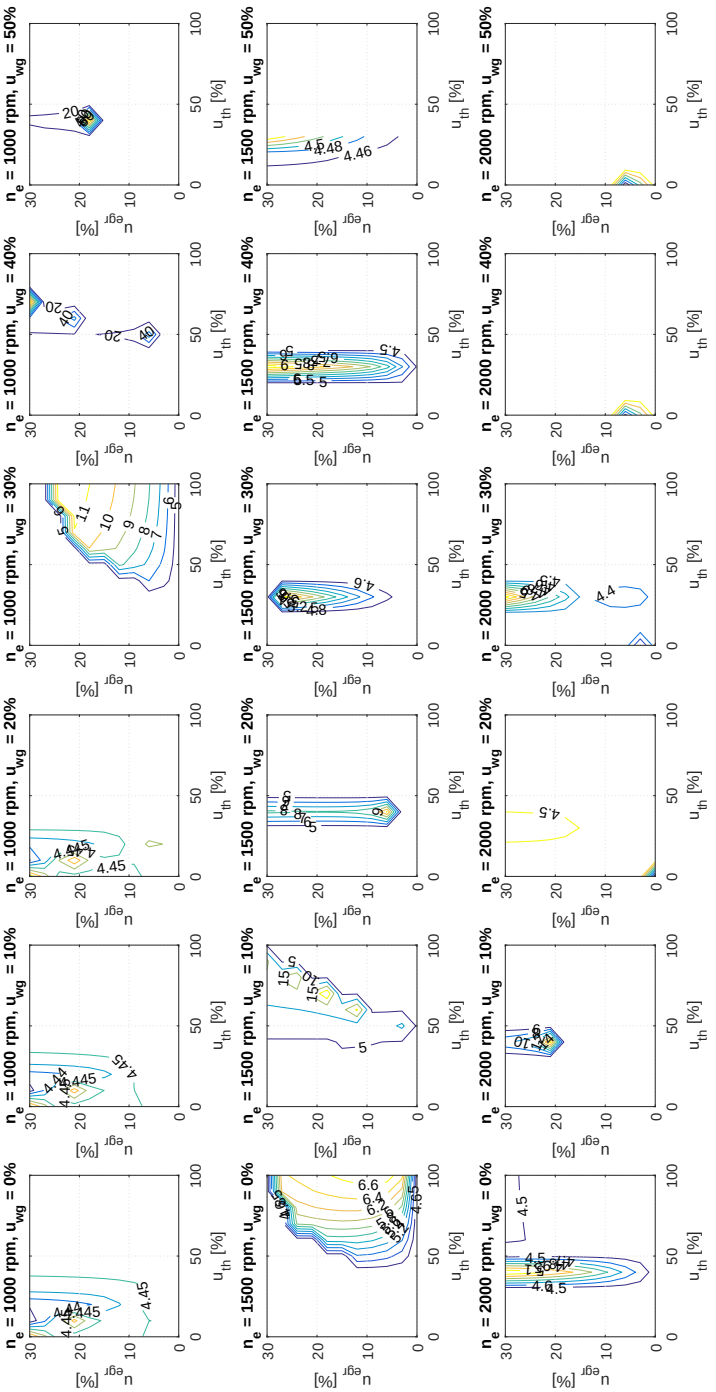

Figure A.17: *Contour plot of the time constant for u_{egr} to x_{egr} of a unit step at 6 different wastegate positions and 3 different speeds.*

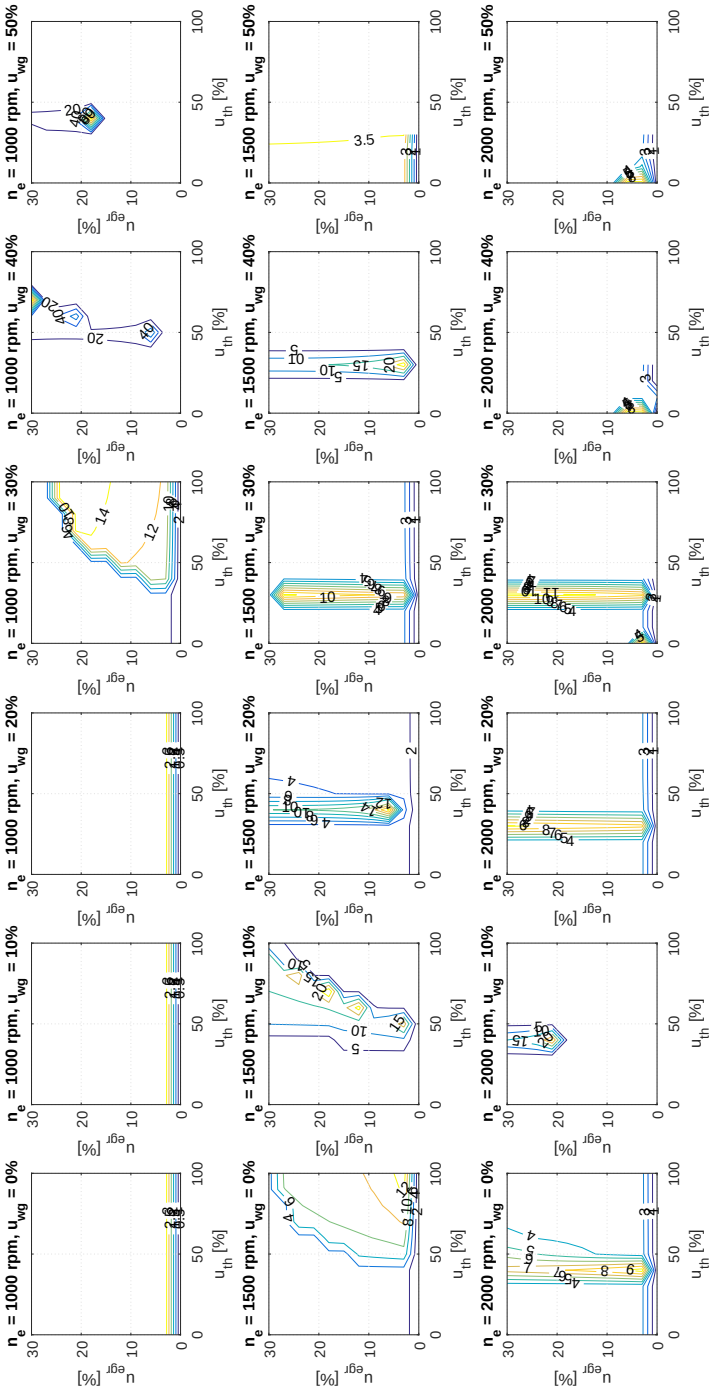

Figure A.18: *Contour plot of the time constant for u_{wg} to x_{egr} of a unit step at 6 different wastegate positions and 3 different speeds.*

A.4 RGA

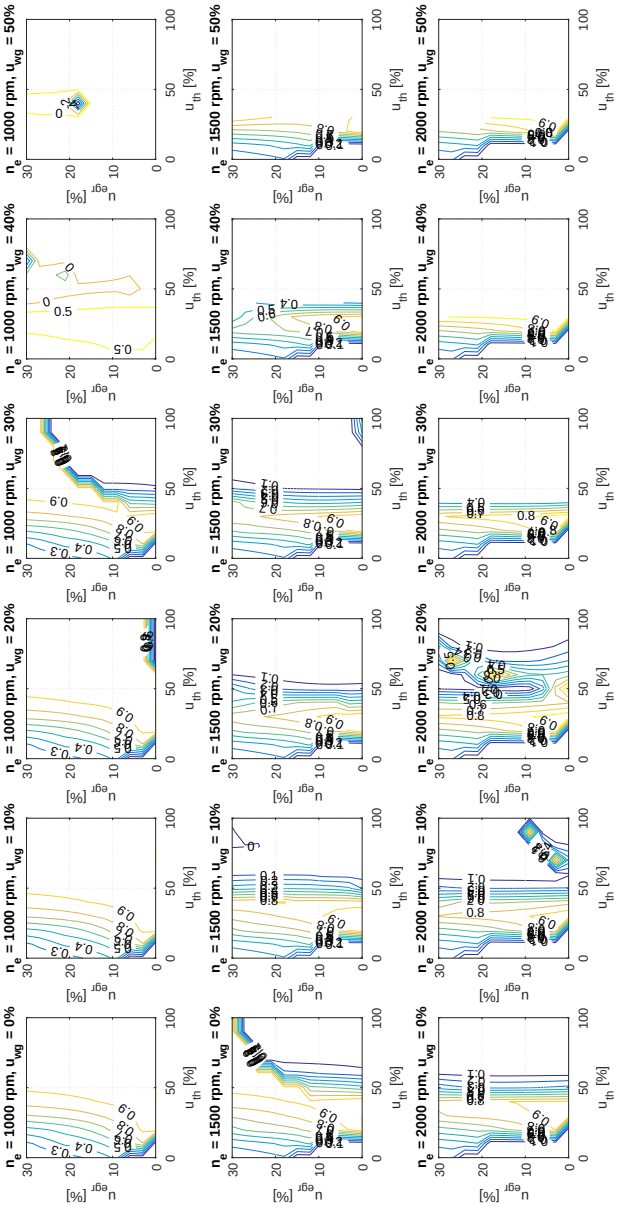

Figure A.19: *RGA analysis for channel u_{th} to p_{im} stationary at 6 different wastegate positions and 3 different speeds.*

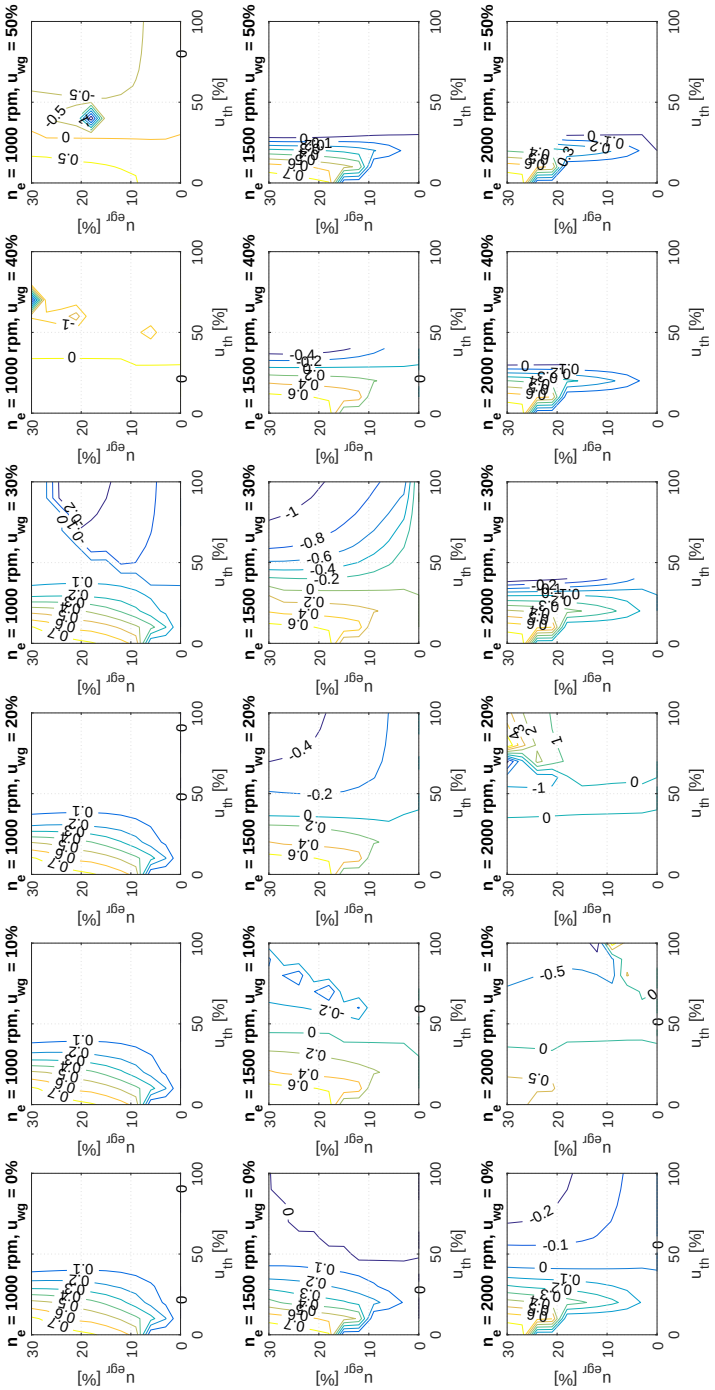

Figure A.20: *RGA analysis for channel u_{egr} to p_{im} stationary at 6 different wastegate positions and 3 different speeds.*

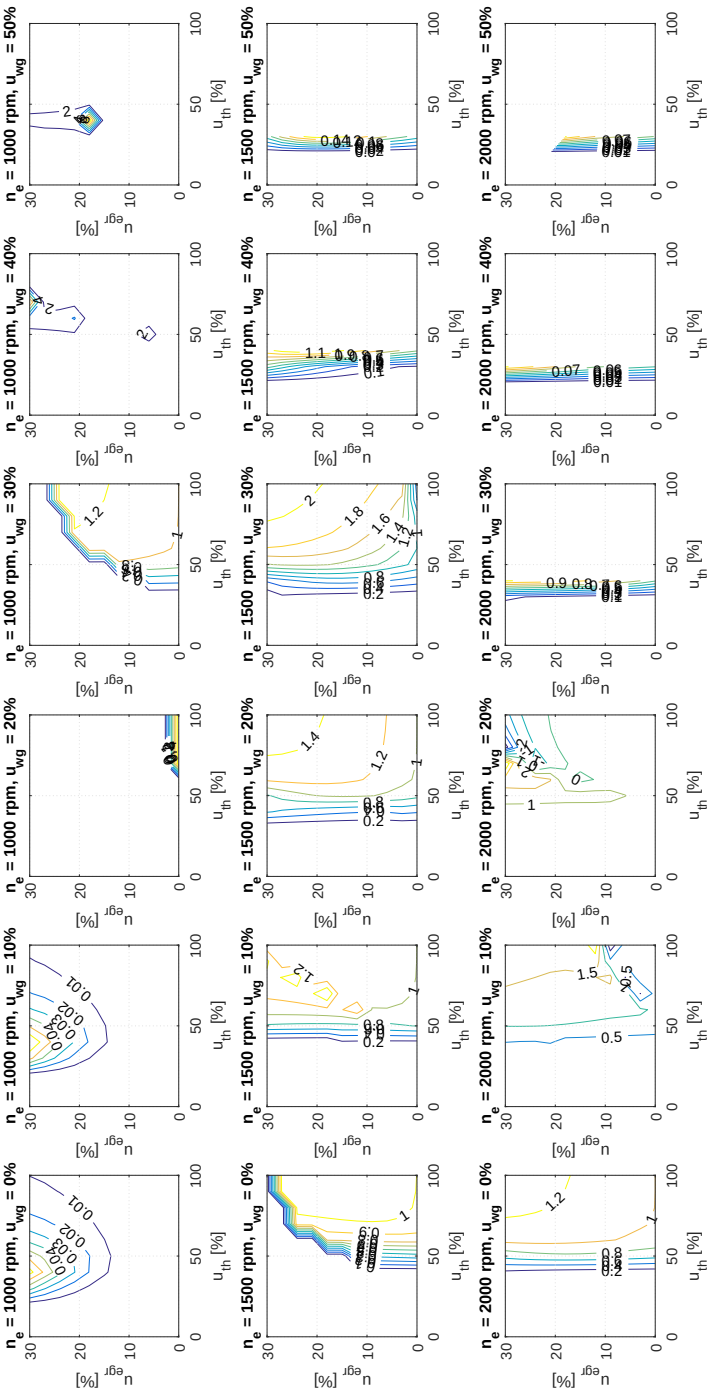

Figure A.21: *RGA analysis for channel u_{wg} to p_{im} stationary at 6 different wastegate positions and 3 different speeds.*

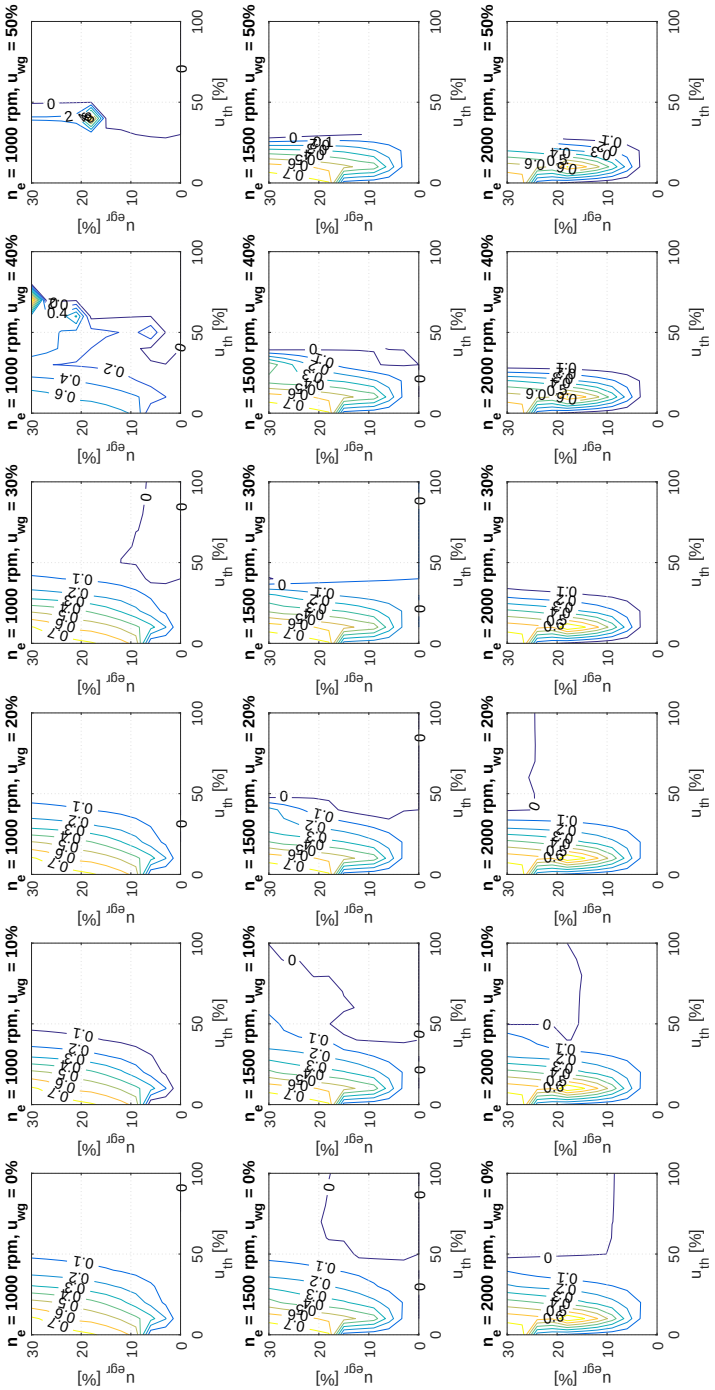

Figure A.22: *RGA analysis for channel u_{th} to x_{egr} stationary at 6 different wastegate positions and 3 different speeds.*

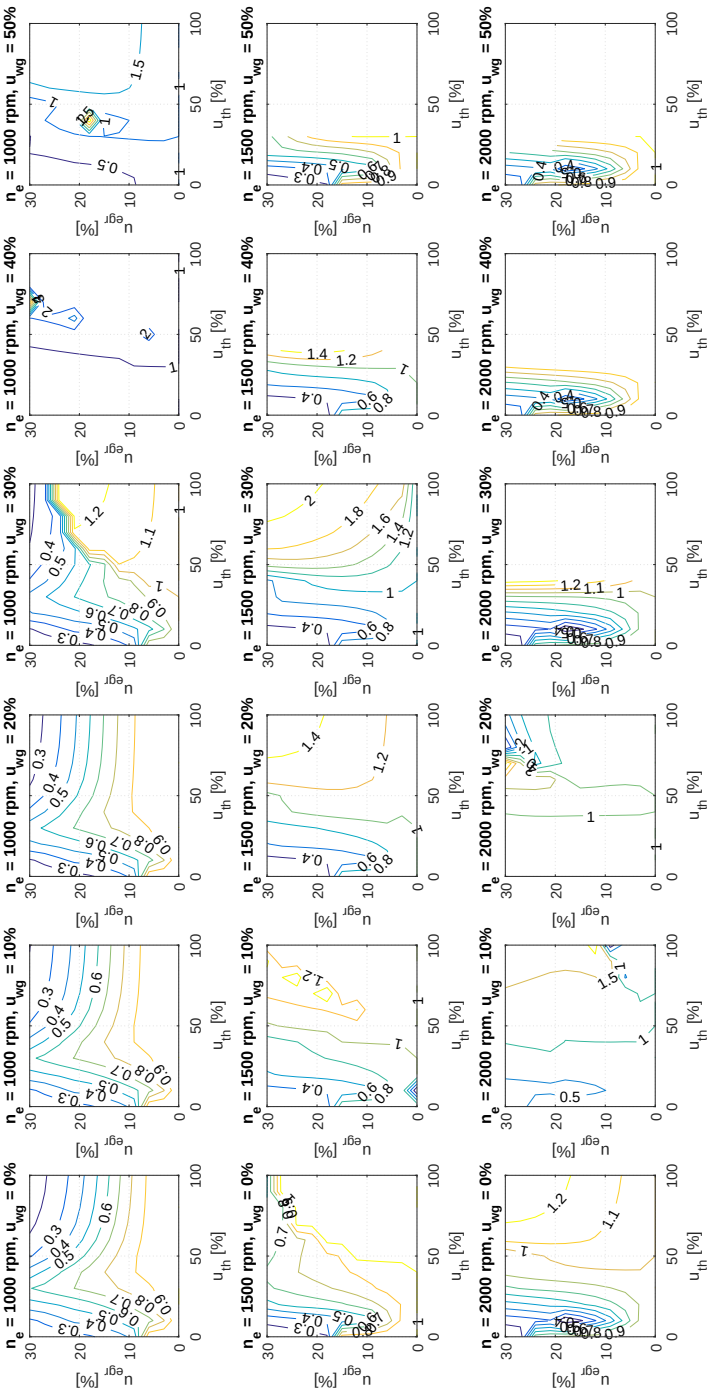

Figure A.23: *RGA analysis for channel u_{egr} to x_{egr} stationary at 6 different wastegate positions and 3 different speeds.*

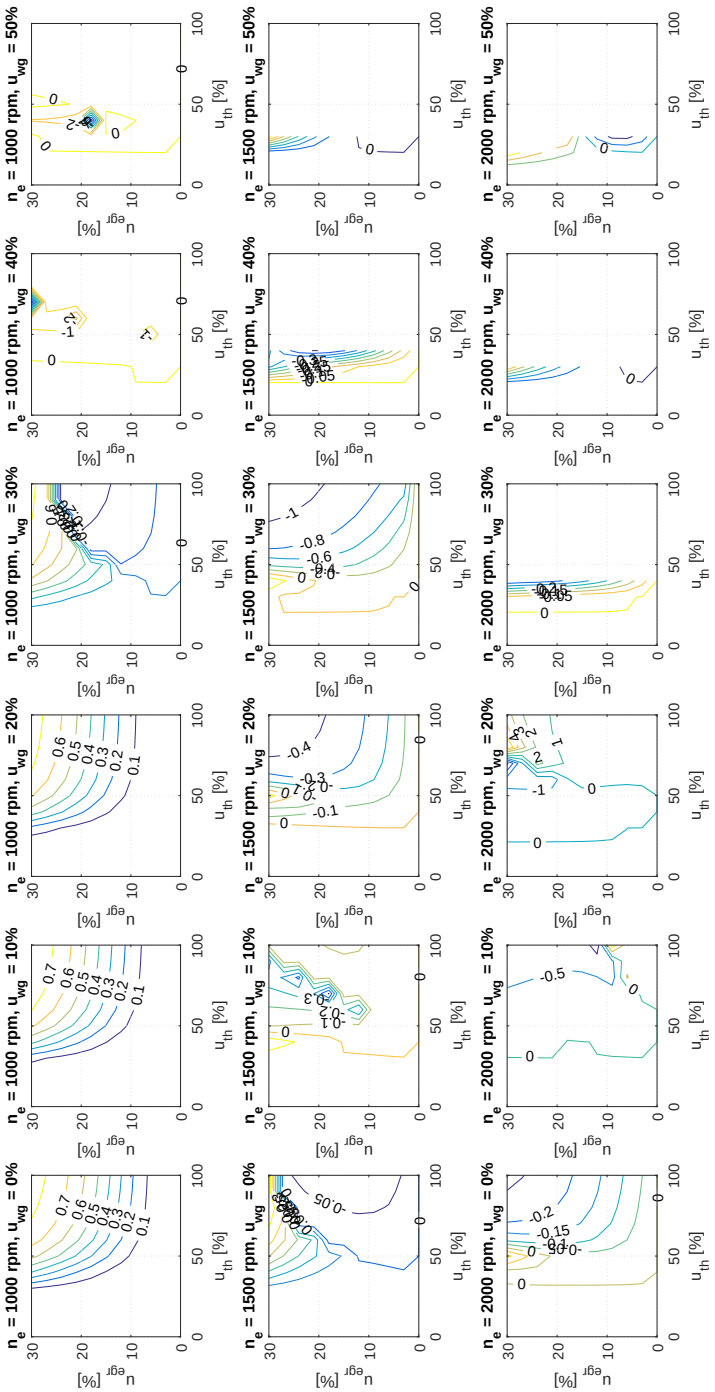

Figure A.24: *RGA analysis for channel u_{wg} to x_{egr} stationary at 6 different wastegate positions and 3 different speeds.*

B

Transient - rise time and overshoot

In Table B.1 to B.4 can the overshoot and the rise time for p_{im} and x_{egr} be found for the different transients made in Section 6.1. In the cases there are no transient for the given signal the overshoot present the biggest deviation from the reference value in percentage.

Table B.1: *Overshoot for p_{im} in % of final value.*

Controller	1	2	3	4	5
Step 1	14.2681	14.2860	14.0381	11.5575	13.8567
Step 2	2.8691	2.8699	2.8851	1.4605	2.8182
Step 3	5.2349	5.3233	5.3672	7.1335	5.3780
Step 4	0.2626	0.4177	0.2618	0.2613	0.6967
Step 5	0.2597	0.3463	0.2474	0.2474	0.2538
Step 6	10.9533	10.9454	10.9114	4.9776	10.9553

Table B.2: *Rise time for p_{im} in seconds.*

Controller	1	2	3	4	5
Step 1	1.1415	1.1407	1.1459	1.4542	1.1424
Step 2	0.0844	0.0841	0.0842	0.7955	0.0800
Step 3	1.1440	1.1440	1.1489	1.2675	1.1441
Step 4	-	-	-	-	-
Step 5	-	-	-	-	-
Step 6	0.6750	0.6796	0.6753	1.0654	0.6754

Table B.3: *Overshoot for x_{egr} in % of final value.*

Controller	1	2	3	4	5
Step 1	24.7856	24.2007	16.1490	23.4294	15.9962
Step 2	132.2324	132.5861	132.2589	15.1054	132.5375
Step 3	-	-	-	-	-
Step 4	0.3866	3.4049	0.3870	0.4016	0.4918
Step 5	0.5607	18.9070	0.5399	0.5520	0.5368
Step 6	0.1012	2.8701	2.3650	0.0896	0.3006

Table B.4: *Rise time for x_{egr} in seconds.*

Controller	1	2	3	4	5
Step 1	-	-	-	-	-
Step 2	-	-	-	-	-
Step 3	-	-	-	-	-
Step 4	2.4218	1.3364	2.4220	2.4217	2.6468
Step 5	2.6908	1.4879	2.6942	2.6958	2.6932
Step 6	1.2955	0.6070	1.0050	1.3558	3.6849

Bibliography

[1] P. Andersson. *Air Charge Estimation in Turbocharged Spark Ignition Engines*. PhD thesis, Linköping University, Linköping, Sweden, 2005. Cited on page 2.

[2] D. Dyntar, C. Onder, and L. Guzzella. Modeling and Control of CNG Engines. *SAE Paper, 2002-01-1295*, 2002. Cited on page 8.

[3] L. Eriksson. Mean Value Models for Exhaust System Temperatures. *SAE Paper, 2002-01-0374*, 2002. Cited on page 24.

[4] L. Eriksson. Modeling and Control of Turbocharged SI and DI Engines. *Oil Gas Sci. Technol. - Rev. IFP*, 62(4):523–538, 2007. Cited on page 7.

[5] L. Eriksson and L. Nielsen. *Modeling and control of engine and drivelines*. Wiley, first edition, 2014. Cited on pages 7, 8, 11, 16, 23, 25, 26, 29, and 46.

[6] Lars Eriksson, Simon Frei, Christopher Onder, and Lino Guzzella. Control and optimization of turbo charged spark ignited engines. IFAC World Congress, Barcelona, Spain, July 2002. Cited on page 50.

[7] M. Fonsa, M. Muller, A. Chevalier, C. Vigild, E. Hendricks, and S. Sorenson. Mean Value Models for Exhaust System Temperatures. *SAE Paper, 1999-01-0909*, 1999. Cited on page 8.

[8] I. Friedrich, C-S Liu, and D. Oehlerking. Coordinated EGR-Rate Model-Based Controls of Turbocharged Diesel Engines via an Intake Throttle and an EGR Valve. *Vehicle Power and Propulsion Conference, 2009. VPPC '09. IEEE*, 2009. Cited on page 8.

[9] L. Glad and T. Ljung. *Reglerteori - Flervariabla och olinjära metoder*. Studentlitteratur AB, second edition, 2003. Cited on pages 9, 37, 41, and 47.

[10] L. Glad and T. Ljung. *Reglerteknik : grundläggande teori*. Studentlitteratur AB, fourth edition, 2006. Cited on page 9.

[11] S. Gunnarsson, P. Lindskog, L. Ljung, J. Löfberg, T. McKelvey, and T. Glad A. Stenman JE. Strömberg M. Enqvist. *Industriell Reglerteknik*. Reglerteknik, Institutionen för Systemteknik, Linköpings universitet, 2014. Cited on pages 9, 47, and 49.

[12] John B. Heywood. *Internal Combustion Engine Fundamentals*. McGraw-Hill, New York, 1988. Cited on page 7.

[13] Inc. The MathWorks. Mathworks. URL `https://se.mathworks.com/`. Cited on page 12.

[14] S. Thomas and R. P. Sharma. Model Based Control of Engines. *SAE Paper, 2007-26-025*, 2007. Cited on page 8.

[15] J. Wahlström. *Control of EGR and VGT for emission control and pumping work minimization in diesel engines*. PhD thesis, Linköping University, Linköping, Sweden, 2009. Cited on pages 2, 7, 19, and 25.

[16] J. Wahlström and L. Eriksson. Mean Value Engine Modelling of a Diesel Engine with EGR, 2005. URL `http://www.fs.isy.liu.se/Software/TCDI_EGR_VGT/`. Cited on pages 2, 3, 4, 7, 11, 15, 20, 21, 25, 29, and 34.

[17] J. Wahlström and L. Eriksson. Modelling diesel engines with a variable-geometry turbocharger and exhaust gas recirculation by optimization of model parameters for capturing non-linear system dynamics. *Journal of Automobile Engineering*, 225(7):960–986, 2011. Cited on pages 7, 8, and 11.

[18] Johan Wahlström and Lars Eriksson. Modeling of a diesel engine with intake throttle, VGT, and EGR. Technical Report LiTH-R-2976, Department of Electrical Engineering, Linköpings Universitet, SE-581 83 Linköping, Sweden, 2010. Cited on page 7.

[19] L. Zhong, M. Musial, R. Reese, and G. Black. EGR Systems Evaluation in Turbocharged Engines. *SAE Paper, 2013-01-0936*, 2013. Cited on pages 2 and 8.